Kobe University Repository : Kernel

PDF issue: 2026-11-25

Engineering Streptomyces Strains for Bioproduct Production through CRISPR Systems and Gene Integration

Apriliana, Pamella

(Degree)
博士（学術）

(Date of Degree)
2025-03-25

(Date of Publication)
2026-03-01

(Resource Type)
doctoral thesis

(Report Number)
甲第9206号

(URL)
https://hdl.handle.net/20.500.14094/0100496487

※ 当コンテンツは神戸大学の学術成果です。無断複製・不正使用等を禁じます。著作権法で認められている範囲内で、適切にご利用ください。

DOCTORAL DISSERTATION

博士論文

Engineering *Streptomyces* Strains for Bioproduct Production through CRISPR Systems and Gene Integration

CRISPR システムと遺伝子導入によるバイオ生産のための

Streptomyces 菌株の遺伝子工学

January, 2025

令和 7 年 1 月

GRADUATE SCHOOL OF ENGINEERING

KOBE UNIVERSITY

PAMELLA APRILIANA

PREFACE

This doctoral dissertation is presented to Kobe University by the author as a partial requirement for the achievement of the Doctor of Engineering degree. The research, conducted from 2021 to 2025, was under the guidance of Professor Chiaki Ogino in the Laboratory of Biochemical and Bioprocess Engineering, Departement of Chemical Science and Engineering, Graduate School of Engineering, Kobe University.

At the outset, the author heartfelt gratitude to الله سبحانه وتعالى for providing the necessary wisdom, strength and guidance that were crucial in accomplishing this academic pursuit. Immense appreciation is owed to the research advisor, Prof. Chiaki Ogino for his relentless support, profound knowledge, and consistent motivation throught the duration of this study. His astute observations, constructive criticisms which sometimes made my heart pound because of his criticism, and his patient mentorship have significantly contributed to the development of this dissertation. Furthermore, the author extends deep thanks to Professor Akihiko Kondo, Associate Professor Prihardi Kahar for his unwavering support, profound expertise, and steadfast encouragement throughout the entirety of this study, I am deeply grateful, Assistant Professor Mori Yutaro, and Dr. Norimasa Kashiwagi for their invaluable mentorship and thoughtful advice, which greatly enriched the research process.

Their contributions were not only essential but also deeply appreciated, significantly enhancing the quality and depth of this academic work.

The author extends her deepest thanks to her parents, Aminjono and Umi Astuti, for their enduring love, consistent prayers, and steadfast support through this endeavor. She also expresses heartfelt gratitude toward her siblings, Ebta, Mega, Wahyu and Lanang. Their collective influence has not only immensely enriched her personal life but has also served as a constant source of motivation and resilience through her academic journey. Indeed, with such strong support network, the author has found both challenges and love to be more readily surmountable, for which she is profoundly grateful. The author wishes to express sincere gratitude to Minami Yara (Mimi chan) for their collaborative. The author extends profound gratitude to Prof. Puspita Lisdiyanti, Dr. Yopi, Dr. Ratih Asmana Ningrum & Dr. Eng. Nanik Rahmani, whose continue to offer valuable insights and guidance to the author. Additionally, heartfelt thanks are conveyed to Hansha Kistamah for consistently spreading positivity and good vibes, Nova rachmadona, Witta Kartika Restu, Bu Titik Istirokhatun, Radityo Pangestu, Dea Fauziah Fitri, Aliyah, Noor Afiqah, Rendi Palar, Daniel Alejandro Alfaro Sayes, Rezky Lastinov Amza (alm.), Taghreed Magdy Abdelrazek Elkasby, Tan Karling, Fahmi Baihaqqi, Hana Nadhifah, Dianti Rahmasari, Winda Tasia and Filemon Jalu. Acknowledgment is also due to the dedicated lab technicians, staff, and student of the Bioproduction Engineering Research Group, whose collaborative spirit and commitment to creating a supportive laboratory environment have

greatly enriched the author's academic experience. The author expresses sincere and deep appreciation to the Japanese Government, and in particular to the Ministry of Education, culture, Sport, Science, and Technology (MEXT), for their generous provision of full financial support, which has been pivotal in advancing the author's studies in the Department of Chemical Science and Engineering at Kobe University.

PAMELLA APRILIANA

Department of Chemical Science and Engineering

Graduate School of Engineering

Kobe University.

CONTENTS

PREFACE ii

CONTENTS v

LIST OF FIGURE vii

LIST OF TABLES xiii

CHAPTER I

Introduction 1

I.1. *Streptomyces* as a Key Producer of Antibiotics, Secondary Metabolites and Lipids 1

I.2. Biotechnology and industrial application 3

I.3. Genetic Engineering and Synthetic Biology in *Streptomyces* 5

I.4. Transforming Oleaginous *Streptomyces* into a Powerful Platform for polymer Biosynthesis 6

CHAPTER II

Utilizing a Target AID system for editing *Streptomyces* genome 17

II.1. Introduction 17

II.2. Materials and Method 20

II.3. Results and Discussion 34

II.4. Conclusions 50

CHAPTER III

Lipid Production in *Streptomyces jeddahensis* Driven by Glucose and Fatty Acid Derivatives 6

III.1. Introduction 6

III.2. Materials and Method 8

III.3. Results and Discussion 11

III.4. Conclusions 16

CHAPTER IV

Development of *Streptomyces jeddahensis* as a Novel Host for Polyhydroxyalkanoate Production Using Sodium Octanoate Medium 51

IV.1. Introduction 51

IV.2. Materials and Methods 54

IV.3. Results and Discussion 64

IV.4. Conclusions 75

CHAPTER V

General Conclusions and Future Research 76

LIST OF PUBLICATIONS 79

REFERENCE 80

LIST OF FIGURES

Figure 2.1 Rewiring metabolic pathway for lipid production in *S. jeddahensis*.

Figure 2.2 Fermentations of *S. jeddahensis* strains. The strain was cultivated for 48 h, with triplicate samples taken. Cell Dry Weight (CDW) was measured from 1 mL samples, and standard deviations were reported. The conditions for each culture are as follows (A) strains culture into medium MSM containing 2.5 g/L glucose, (B) strains culture into medium MSM containing 2.5 g/L Hexanoate, (C) strains culture into medium MSM containing 2.5 g/L Octanoate, (D) strains culture into medium MSM containing 2.5 g/L Decanoate.

Figure 2.3 Fermentations of *S. jeddahensis* strains. The strain was cultivated for 48 h, with triplicate samples taken. Cell Dry Weight (CDW) was measured from 1 mL samples, and standard deviations were reported. The conditions for each culture are as follows (A) strains culture into medium MSM containing 2.5 g/L glucose, (B) strains culture into medium MSM containing 2.5 g/L Hexanoate, (C) strains culture into medium MSM containing 2.5 g/L Octanoate, (D) strains culture into medium MSM containing 2.5 g/L Decanoate.

Figure 3.1 Sequence position of CasPmCDA-UGI and degradation tag

Figure 3.2 Utilizing NdeI and BamHI enzymes, the basic pGM1190 plasmid is electroporated (evidenced by bands 2-4). Similarly, the pMA RQ_UGI_dCasPmCDA1 is cleaved with BamHI and NdeI enzymes to isolate the CasPmCDA1 site, as indicated by bands 5-7.

Figure 3.3 The successful integration of the casPmCDA1 into the pGM1190 plasmid was confirmed through the electroporation of PCR findings.

Figure 3.4 The outcomes of the binding between pGM1190 and CasPmCDA1 plasmid were re-verified through digestion with an alternate retriction enzyme. In one instance, the plasmid was cleaved using SnaBI, while in another a dual enzymatic approach was employed involving NdeI and BamHI.

Figure 3.5. Theoutcomes of the gel electrophoreses step reveal the gRNA component, the ermE-target and combine between gRNA-ermE target by overlap PCR.

Figure 3.6 The process of confirming the results of target infusion into the pGM1190-dCasPmCDA-UGI-AAV plasmid with gRNA-ermE target.

Figure 3.7 The process of confirming the results of target infusion into the pGM1190-dCasPmCDA-UGI-AAV/LVA plasmid with gRNA-ermE target

Figure 3.8 Overview of genome editing using CRISPR-dCas9-PmCDA-UGI in *S. coelicolor*.

Figure 3.9 Plasmid construction. (A) Step to prepare ermE promoter and gRNA region. (B) The construction of vector backbones integrating the fused dCasPmCDA1-UGI. (C) Complete vector.

Figure 3.10 Essential genes for actinorhodin production. (A) Actinorhodin gene cluster. (B) Mutated target gene actVA-ORF4. The positions of PAM sequence (GGC) and target 10 are given. (C) The position of SCO5079 protein (actVA-ORF4) in actinorhodin biosynthesis.

Figure 3.11 Genome editing using dCas9-PmCDA-UGI-AAV system. (A) Phenotypical analysis of five mutants selected and grew on ISP2 medium agar, the mutant with targeted actVA-ORF4. Wild-type *S. coelicolor*, pGM1190, and Empty vector (dcas9-PmCDA-UGI-AAV without target) were used as control experiments. (B) Sequence alignment between Wild type and target 10 (actVA-ORF4) edited by dCas9-PmCDA-UGI-AAV. The PAM sequence is shown in the red box, and the site targeted by sgRNA is indicated by a brown underline. Uncolored bases are seen in single mutation results. (C) A typical sequencing chromatogram showing the mutation from C to T in the target location. *S. coelicolor* wild-type strain was used as a control.

Figure 3.12 The actinorhodin color differences from the cultures of WT (Wild type), Empty (plasmid CRISPR system with no expected target), Target 10 (plasmid CRISPR system with 20 nucleotides from gen

actVA-ORF4 as targets) At a pH of 2, actinorhodin undergoes a color change, shifting from its initial blue to a distinct red are depicted in the photograph (A) and observed at various absorbances (B).

Figure 3.13 The outcome of assessing mutations in the open reading frame (ORF) genome plays a crucial role in producing actinorhodin. (A) The mutated gene critical for actinorhodin production was analyzed and compared to the reference sequence from the *S. coelicolor* wild type. The study recorded the total count of single nucleotide variants (SNVs) in this analysis. (B) The number of mutations based on the mutation types, including SNVs, deletions, and insertions, were observed in the critical genes. (C) The single nucleotide variations (SNPs) are observed in multiple ORFs, these mutations do not result in the creation of a stop codon

Figure 4.1 The Illustration of the construction and restriction maps for plasmids 3TYM-ermE, 3TYM-ermEAB, and 3TYM-ABCGC.

Figure 4.2 Rewiring metabolic pathway for enabling polyhydroxyalkanoate (PHA) production in *S. jeddahensis.*

Figure 4.3 Fermentations of *S. jeddahensis* wild-type and SJ-D2 engineered strains. The strain was cultivated for 144 h by repeated batch fermentation, with triplicate samples taken. Cell Dry Weight (CDW) was measured from 1 mL samples, and standard deviations

were reported. The conditions for each culture are as follows: (A) *S. jeddahensis* wild-type grown in MSM medium with 2.5 g/L sodium octanoate; (B) *S. jeddahensis* wild-type grown in TSB medium with 1 g/L glucose and 2.5 g/L sodium octanoate; (C) *S. jeddahensis* SJ-D2 strain grown in MSM medium with 2.5 g/L sodium octanoate; (D) *S. jeddahensis* SJ-D2 strain grown in TSB medium with 1 g/L glucose and 2.5 g/L sodium octanoate.

Figure 4.4 Observation of PHA accumulation in *S. jeddahensis* SJ-D2 strain. Wild-type strain was used as a background. The panel displays images of both strains as observed through Nile Red staining, phase-contrast microscopy (Brightfield), and merged (bars, 10μm). (A) strains culture into medium MSM containing 2.5 g/L sodium octanoate. (B) strains culture into medium TSB0.5 containing 1 g/L glucose and 2.5 g/L sodium octanoate.

Figure 4.5 Gas chromatography analysis detects P (3HB-co-3HHx-co-3HO), indicating successful PHA production by the engineered strain (SJ-D2). (A) Standard P(3HB). (B) Standard P(3HB-co-3HV-co-3HHx). (C) *S. jeddahensis* wild-type strain cultured in MSM medium containing 2.5 g/L sodium octanoate. (D) *S. jeddahensis* wild-type strain cultured in TSB0.5 medium containing 1 g/L glucose and 2.5 g/L sodium octanoate. (E) *S. jeddahensis* SJ-D2 strain cultured in MSM medium containing 2.5 g/L sodium

octanoate. (F) *S. jeddahensis* SJ-D2 strain cultured in TSB0.5 medium containing 1 g/L glucose and 2.5 g/L sodium octanoate. IS indicates the internal standard peak.

LIST OF TABLES

Table 3.1 Strain and plasmids used in this study.

Table 3.2 Primers used in this study.

Table 3.3 Target sequence position in *S. coelicolor* NBRC15146 genome.

Table 4.1 Strains and plasmids used in this study.

Table 4.2 Primers were used for 3TYM-ABCGC plasmid construction in this study.

Table 4.3 Production of P(3HB-co-3HHx-co-3HO) in *S. jeddahensis* wild type and SJ-D2 strains.

CHAPTER I

INTRODUCTION

I.1. *Streptomyces* as a Key Producer of Antibiotics and other Secondary Metabolites.

The genus *Streptomyces*, belonging to the Actinobacteria phylum, is pivotal in microbiology and biotechnology due to its exceptional ability to produce a wide variety of secondary metabolites. These compounds hold significant value in medicine, agriculture, and industry. As filamentous, Gram-positive bacteria predominantly found in soil, *Streptomyces* plays a vital ecological role in nutrient cycling and organic matter decomposition through enzymatic activities like cellulase and chitinase production. These enzymes enable the breakdown of complex biopolymers, facilitating nutrient recycling in ecosystems[1]. The genus is also known producing geosmin, a volatile compound responsible for the distinctive "earthy" smell of soil, showcasing its close relationship with the environment[2]. Among Actinobacteria, *Streptomyces* is the most prolific producer of bioactive compounds, including over two-thirds of known antibiotics, as well as antifungal, antiparasitic, and anticancer agents[3]. Its filamentous structure, resembling fungal hyphae, allows it to thrive in complex soil environments. A unique feature of *Streptomyces* is its linear chromosomes with a high guanine-cytosine (GC) content, which confer genetic flexibility and support the biosynthesis of diverse secondary metabolites[1].

These bacteria inhabit a range of environments, from temperate soils to extreme ecosystems such as saline habitats and acidic forests. Their genomic adaptability, driven by lateral gene transfer and gene duplication, enhances their ability to produce antimicrobial and stress-responsive compounds[4]. Habitat-specific adaptations, shaped by environmental factors like pH and salinity[5], futher refine this capacity. Ecologically, *Streptomyces* forms symbiotic relationships with plants, aiding in growth promotion and pathogen resistance through the production of antifungal and antibacterial metabolites. Marine-associated species, found in organisms like sponges and cone snails, contribute to host defense by synthesizing unique bioactive compounds[6,7].

The discovery of antibiotics such as streptomycin and tetracycline from *Streptomyces* revolutionized modern medicine, highlighting its immense pharmaceutical value[8]. Beyond healthcare, the genus produces agriculturally relevant products like herbicides and insecticides, demonstrating its broad biotechnological potential[9]. Its complex developmental cycle, involving sporulation and hyphal differentiation, is intricately linked to secondary metabolite production. This process is regulated by genetic networks that integrate environmental cues to optimize production[2].

I.2. Expanding Streptomyces Applications: Lipids and Biopolymers

The exceptional ability of *Streptomyces* to produce diverse bioactive compounds has established it as a key player in biotechnology and industrial innovation, profoundly influencing fields such as medicine, agriculture, and environmental sustainability. Beyond these well-documented capabilities, *Streptomyces* species have garnered attention for their potential in lipid biosynthesis and biopolymer production, presenting promising avenues for biotechnological and industrial applications.

I.2.1 Lipid production in *Streptomyces*

The potential to engineer *Streptomyces* for enhanced lipid production offers significant promise for industrial applications. These bacteria are capable of synthesizing diverse lipids, including fatty acids, phospholipids, and triacylglycerols (TAGs), which are essential for energy storage, membrane structure, and secondary metabolism. Among these, TAGs have garnered attention for their ability to be converted into biodiesel and other biofuels, presenting a sustainable alternative to fossil fuels. The structural diversity of lipids produced by *Streptomyces* also opens avenues for developing specialty chemicals, pharmaceuticals, and food additives. Central to this process is fatty acid synthase (FAS), an enzyme that catalyzes the formation of long-chain fatty acids from acetyl-CoA and malonyl-CoA precursors. Advances in understanding the structural and functional aspects of FAS have illuminated its critical role in lipid metabolism and revealed its potential for metabolic engineering to increase lipid

production, a valuable step toward renewable lipid-based biofuels and biochemicals[10,11].

Certain *Streptomyces* species, including *Streptomyces coelicolor* (*S. coelicolor*), *Streptomyces avermitilis* (*S. avermitilis*), and *Streptomyces jeddahensis* (*S.jeddahensis*,), have demonstrated significant lipid production capacity. *S. jeddahensis*, in particular, is noted as an oleaginous bacterium capable of accumulating TAGs that comprise up to 60% of its total lipid content during the stationary growth phase[11,12]. The biosynthesis of these lipids relies on primary metabolic precursors such as acetyl-CoA and malonyl-CoA, which feed into fatty acid biosynthetic pathways. The activity of FAS, which facilitates the synthesis of long-chain fatty acids, is tightly regulated by substrate availability and energy status. Additionally, TAG production is driven by acyltransferases, enzymes responsible for esterifying diacylglycerol with fatty acids. Studies have identified genes like sco0958 as crucial for TAG biosynthesis, where its deletion significantly reduces TAG accumulation, while its overexpression enhances lipid production. These insights underline the intricate enzymatic and genetic regulation of lipid metabolism in *Streptomyces*, presenting opportunities to optimize these pathways for biotechnological applications[10]. These developments will be discussed in detail in Chapter III, where the focus is on optimizing production conditions.

I.2.2 Exploring Biopolymer (PHA) Production Potential in *Streptomyces*

Polyhydroxyalkanoates (PHAs) are biodegradable polymers synthesized by various microorganisms, including *Streptomyces*, under nutrient-limited

conditions. These biopolymers offer a sustainable alternative to conventional plastics due to their renewable origin and biodegradability. Several studies reporting the *Streptomyces* can accumulate PHA[13,14], *Streptomyces aureofaciens*[15], *Streptomyces coelicolor*[16], genes have been utilized in recombinant systems to enhance PHA production. For instance, an engineered Escherichia coli harboring genes from *S. aureofaciens* was able to produce highly crystalline polyhydroxybutyrate (PHB) with remarkable thermal stability[15].

Building on *Streptomyces*' remarkable capabilities, the next chapter delves deeper into the transformative potential of genetic engineering and synthetic biology in unlocking novel applications. By harnessing advanced tools like CRISPR and genome-editing technologies, the chapter will explore how tailored modifications can amplify metabolic efficiency and enable the synthesis of unprecedented bioactive compounds. This exploration will extend into the realm of sustainable biotechnology, showcasing how synthetic biology can transform industrial production, environmental sustainability.

I.3. Advancing Streptomyces Applications Through Genetic Engineering and Synthetic Biology

The integration of genetic engineering and synthetic biology has transformed the biotechnological landscape of Streptomyces. Techniques such as CRISPR, advanced genome-editing tools, and synthetic biology frameworks enable precise manipulation of metabolic pathways, allowing the tailoring of Streptomyces strains to produce novel bioactive compounds and optimize existing

ones. These modifications can amplify the production of lipids and biopolymers, positioning Streptomyces as a sustainable platform for industrial biotechnology. For instance, CRISPR-Cas systems have been employed to delete or enhance genes associated with secondary metabolism, leading to the overproduction of target compounds. Similarly, synthetic biology approaches enable the construction of artificial gene clusters, facilitating the synthesis of novel metabolites. These transformative methodologies will be explored in subsequent chapters, showcasing the vast potential of Streptomyces as a microbial chassis for industrial innovation.

I.4. Bridging Metabolic Pathways for Enhanced Polymer Production

A key focus of this study is the dual application of Streptomyces in lipid and biopolymer production. The ability of *S. jeddahensis* to thrive in diverse environments and its high lipid accumulation capacity make it an ideal candidate for developing sustainable biotechnological solutions. By leveraging genetic tools to redirect metabolic fluxes, this research aims to optimize the simultaneous production of lipids and PHAs. This dual approach not only enhances the efficiency of resource utilization but also addresses industrial demands for renewable materials. The following chapters will delve deeper into these aspects. **Chapter II** will explore strategies for optimizing lipid production in *S. jeddahensis*, focusing on environmental and genetic factors influencing metabolic output. **Chapter III**, introduce *S. jeddahensis* as a novel host for polyhydroxyalkanoate

(PHA) synthesis. This chapter will detail the integration of biosynthetic gene clusters and the role of metabolic engineering in optimizing production. The approach involves a combination of traditional genetic modification and advanced genome editing technologies. Specifically, the traditional method is used to insert key genes required for PHA synthesis (*phbA*, *phbB*, *phaC1*, *phaG*, and *phaC2*), while advanced genome editing employs the CRISPR FnCpf1 system to knock out the *DGAT* gene, enhancing the metabolic pathway. This dual strategy demonstrates the synergy between conventional and next-generation genetic modification techniques. Chapter IV details the development of a novel CRISPR-based system designed for genome editing in Streptomyces. This system specifically targets the AID (activation-induced cytidine deaminase) system fused with a UGI-degradation tag, optimizing its functionality for precise genetic modifications. For the initial phase of this research, Streptomyces coelicolor was employed as a model organism to validate and refine the experimental approach. Finally, Chapter V will discuss the broader implications of these advancements, highlighting their contributions to sustainable biotechnology and industrial scalability

CHAPTER II

Lipid Production in *Streptomyces jeddahensis* Driven by Glucose and Fatty Acid Derivatives

II.1. Introduction

The growing global need for sustainable and renewable energy has sparked considerable interest in microbial lipid production as a potential eco-friendly alternative to fossil-based oils. Among the lipid-producing microorganisms, certain *Streptomyces* species have garnered attention fot their ability to accumulate lipids, especially triacylglycerols (TAGs), which are precusors for biodiesel and various industrial products. These microorganisms can produce lipid that make up 20% to 80% of their biomass when grown under nitrogen-limited conditions[12,17–19], making them a promising option for large-scale lipid production. Oleaginous microbes like *Rhodococcus opacus* and *Cryptococcus curvatus* have been widely researched for their ability to accumulate

TAGs[18,20]. Rhodococcus species are renowned for their capacity to degrade various hydrocarbons and accumulate lipids, a process facilitated by their versatile central metabolism. This includes key metabolic pathways such as glycolysis, gluconeogenesis, and the tricarboxylic acid cycle[21,22]. These metabolic adaptations are crucial for understanding the potential of *S. jeddahensis* in biodiesel production. Specifically, the formation of triacylglycerols (TAG) in *S. jeddahensis* represents a key aspect of its metabolic flexibility, as illustrated in Figure 3.1. This ability allows them to convert inexpensive, renewable feedstocks into valuable lipids, showcasing their economic and environmental benefits[21,23]. Despite the extensive research on these organisms, *Streptomyces* species remain relatively underexplored. However, they show significant potential for lipid production, especially in synthesizing branched-chain fatty acids and high-value lipids when cultivated with carbon sources like glucose or cellobiose.

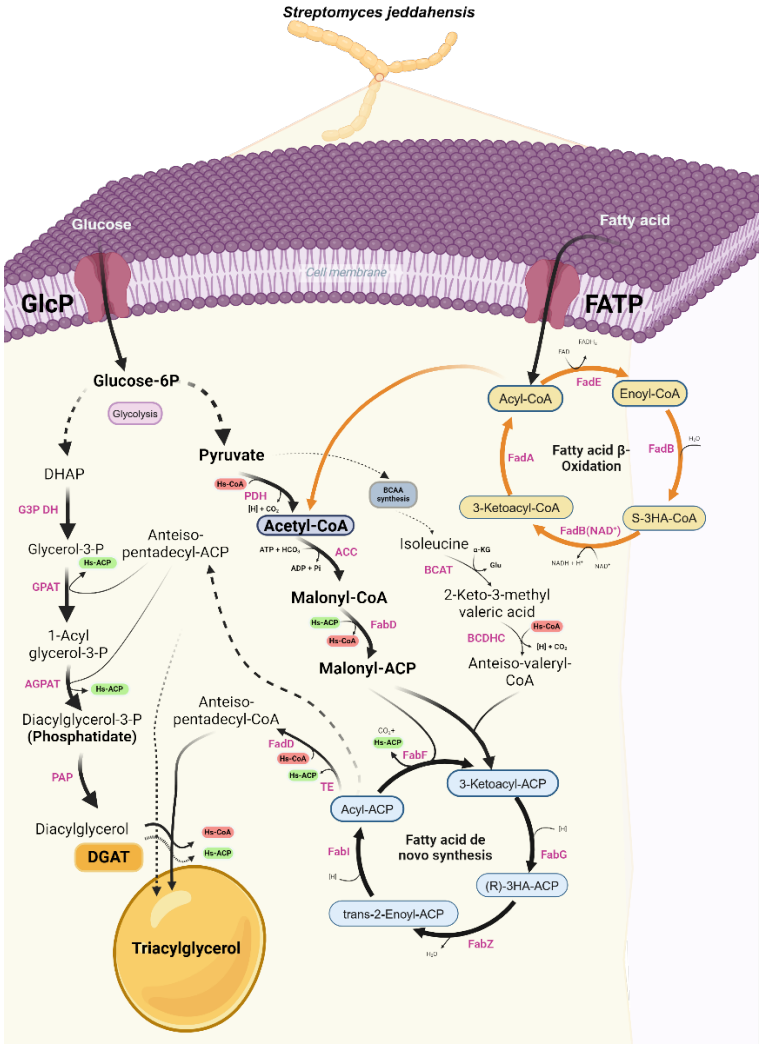

Figure 2.1 Rewiring metabolic pathway for lipid production in *S. jeddahensis*.

Among them, *Streptomyces jeddahensis* is particularly notable for its metabolic diversity and exceptional lipid accumulation, producing lipids up to 64% of its dry cell weight. This species can thrive across a wide range of temperatures, up to 50°C, making it suitable for industrial-scale production. Additionally, *S. jeddahensis* can utilize various low-cost carbon sources, including industrial waste, which helps reduce production costs and addresses waste

management challenges. These attributes make it a novel and promising host for the biotechnological development of lipid-based products[24].

Triacylglycerols (TAGs) produced by oleaginous microbes have gained considerable attention due to their crucial role in the synthesis of polyhydroxyalkanoates (PHAs), which are biodegradable plastics offering an environmentally friendly alternative to petrochemical-based plastics. The metabolic pathways for lipid and biopolymer production share key intermediates and enzymatic components, such as acyl-CoA derivatives and acyl-carrier proteins (ACP). By delving into the metabolic processes in *Streptomyces*, we can potentially enhance the production of both lipids and PHAs, leveraging their shared biochemical pathways[25–27]

This study aims to optimize lipid production in *Streptomyces jeddahensis* by using glucose and fatty acid derivatives such as sodium hexanoate, sodium octanoate, and sodium decanoate as carbon sources. Glucose is commonly used due to its availability, low cost, and efficient metabolism through glycolysis to produce acetyl-CoA, a precursor for fatty acid synthesis [28]. Medium-chain fatty acids, such as hexanoate, octanoate and decanoate, activate specific biosynthetic pathways, including β-oxidation, and enhance lipid accumulation [27,29–32]. By leveraging these substrates, this research aims to elucidate the metabolic potential of *S. jeddahensis* and its ability to serve as a sustainable platform for lipid production.

II.2. Materials and Methods

II.2.1 Medium, bacterial strains and maintenance

The Glucose and other reagents were procured from Sigma-Aldrich (Tokyo, Japan) and Nacalai Tesque, Inc. (Kyoto, Japan). Sodium hexanoate, sodium octanoate, and sodium decanoate were obtained from Tokyo Chemical Industry Co., Ltd (Tokyo, Japan). The oleaginous microorganism used in the experiments was *Streptomyces jeddahensis* (DSM 101878), sourced from the Leibniz Institute DSMZ-German Collection of Microorganisms and Cell Cultures. The *Streptomyces* strains were maintained on TSB agar medium, which contained 17 g/L peptone from casein, 3 g/L peptone from soymeal, 2.5 g/L D(+)-glucose, 5 g/L NaCl, 2.5 g/L K_2HPO_4, and 20 g/L agar.

III.2.2 Culture Process

Lipid accumulation in *Streptomyces jeddahensis* cells was assessed using a modified protocol based on Sass P *et al*[83]. The experiments were conducted in 300 mL Erlenmeyer flasks. Pre-seed Culture: Approximately 1 cm^2 of *S. jeddahensis* was introduced into 45 mL of Tryptic Soy Broth (TSB) liquid medium and incubated at 30°C with agitation at 160 rpm for 2 days. For seed culture, 5 mL of the pre-seed culture was transferred into 50 mL of TSB medium and incubated under the same conditions for 18 hours. For fermentation Phase, the seed culture, adjusted to an OD of 1, was transferred into 60 mL of Mineral Salts Medium (MSM) to promote triacylglycerol (TAG) accumulation. Various carbon sources, including glucose, sodium hexanoate, sodium octanoate, and sodium

decanoate, were tested. For cultivation conditions, the flasks were placed on an orbital shaker at 160 rpm and incubated at 30°C for 48 H. MSM with reduced nitrogen content (0.25 g/L urea, 0.16 g/L yeast extract, 0.02 g/L $CaCl_2$, 1.52 g/L KH_2PO_4, 0.52 g/L $MgSO_4 \cdot 7H_2O$, 4 g/L Na_2HPO_4) was supplemented with 2.5 g/L of each carbon source. TSB was used as a comparative medium. Cells were harvested by centrifugation at 10,000 x g for 5 minutes at 4°C, washed with MQ water, frozen at -20°C overnight, and then freeze-dried for 48 hours.

II.2.3 Dry cell weight measurement

Cells from each culture were harvested by centrifugation at 5000 x g for 5 minutes. The wet weight of the cell pellets was measured. The pellets were then washed with sterile water and reweighed. The washed cell pellets were freeze-dried for 48 hours. After freeze-drying, the dry weight of the cell material was recorded before lipid extraction.

II.2.4 Lipid contents

To prepare bacterial cell samples for lipid extraction, 30 mg of freeze-dried cells were combined with 0.6 mm zirconia beads in a 2 mL Eppendorf tube. The cell mixture was treated with lysozyme (5 mg/mL) to lyse the bacterial cell walls and incubated for 30 minutes. After incubation, the samples were freeze-dried again. Chloroform (1 mL) and methanol (0.5 mL) were added to the mixture. The samples were disrupted using a Shake Master Neo at 1500 rpm for 5 minutes, repeated three times to ensure thorough mixing. Following disruption, the samples were centrifuged at 14,000 rpm for 5 minutes to separate the

supernatant from the pellet. The supernatant was carefully removed, and 1.5 mL of MilliQ water was added to the pellet. The samples underwent another round of disruption under the same conditions. After the second disruption, the supernatant was discarded, and the remaining sample was dried in a block incubator set at 60°C for 3 days. The final dry weight of the samples was recorded to calculate the lipid content by comparing it with the initial weight of the freeze-dried bacterial cells.

II.2.5 Identify and quatify fatty acid by using Fatty Acid methyl Ester (FAME) analysis

The cellular fatty acid composition was analyzed using a gas chromatograph-mass spectrometer (GCMS-QP2020 NX, Shimadzu Corporation). Chromatographic separation was achieved on a DB-23 column (60 m x 0.25 mm x 0.15 µm; Agilent Technologies, Palo Alto, CA). The temperature program began at 50°C for 2 minutes, followed by a ramp of 25°C per minute to 175°C, and then a slower ramp of 4°C per minute to a final temperature of 230°C. Approximately 30 mg of freeze-dried bacterial cells were accurately weighed and combined with 0.6 mm zirconia beads in a 2 mL microcentrifuge tube. The mixture was treated with 500 µL of Reagent A and Reagent B, following the instructions of the fatty acid methylation kit (Fatty Acid Methylation Kit, Nacalai Tesque, Kyoto). Cell lysis was performed by agitating the mixture with a Shake Master Neo at 1500 rpm for three cycles of 5 minutes each. After lysis, the sample was incubated at 37°C for 60 minutes on a heat block

to allow for the methylation of glycerides and sterol esters. Next, 500 µL of Reagent C (from the same kit) was added to the mixture, which was then subjected to the same cell disruption protocol followed by a 20-minute incubation at 37°C to promote the methylation of free fatty acids. After the methylation process, 1 mL of the kit's extraction solvent was added. The mixture was centrifuged at 14,000 rpm for 1 minute, and the clear supernatant was transferred into a new microcentrifuge tube. For Gas Chromatography-Mass Spectrometry (GC-MS) analysis, 90 µL of the supernatant was combined with 10 µL of an Internal Standard (IS) solution in a glass vial. The IS was prepared by diluting 10 µL of methyl benzoate in 990 µL of hexane, resulting in a final volume of 1 mL.

II.2.6 Quatified lipid inside cell by Bodipy

BodipyTN 493/503 (4,4-difluoro-5,7-dimethyl-4-bora-3a,4a-diaza-s-indacene) from Invitrogen (Thermo Fisher Scientific) was used for staining. A 5 mg/mL stock solution of the dye was prepared by dissolving it in ethanol and stored at -20°C, protected from light. Approximately 100 µL of cell cultures were centrifuged at 13,000 rpm for 30 seconds, and the supernatant was discarded. The cell pellets were washed with 100 µL of phosphate-buffered saline (PBS) at pH 7, and after removing the supernatant, they were resuspended in 100 µL of the same buffer. To this suspension, 1 µL of Bodipy staining solution was added and mixed thoroughly. The stained cells were incubated at room temperature for 10 minutes.

10 µL sample of the stained cell suspension was placed on a microscope slide and observed using a Keyence BZ-X810 fluorescence microscope.

II.2.7 qPCR analysis of gene transcript levels in *S. jeddahensis* strain

To investigate gene expression, *S. jeddahensis* strains were grown to an OD600 of 1. cDNA was synthesized from DNase-treated 0.5 µg of total RNA in a 20 µL reverse transcription reaction using random hexamers and SuperScript III reverse transcriptase (Invitrogen). Real-time PCR reactions were performed with a Bio-Rad iCycler (iQ5 system), using primers listed in Table 3.1. Changes in gene expression were calculated using the $2^{-\Delta\Delta Cq}$ formula, as previously decribed [34]. Gene expression data for each run were organized into a matrix labeled "countData," with rows representing genes and columns representing samples. Metadata, referred to as "colData," included details on sample conditions and biological replicates (numbered 1, 2, or 3). Differentially expressed genes (DEGs) were identified by analyzing expression level variations between two groups of samples using the DESeq2 package in R, which applies a negative binomial distribution. DEGs were defined based on a threshold of |log2-fold change (LFC)| ≥ 2 and an adjusted p-value ≤ 0.05 (equivalent to -log10 adjusted p-value ≥ 1.30). A list of DEGs meeting these criteria was compiled.Protein-Protein Interaction (PPI) Network analysis of the DEGs was performed using STRING (https://string-db.org/) version 11.5.

Table 2.1. List of Primers Used for Measuring Gene Expression via Quantitative PCR

Gene	Forward primer (5'→3')	Reverse primer (5'→3')
STSP_00760 (*plsC_1*)	CCGTGAACCACTCCCACAA	ACCTTCAGCTGGCCGATTC
STSP_00850	GCCAGTGCGTACCGAGATAG	CTCGCCTATATGGCCTCGAC
STSP_01000 (*inhA_1*)	CAGGTTGCAGCGGATGTTCT	CGCAGTACGACTGGATGGG
STSP_01010 (*fabG1_1*)	CTCCAGTGATGTACGAGGCG	TCGACACCGACATGACCAAG
STSP_03080 (*DGAT*)	GATCGACGGGGTCCATCAC	TTCGCCGTGCTGTTCAAGTT
STSP_12530	TAGCCCCACTCGAAGTTGTC	CGGACCGTATCGCGTATCTG
STSP_17580 (*bkdA_1*)	GTTGACACCACGGAACATGC	GACGACTACGTCTTCCCGAC
STSP_19060 (*gpsA*)	GATGGTCTCCTCCAGGGTCA	CATGACCTTCTCCGGACTCG
STSP_28680 (*accD5_1*)	CATCAAGCAGCTCCTGTCGT	CTCGATGACCTCGTGCATGT
STSP_45110 (*tesB_2*)	GTACTTCGGCAGTGACTCGG	GCAGCCGATCTTCCATCTGT
STSP_45150 (*accA1_2*)	CGGAGAGCTATCTGTCGGTG	CTCGGCGAGGAATCCGTATC
STSP_50580 (*FabZ*)	CCGACCTCTTTGGCGAACTT	GCCCAGACCTTCAACGTGAC
STSP_61390 (*ilvE*)	TGACGATCAAGTGGACGGAG	CGAAGATCTCCTGGGCGTAG
STSP_67970 (*fabD*)	GCGTACGTCTCGAACAAGGA	TCTGGAACGTCTCCATGCAC
STSP_67980 (*fabH_2*)	AGCTGATCAAGCAGACCGTG	GGAACTTGATGTCGCCGTTG
STSP_68010 (*fabF*)	CGATCGAGATGATCCGCACC	TGTTCTTGGACATCGCCATCA

STSP_72400 (*lcfB-5)*	CACGAGACGGTCTA CATCGG	ATCGTCACAGCTCAA CTCGG
STSP_74190	TACCTGGTCCGTCA GGTTGA	AAGTGGACGATCCAG TTCGG
rpoB[1]	GTAGTTGTGACCCT CCCACG	GACTACATCACCACC GCCAA

[1] Housekeeping gen.

II.3. RESULTS AND DISCUSSION

II.3.1. Effect of temperature and carbon source on *S. jeddahensis* growth

Microorganisms need to absorb carbon sources and other nutrients from their environment to support cell growth and maintain metabolic balance[35]. Temperature is also a critical factor in regulating bacterial growth. This study examined the growth dynamics and metabolic efficiency of *S. jeddahensis* under different carbon sources and incubation temperatures, providing insights into how these factors influence the bacterium's growth and metabolism. three distinct temperatures (30°C, 37°C, and 45°C) were chosen to encompass a range that supports optimal growth and enzyme activity. These temperatures represent mild, moderate, and higher thermal conditions, allowing for a comprehensive examination of their effects on the biological processes under investigation[36–38].

Glucose is typically the preferred carbon source and serves as the primary energy source for many organisms[39]. Sodium hexanoate has been shown to support the growth of various bacterial strains, such as *Cupriavidus necator*[40]. Similarly, sodium octanoate is an effective carbon source for *C. necator*[41],

196 promoting efficient biomass production without adverse effects. Several bacterial
197 species can also utilize decanoate as a carbon and energy source[42]. In this study,
198 glucose, sodium hexanoate, sodium octanoate, and sodium decanoate were used
199 as carbon sources. Growth was monitored at three temperatures: 30°C, 37°C, and
200 45°C. Cell dry weight (CDW) measurements were taken at 0, 12, 24, and 48 hours,
201 with triplicate samples at each time point to ensure data reliability. The results
202 showed that *S. jeddahensis* achieved the highest CDW values at 30°C across all
203 tested carbon sources, indicating that this temperature is optimal for growth
204 (Figure 2A, E, C, G). At 30°C, the bacterium exhibited robust growth, making it
205 the best condition for biomass production. Conversely, at 45°C, there was a
206 significant decline in CDW for all carbon sources, suggesting a critical thermal
207 tolerance threshold for this strain. The reduced growth at higher temperatures
208 may be due to cellular damage, protein denaturation, or impaired enzymatic
209 activity, as noted by Schroda *et al*[43]. The temperature sensitivity of *S. jeddahensis*
210 could also be related to its inability to maintain essential metabolic processes for
211 cell division and growth under thermal stress.

212 Among the carbon sources tested, sodium octanoate was the most
213 efficient substrate for biomass production, with the highest CDW variability
214 observed at 30°C (Figure 2.2E). Sodium hexanoate and sodium octanoate were
215 consumed within 24 hours at 30°C and 37°C (Figure 2.2D-F). However, at 45°C,
216 the consumption rate slowed significantly, indicating that elevated temperatures
217 inhibit key metabolic processes such as carbon source uptake, utilization, and

enzyme activities crucial for substrate metabolism[44]. This study confirmed that bacteria readily utilize medium-chain fatty acids like sodium hexanoate and sodium octanoate for growth. This was evident in the present study[40,41]. In contrast, glucose showed the most significant reduction in residual levels at 45°C, with no measurable glucose remaining after 12 hours (Figure 2.2B). The rapid glucose consumption at 45°C suggests that glucose is quickly metabolized at higher temperatures.

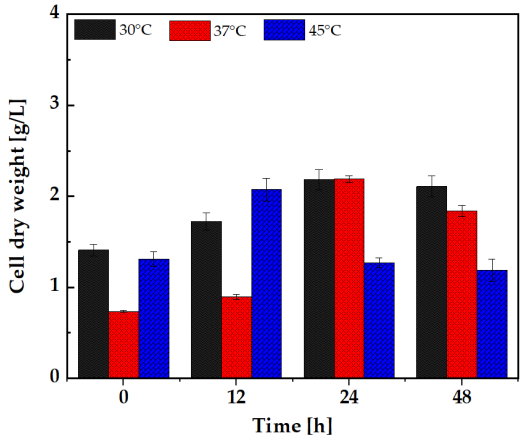

(A)

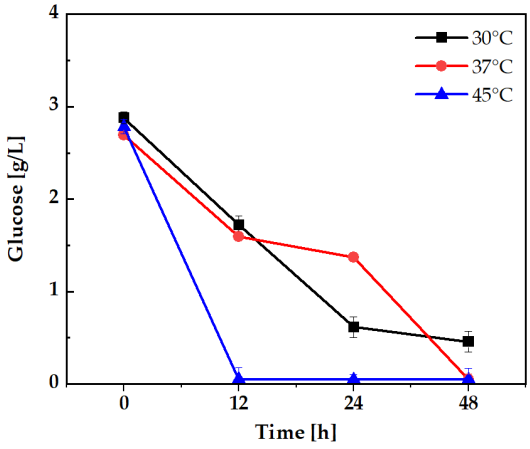

(B)

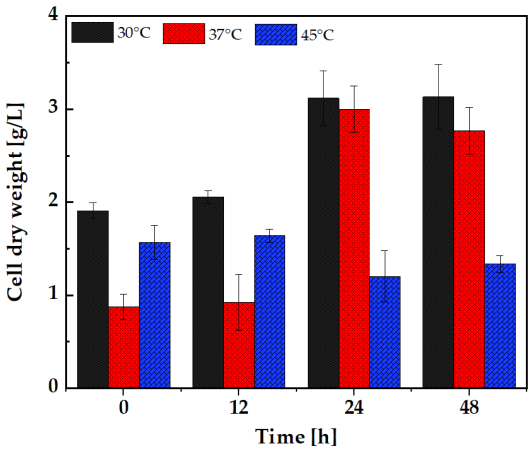

(C)

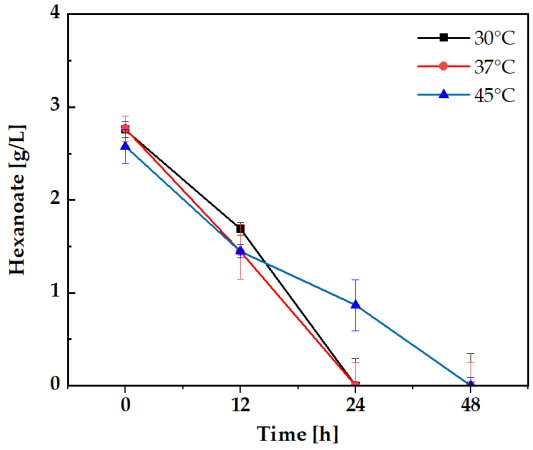

(D)

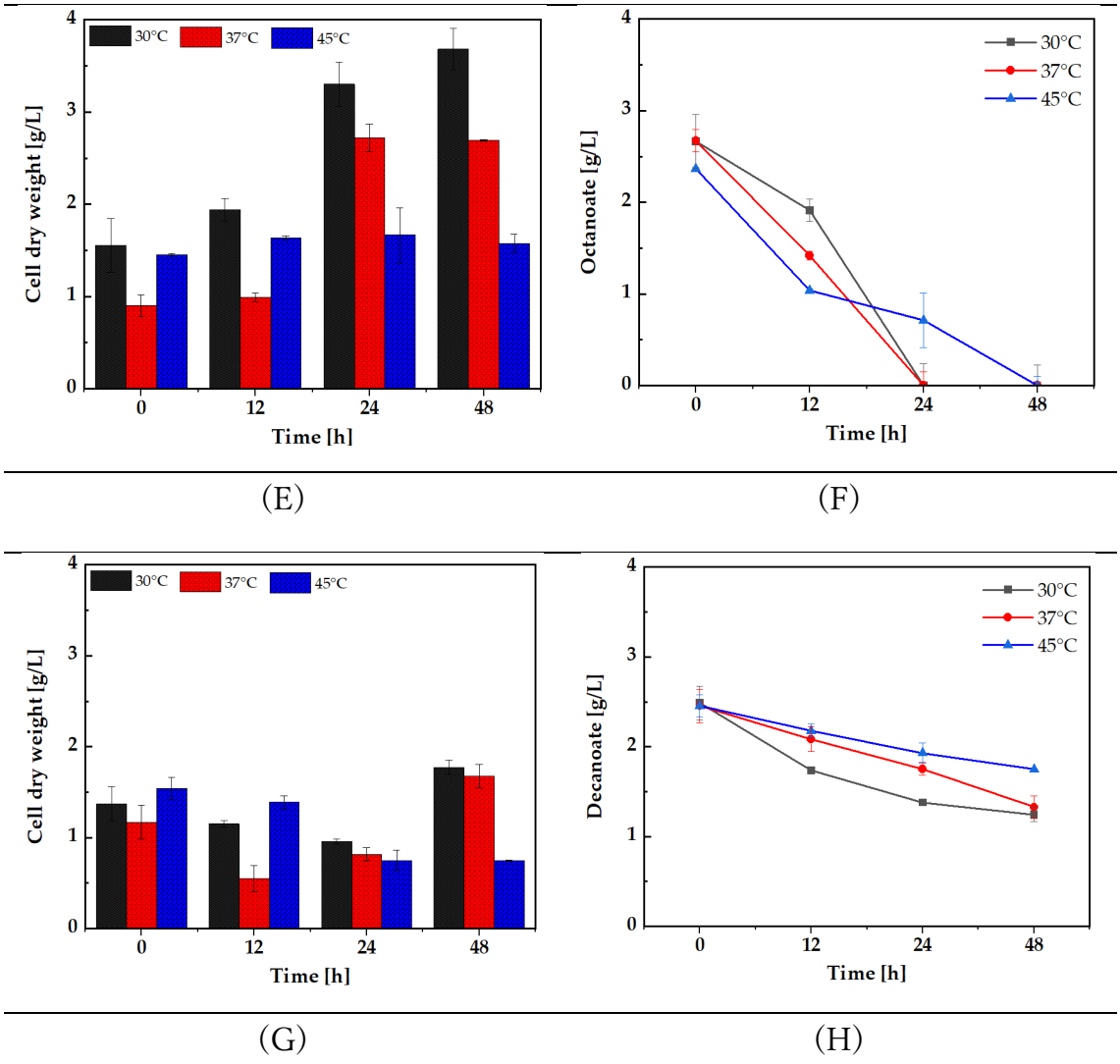

225

226 **Figure 2.2** Fermentation of S. jeddahensis strains under various conditions. The strains were
227 cultured for 48 hours in minimal salt medium (MSM) with different carbon sources, and triplicate
228 samples of 1 mL were taken for measurement. (A) Cell dry weight (CDW) of the strain cultured
229 in MSM with 2.5 g/L glucose. (B) Glucose consumption by the strains. (C) CDW of the strain
230 cultured in MSM with 2.5 g/L sodium hexanoate. (D) Sodium hexanoate consumption by the
231 strains. (E) CDW of the strain cultured in MSM with 2.5 g/L sodium octanoate. (F) Sodium
232 octanoate consumption by the strains. (G) CDW of the strain cultured in MSM with 2.5 g/L
233 sodium decanoate. (H) Sodium decanoate consumption by the strains.

234

235

236 ## II.3.2. Lipid accumulation in *S. jeddahensis*

237 Storage lipids serve vital functions in cellular processes, including the
238 regulation of membrane fatty acid composition, acting as reservoirs for reducing
239 equivalents and metabolic intermediates, and serving as precursors for lipid
240 biosynthesis, which are essential for maintaining metabolic balance under varying
241 environmental conditions[45]. This study assessed lipid accumulation in *S.*
242 *jeddahensis* cultured with different carbon sources—glucose, sodium hexanoate,
243 sodium octanoate, and sodium decanoate—at three temperatures (30°C, 37°C,
244 and 45°C). Lipid content was quantified as a percentage of cell dry weight (%,
245 w/w), and Bodipy staining was employed to visualize intracellular lipid
246 accumulation. Figure 2.3 illustrates lipid accumulation in *S. jeddahensis* at 37°C
247 with glucose (Figure 2.3A), sodium hexanoate (Figure 2.3B), sodium octanoate
248 (Figure 2.3C), and sodium decanoate (Figure 2.3D), highlighting visible lipid
249 storage within cells. Additional visualizations for lipid accumulation at 30°C and
250 45°C are presented in Figures 2.4 and 2.5, respectively. The data underscore the
251 influence of carbon source and temperature on lipid biosynthesis, demonstrating
252 that both factors significantly modulate lipid storage in *S. jeddahensis*.
253

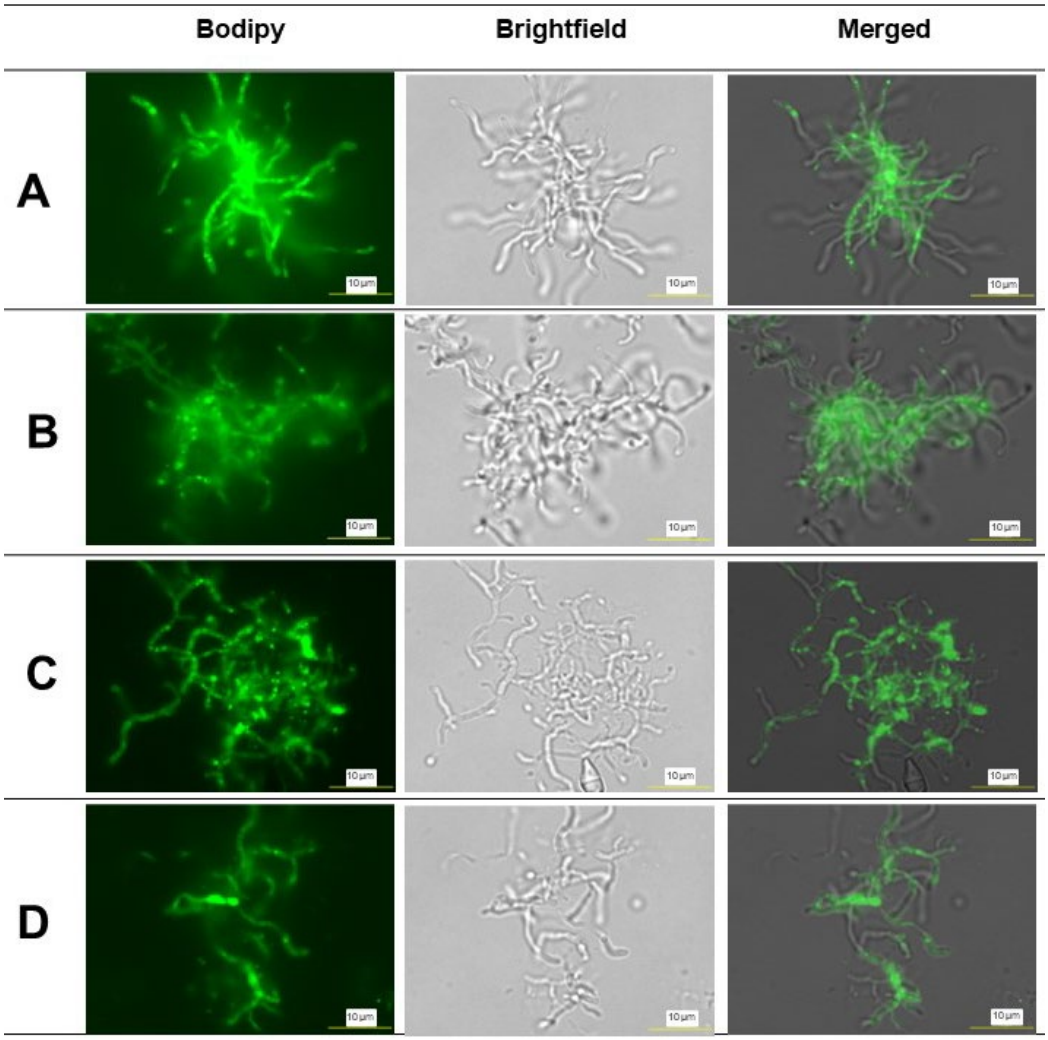

Figure 2.3 Observation of lipid accumulation in *S. jeddahensis*., culture process on 30°C. The displays images of both strains as observed through Bodipy staining, phase-contrast microscopy (Bright-field), and merged (bars, 10μm). (A) Culture in MSM medium with 2.5 g/L glucose, with the cropped and magnified area (red box) highlighting lipid accumulation (green) within the cells. (B) Culture in MSM medium with 2.5 g/L sodium hexanoate. (C) Culture in MSM medium with 2.5 g/L sodium octanoate. (D) Culture in MSM medium with 2.5 g/L sodium decanoate.

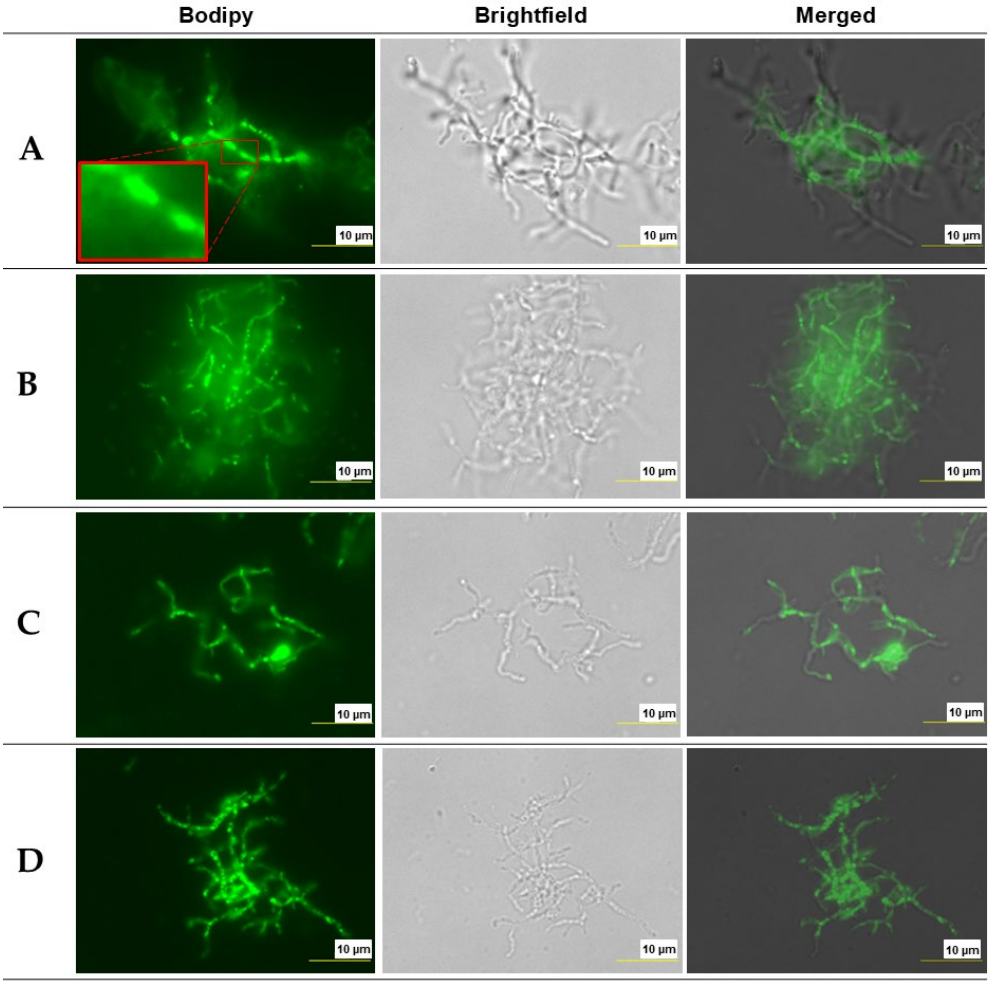

Figure 2.4 Observation of lipid accumulation in *S. jeddahensis.*, culture process on 37°C. The displays images of both strains as observed through Bodipy staining, phase-contrast microscopy (Bright-field), and merged (bars, 10µm). (A) Culture in MSM medium with 2.5 g/L glucose, with the cropped and magnified area (red box) highlighting lipid accumulation (green) within the cells. (B) Culture in MSM medium with 2.5 g/L sodium hexanoate. (C) Culture in MSM medium with 2.5 g/L sodium octanoate. (D) Culture in MSM medium with 2.5 g/L sodium decanoate.

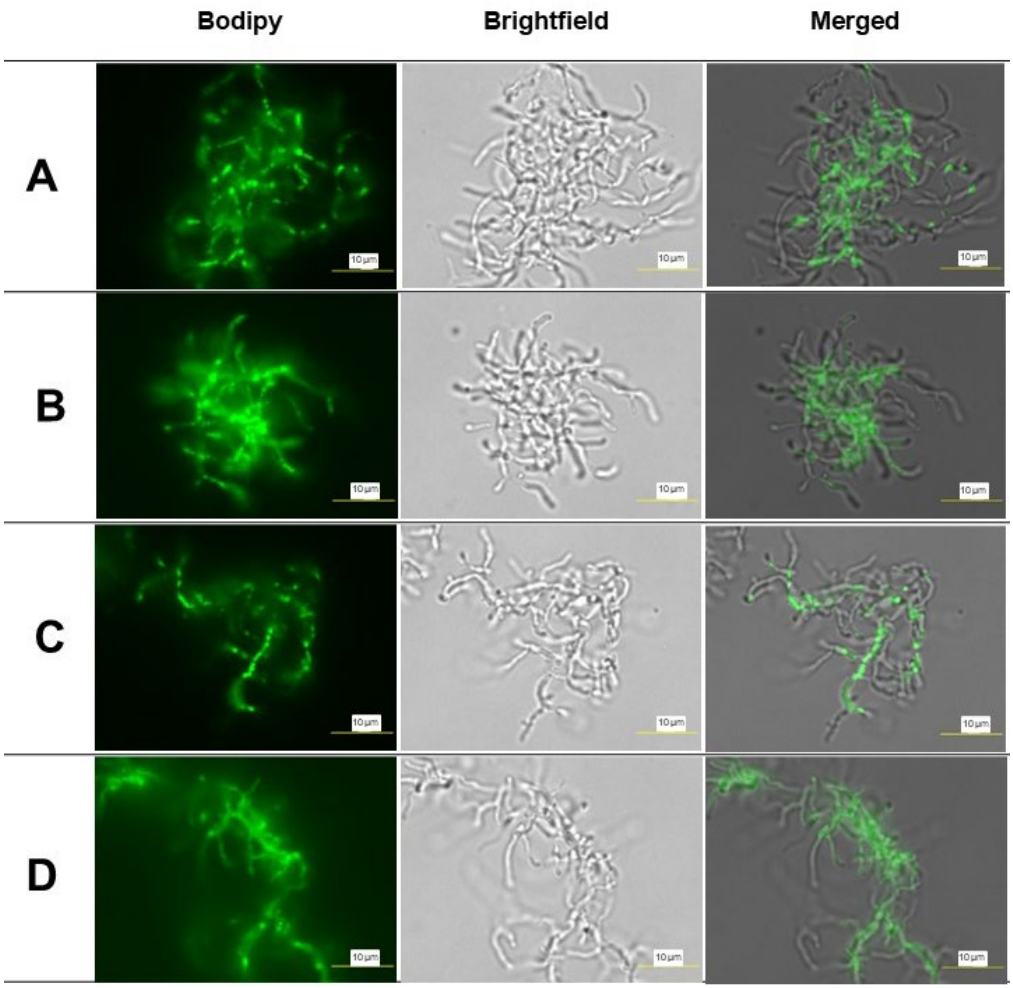

Figure 2.5 Observation of lipid accumulation in *S. jeddahensis.*, culture process on 40°C. The displays images of both strains as observed through Bodipy staining, phase-contrast microscopy (Bright-field), and merged (bars, 10μm). (A) Culture in MSM medium with 2.5 g/L glucose, with the cropped and magnified area (red box) highlighting lipid accumulation (green) within the cells. (B) Culture in MSM medium with 2.5 g/L sodium hexanoate. (C) Culture in MSM medium with 2.5 g/L sodium octanoate. (D) Culture in MSM medium with 2.5 g/L sodium decanoate.

Figure 2.6 presents the quantitative analysis of lipid content (% w/w) under different temperatures and carbon sources, showing that both factors significantly influence lipid accumulation in *S. jeddahensis*. At 30°C, lipid content was consistently lower across all carbon sources, with glucose yielding the highest accumulation. The optimal temperature for lipid production was 37°C, where

sodium octanoate resulted in the highest lipid content, followed by glucose and sodium hexanoate. At 45°C, lipid accumulation declined significantly across all carbon sources, demonstrating the adverse effect of higher temperatures on lipid biosynthesis. These findings highlight the critical roles of carbon source and incubation temperature in lipid production by *S. jeddahensis*.

The highest lipid yield observed at 37°C with sodium octanoate indicates that medium-chain fatty acids are efficiently utilized for lipid biosynthesis under these conditions. This is consistent with previous studies emphasizing the importance of carbon source selection and environmental optimization for lipid production in oleaginous microbes. For instance, Yang *et al*[46] reported that lipid synthesis in oleaginous microbes is strongly influenced by carbon source and cultivation conditions such as temperature and nutrient availability. Similarly, Koreti *et al*[47] highlighted that medium-chain fatty acids, like those used in this study, are particularly effective in enhancing lipid accumulation under optimized conditions. The higher lipid accumulation observed with sodium octanoate and sodium hexanoate may be attributed to the metabolic pathways involved in fatty acid conversion. Oleaginous bacteria, including *S. jeddahensis*, convert excess carbon into storage lipids such as triacylglycerols (TAGs), and the efficiency of this process depends on the chain length of the supplied fatty acids. In this study, Bodipy staining was used to visualize lipid droplets in cells, offering a reliable and specific method for lipid detection. As Patel et al[48] discussed Bodipy is highly specific and photostable, making it a valuable tool for assessing lipid accumulation

in microbial research. These results emphasize the importance of selecting the appropriate carbon source and optimizing environmental conditions to enhance lipid production in *S. jeddahensis*, which is crucial for applications in biotechnology and renewable energy production.

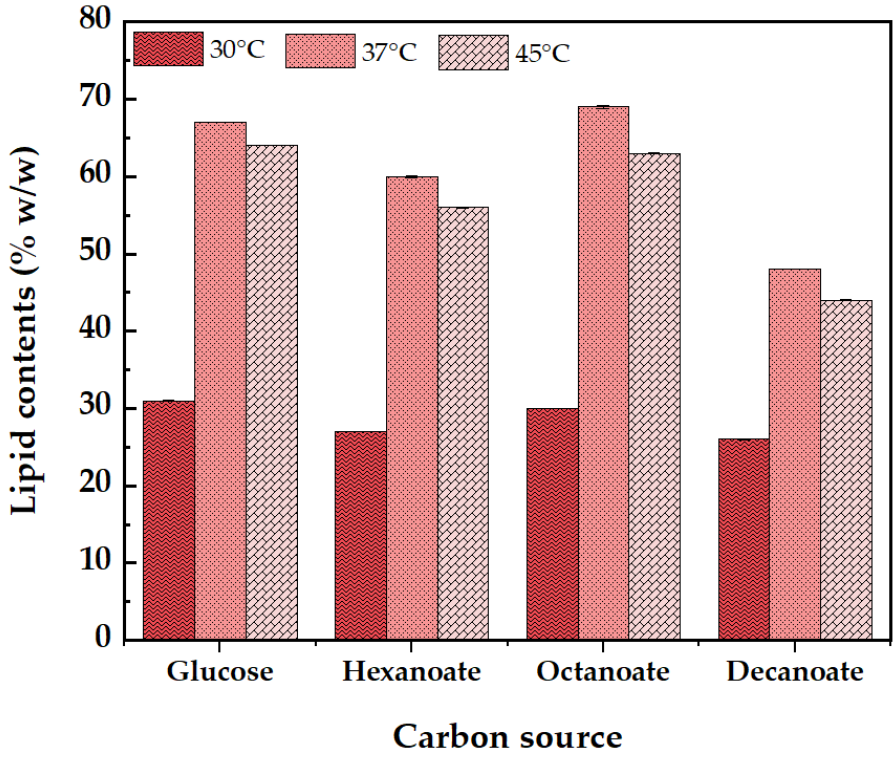

Figure 2.6 Bioconversion of various carbon sources into lipids by S. jeddahensis cultivated for 48 hours in MSM medium with different carbon sources at 30°C, 37°C, and 45°C. The lipid content (% w/w) is depicted as a bar graph showing the average value and standard deviation (n = 3).

II.3.3. Total fatty acid in *S. jeddahensis*

The total fatty acid (FA) composition of *S. jeddahensis* under varying carbon sources and incubation temperatures was investigated using a stacked bar chart (Figure 2.7). The study utilized glucose, sodium hexanoate, sodium octanoate, and sodium decanoate as carbon sources, with cultures incubated at 30 °C, 37°C, and 45°C. This analysis demonstrated the intricate relationship between

322 carbon source utilization and environmental conditions in modulating fatty acid
323 metabolism in *S. jeddahensis*. The observed shifts in fatty acid proportions across
324 conditions underscored the strain's remarkable metabolic flexibility, with
325 implications for its potential application in industrial biotechnology. The type of
326 carbon source strongly influenced fatty acid profiles. Cultures grown on glucose,
327 a simple carbon source, exhibited a relatively balanced distribution of fatty acids,
328 with C16:1 (cis-9) and 3-OH C14:0 predominating across all temperatures. This
329 suggests that glucose supports a generalist metabolic pathway, producing
330 medium- and long-chain fatty acids in stable proportions. Conversely, sodium
331 hexanoate promoted a notable increase in 2-OH C16:1 and C16:0, especially at
332 30°C. This trend indicates hexanoate's role as a direct substrate for elongation and
333 desaturation pathways, enhancing medium-chain fatty acid production. Similarly,
334 sodium octanoate increased the proportions of 2-OH C16:0 at 30°C and 37°C,
335 C16:1 (cis-9) dominating across all temperature, for C16:0 was noted at 45°C
336 highest compared the another temperature. The presence of octanoate appears to
337 promote the synthesis of longer-chain unsaturated fatty acids, suggesting its
338 involvement in elongating fatty acid chains. This effect likely occurs through
339 intermediates produced during β -oxidation, indicating that octanoate plays a key
340 role in the extension of fatty acid chains.
341 In contrast, sodium decanoate, a longer-chain fatty acid precursor,
342 induced distinct profiles, particularly an increase in C15:0 at across all
343 temperature. This suggests that decanoate facilitates the biosynthesis of

polyunsaturated fatty acids under high-temperature conditions, reflecting a possible stress adaptation mechanism. These results emphasize the strain's capability to metabolize diverse substrates into specific fatty acid profiles, a characteristic with promising industrial applications. Temperature also played a crucial role in shaping fatty acid composition. At 37°C, cultures exhibited a balanced distribution of saturated and unsaturated fatty acids, indicating optimized enzymatic activity for chain elongation and desaturation. For example, cultures grown on glucose and sodium octanoate produced higher levels of long-chain unsaturated fatty acids, such as C18:2 (all cis-9,12), reflecting heightened biosynthetic activity. In contrast, at 45°C, significant shifts were observed, particularly in cultures supplemented with sodium decanoate. At this temperature, polyunsaturated fatty acids such as C18:2 (all cis-9,12) were prominent, suggesting an adaptive response to thermal stress. Elevated temperatures likely enhance desaturase enzyme activity, introducing double bonds that increase membrane fluidity and maintain cellular integrity under heat stress. These findings align with prior studies that reported increased polyunsaturated fatty acid production in bacteria subjected to high temperatures.

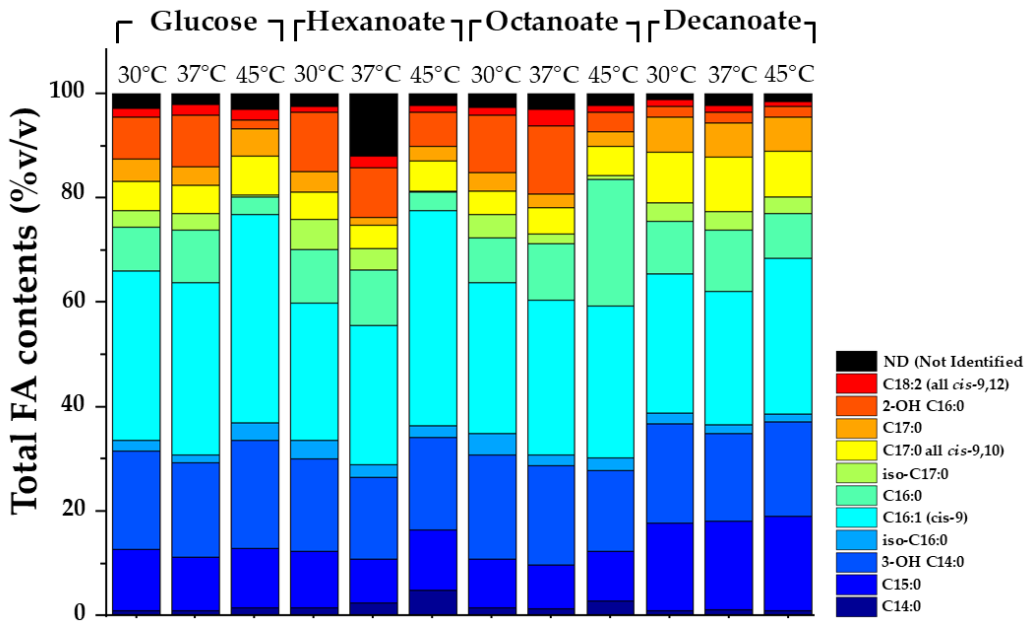

Figure 2.7 Total fatty acid (TFA) content of S. jeddahensis strains grown in minimal salt medium (MSM) supplemented with different carbon sources (2.5 g/L glucose, sodium hexanoate, sodium octanoate, or sodium decanoate) at varying temperatures (30°C, 37°C, and 45°C) for 48 hours. Experimental conditions included MSM + glucose (30°C, 37°C, 45°C), MSM + sodium hexanoate (30°C, 37°C), MSM + sodium octanoate (30°C, 37°C, 45°C), and MSM + sodium decanoate (30 °C, 37°C, 45°C). The results demonstrate the influence of carbon source and temperature on total fatty acid production under controlled growth conditions.

This study highlights the metabolic flexibility of *S. jeddahensis* and its potential for biotechnological applications. Tailoring fatty acid profiles by manipulating carbon sources and incubation temperatures could enable the production of specific fatty acids for industrial purposes. The results also revealed higher GC-MS peaks at 37°C and 45°C compared to 30°C, although these peaks could not be fully identified due to the absence of corresponding standards in the BAME reference (Figures 2.8–2.11). These findings align with and expand upon prior research, such as Gorte et al[49], which demonstrated the significant influence of carbon sources and temperature on microbial lipid profiles.

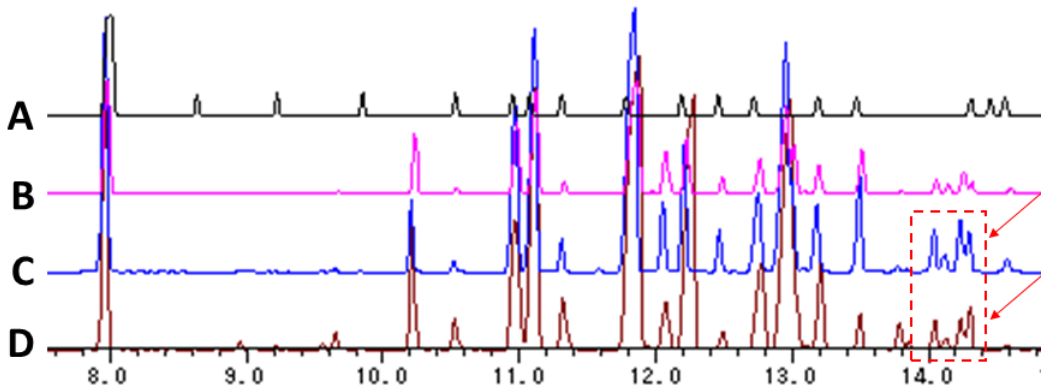

Figure 2.8 GC analysis detecting fatty acids from *S. jedahhensis* cultured in MSM glucose (2.5 g/L): (A) Standard BAME, (B) 30°C, (C) 37°C, (D) 45°C. The red arrows indicate that at 37°C and 45°C, there are higher peaks of fatty acids compared to 30°C.

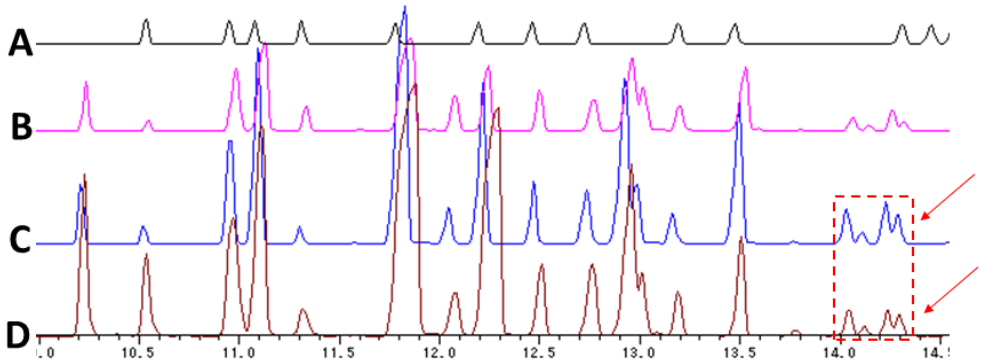

Figure 2.9 GC analysis detecting fatty acids from *S. jedahhensis* cultured in MSM sodium hexanoate (2.5 g/L): (A) Standard BAME, (B) 30°C, (C) 37°C, (D) 45°C. The red arrows indicate that at 37°C and 45°C, there are higher peaks of fatty acids compared to 30°C.

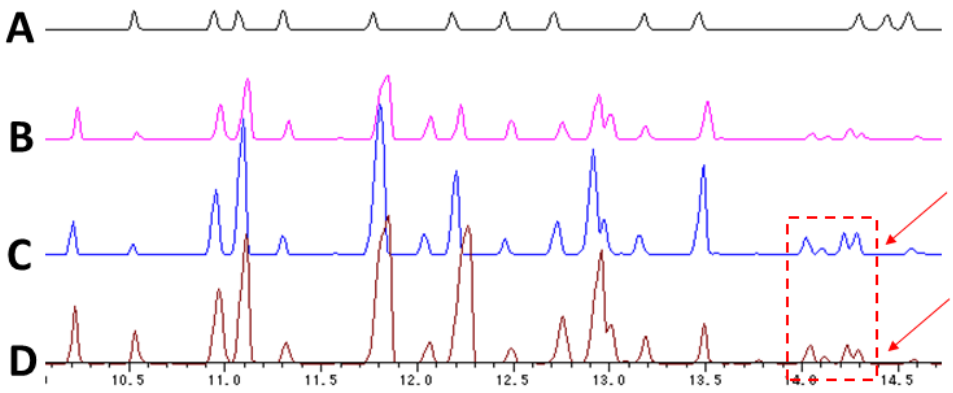

Figure 2.10 GC analysis detecting fatty acids from *S. jedahhensis* cultured in MSM sodium octanoate (2.5 g/L): (A) Standard BAME, (B) 30°C, (C) 37°C, (D) 45°C. The red arrows indicate that at 37°C and 45°C, there are higher peaks of fatty acids compared to 30°C.

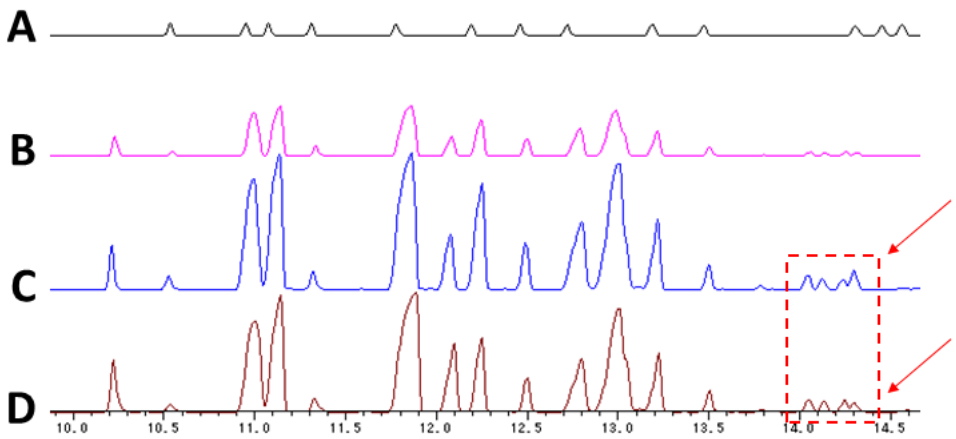

Figure 2.11 GC analysis detecting fatty acids from *S. jedahhensis* cultured in MSM sodium decanoate (2.5 g/L): (A) Standard BAME, (B) 30°C, (C) 37°C, (D) 45°C. The red arrows indicate that at 37°C and 45°C, there are higher peaks of fatty acids compared to 30°C.

II.3.4. Gene Expression Analysis

The Our findings indicate that sodium octanoate as a carbon source at 37 °C yielded the highest lipid content, although the cell dry weight (CDW) was greatest at 30°C. Interestingly, significant lipid accumulation was still observed at 45 °C, even though the CDW was relatively low (Figure 2.2). The observed phenomenon can be attributed to a combination of factors related to the strain's metabolic and physiological adaptations. Originating from desert soil, this strain may have developed the ability to store lipids as a survival mechanism, particularly under conditions of nutrient scarcity and high temperatures[24]. Its versatility in utilizing various carbon sources further facilitates lipid production across different growth environments. Moreover, the presence of key enzymes such as wax ester synthase/acyl-CoA:diacylglycerol acyltransferase [50], suggests a complex metabolic

pathway that supports lipid synthesis, even when exposed to stressful environmental.

Bacteria exhibit responses to temperature fluctuations by activating heat-shock proteins and other genes associated with stress when exposed to elevated temperatures[51]. To further investigate the molecular mechanisms behind lipid biosynthesis, we performed gene expression analysis at 37°C and 45°C using sodium octanoate. We focused on genes involved in lipid metabolism, with *rpoB* used as a housekeeping gene for normalization (Table 2.1). Our analysis revealed that genes crucial for lipid synthesis, such as *accD5_1* (acetyl-CoA carboxylase), *fabF*, and *fabG*, showed strong expression at higher temperatures.

The STRING analysis highlighted the significant role of *accD5_1*, emphasizing its position as a key regulator in fatty acid biosynthesis by catalyzing the first committed step in the pathway. The interactions between *fabF* and *fabG* further reinforce the prioritization of lipid production, with these genes playing essential roles in elongation and reduction during fatty acid synthesis[52]. Additionally, proteins involved in glycerolipid biosynthesis, such as *plsC* (1-acyl-sn-glycerol-3-phosphate acyltransferase) and *gpsA* (glycerol-3-phosphate dehydrogenase), were identified, further supporting the focus on lipid synthesis under varying environmental conditions. Peripheral interactions with plsC_1 indicate its involvement in the biosynthesis of glycerolipids and polyketides. More specifically, *plsC_1*, a bacterial 1-acyl-sn-glycerol-3-phosphate acyltransferase, facilitates the acylation of lysophosphatidic acid, resulting in the formation of

phosphatidic acid, which serves as a precursor for membrane glycerophospholipids[53]. The bacterium's dependence on lipid biosynthesis during heat stress is consistent with findings in other oleaginous microorganisms, where lipid accumulation serves as a protective strategy. Regulatory proteins such as *pucR* were also identified, suggesting they may play a role in modulating stress responses, including the regulation of heat shock proteins under elevated temperatures[54].

Regulatory proteins, such as *pucR*, were also observed, pointing to their potential involvement in modulating stress responses. Similar regulatory elements have been shown to control heat shock protein expression under thermal stress in other bacterial species. These results indicate that *S. jeddahensis* adapts to higher temperatures by upregulating lipid biosynthesis pathways, with acyl carrier proteins being crucial in this process. Gaining insight into these mechanisms provides a basis for exploring heat-induced metabolic pathways and their potential industrial applications, including biofuel production[46].

The RNA-Seq analysis compared the transcriptomes of *S. jeddahensis* at 37ºC and 45ºC using DESeq2, shedding light on temperature-dependent gene expression patterns that are crucial for understanding the bacterium's metabolic adaptations under varying thermal conditions. The differential gene expression was visualized using volcano plots, bar charts, and heatmaps, offering a comprehensive overview of the data. The volcano plot (Figure 2.13A) indicates that most genes have moderate log2 fold changes (FC) and low statistical

significance. However, a subset of genes show large log2 FC values and high statistical significance (p-value < 0.05), suggesting that they may play a key role as metabolic regulators under specific temperature conditions. Genes at the extremes of the plot are likely involved in medium-chain fatty acid metabolism. Overall, only a small number of genes exhibit significant differential expression. Genes with high |log2 FC| (far left or right) and significant -log10(p-value) are notably upregulated or downregulated. The bar chart (Figure 2.13B) visualizes the differential expression, with upregulated genes (marked in red), such as STSP_67970 (*fabD*) and STSP_03080 (*DGAT*), and downregulated genes (marked in blue), like STSP_12530. This suggests that *S. jeddahensis* undergoes substantial metabolic and regulatory adjustments in response to varying temperatures. The upregulated genes are likely involved in carbon metabolism, heat stress response, or biosynthesis, aligning with typical stress responses triggered by altered carbon sources and elevated temperatures. On the other hand, the downregulated genes may indicate the suppression of certain pathways, such as glucose metabolism, in favor of utilizing fatty acids[55]. For example, a study by Bucca *et al*[56] on *S. coelicolor* under heat stress identified similar upregulation of genes involved in heat shock protein metabolism, highlighting conserved stress responses across *Streptomyces* species and providing further insights into their adaptive mechanisms. The heatmap (Figure 2.13C) reveals clear gene clusters with higher expression levels at 45°C compared to 37°C. For example, genes like STSP_12530, STSP_01010 (*fabG1_1*), and STSP_19060 (*gpsA*) show elevated

478 expression at 45°C. These genes are likely linked to essential metabolic processes,
479 including fatty acid biosynthesis and stress responses. Notably, STSP_28660
480 (*accD5_1*), associated with acetyl-CoA carboxylase activity, also showed a
481 significant increase in expression, suggesting that higher temperatures might
482 promote lipid metabolism, potentially to compensate for changes in membrane
483 fluidity at elevated temperatures.
484
485

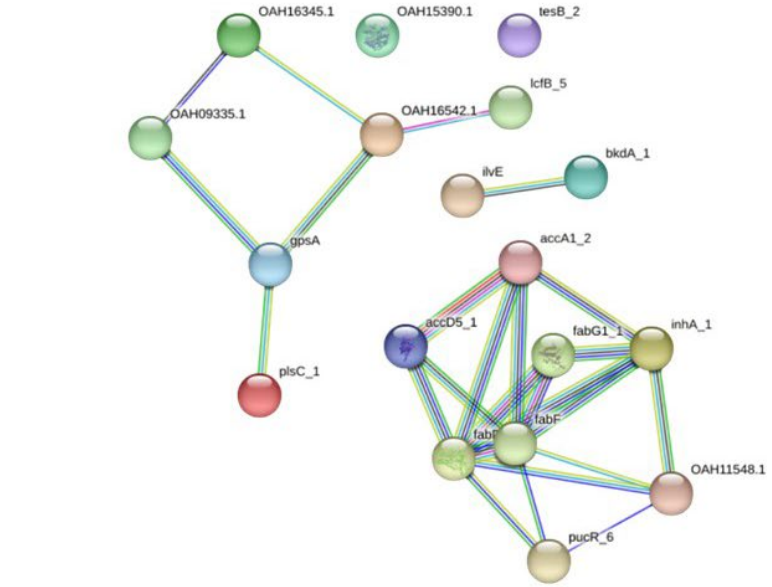

plsC_1	*1-acyl-sn-glycerol-3-phosphate acyltransferase*
OAH16542.1/ STSP_00850	*PAP2 superfamily protein*
inhA_1	*Enoyl-[acyl-carrier-protein]reductase [NADH]*
fabG1_1	*3-oxoacyl-[acyl-carrier-protein] reductase FabG1; Catalyzes the NADPH-depent reduction of beta-ketoacyl-ACP substrates to beta-hydroxyacyl-ACP products, the first reductive step in the elongation cycle of fatty acid biosynthesis. Belongs to the short-chain dehydrogenase/ reductases (SDR) family*
OAH16345.1/ STSP_03080	*Putative diacylglycerol O-acyltransferase; Belongs to the long-chain O-acyltransferase family*
OAH15390.1/ STSP_12530	*Bifunctional beta-D-glucosidase/beta-D-fucosidase*
bkdA_1	*3-methyl-2-oxobutanoate dehydrogenase subunit alpha*
gpsA	*Glycerol-3-phosphate dehydrogenase [NAD(P)+]; Belongs to the NAD-dependent glycerol-3- phosphate dehydrogenase family*
accD5_1	*Putative propionyl-CoA carboxylase beta chain 5*
tesB_2	*Acyl-Coa thioesterase 2*
accA1_2	*Acetyl-/propionyl-coenzyme A carboxylase alpha chain*
OAH11548.1 /STSP_50580	*Bifunctional enoyl-CoA hydratase/ phosphate acetyltransferase*
ilvE	*Branched-chain-amino-acid aminotransferase*
pucR_6	*Purine catabolism regulatory protein*
fabD	*Malonyl CoA-acyl carrier protein transacylase*
fabF	*3-oxoacyl-[acyl-carrier-protein] synthase 2; Catalyzes the condensation reaction of fatty acid synthesis by the addition to an acyl acceptor of two carbons from malonyl-ACP*
lcfB_5	*Long-chain-fatty-acid-CoA ligase*
OAH09335.1 /STSP_74190	*2-acyl-glycerophospho-ethanolamine acyltransferase*

Figure 2.12 The STRING interaction network of the analyzed genes, where each filled node represents a gene, and the edges between nodes indicate interactions between the corresponding protein products. The edges are color-coded to reflect the types of evidence supporting these interactions, while the genes are color-coded according to their names and functional categories.

492 At 45 ° C, several genes showed decreased expression, including
493 STSP_45150 (*accA2_1*) and STSP_45110 (*tesB_2*), suggesting that these genes
494 are involved in alternative metabolic pathways that may be downregulated in favor
495 of others more suitable for heat stress adaptation. The clustering of gene
496 expression patterns supports the idea that gene functions are temperature-
497 dependent, reflecting a shift in the metabolic network of *S. jeddahensis* in
498 response to environmental conditions. These findings confirm that temperature
499 plays a crucial role in modulating secondary metabolism in *Streptomyces.* High
500 temperatures likely trigger stress-response mechanisms that enhance the
501 production of secondary metabolites, which are vital for the organism's survival
502 under unfavorable conditions. Additionally, sodium octanoate as a carbon source
503 seems to further intensify these effects, particularly by activating pathways related
504 to lipid metabolism and energy production. This observation is consistent with
505 previous studies showing the influence of both carbon sources and temperature
506 on *Streptomyces* metabolism.
507

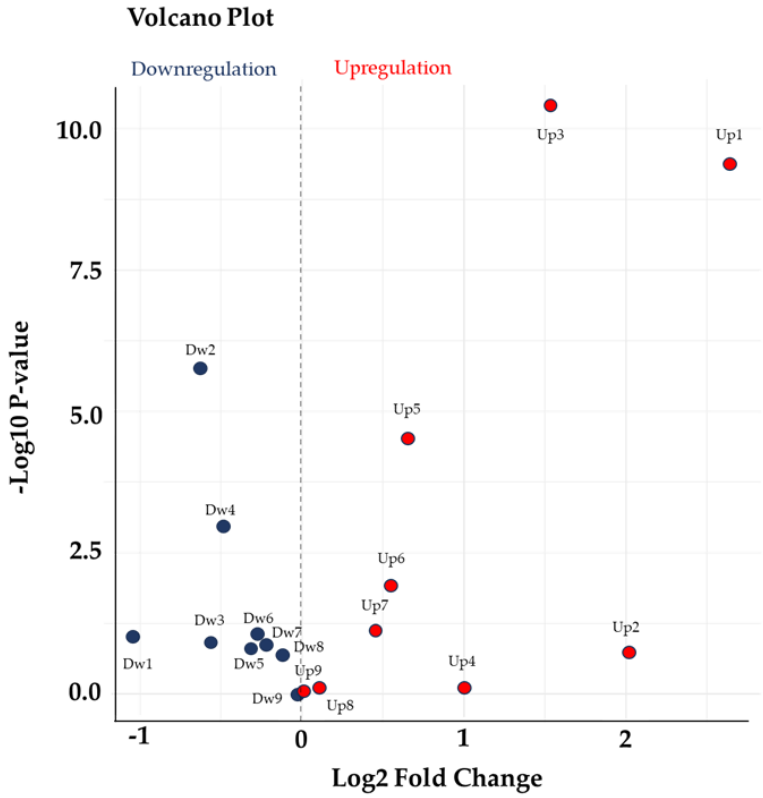
Volcano Plot
Downregulation
Upregulation
10.0
7.5
5.0
2.5
0.0
-Log10 P-value
-1
0
1
2
Log2 Fold Change
Up3
Up1
Dw2
Up5
Dw4
Up6
Up7
Up2
Dw3
Dw6
Dw7
Dw8
Dw1
Dw5
Up9
Up4
Dw9
Up8

(A)

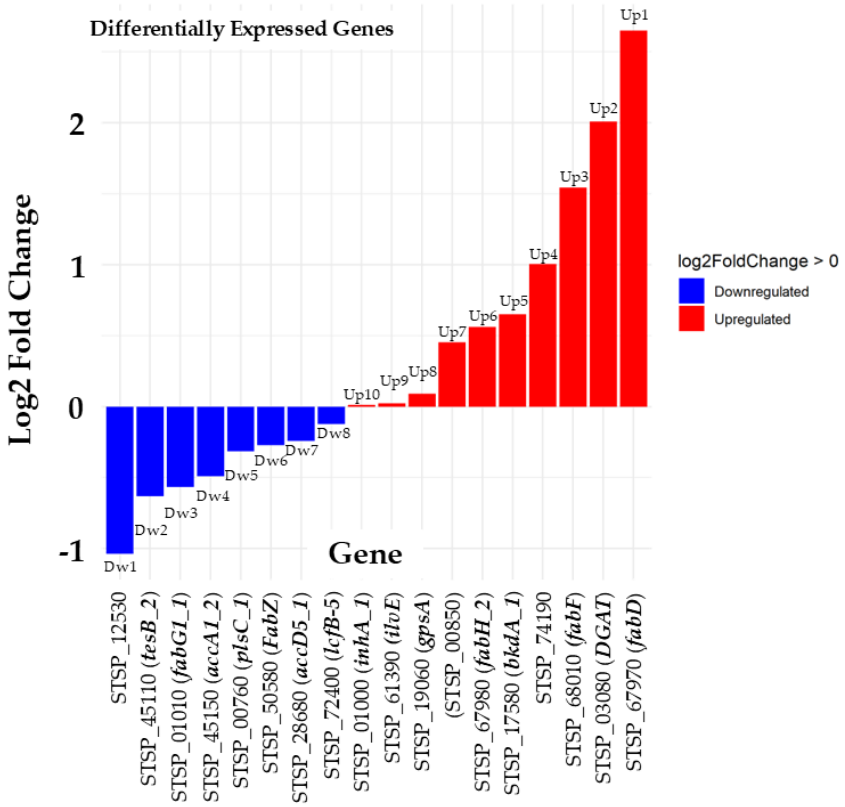
Differentially Expressed Genes
Log2 Fold Change
2
1
0
-1
Gene
log2FoldChange > 0
Downregulated
Upregulated
Up1
Up2
Up3
Up4
Up5
Up6
Up7
Up8
Up9
Up10
Dw1
Dw2
Dw3
Dw4
Dw5
Dw6
Dw7
Dw8
STSP_12530
STSP_45110 (tesB_2)
STSP_01010 (fabG1_1)
STSP_45150 (accA1_2)
STSP_00760 (plsC_1)
STSP_50580 (FabZ)
STSP_28680 (accD5_1)
STSP_72400 (lcfB-5)
STSP_01000 (inhA_1)
STSP_61390 (ilvE)
STSP_19060 (gpsA)
(STSP_00850)
STSP_67980 (fabH_2)
STSP_17580 (bkdA_1)
STSP_74190
STSP_68010 (fabF)
STSP_03080 (DGAT)
STSP_67970 (fabD)

(B)

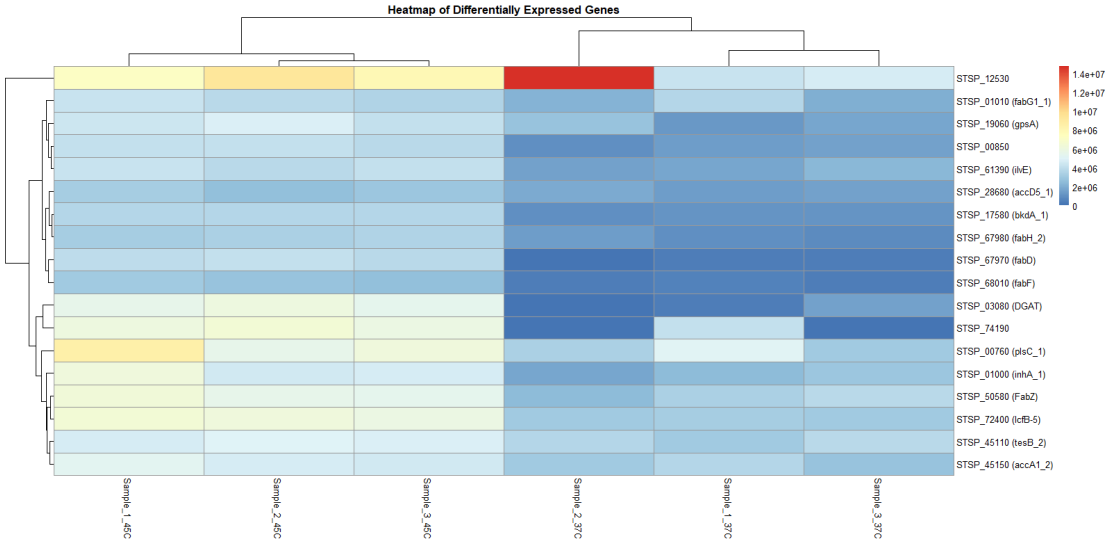

(C)

Figure 2.13 Visualization of Differential Gene Expression Using DESeq2. (A) Volcano plot illustrating gene expression differences between 37°C and 45°C, with significant genes (log2FC > 1 or < -1, $p < 0.05$) represented as dots. (B) Bar chart showing log2 fold changes for selected genes, with upregulated genes depicted in red and downregulated genes in blue. (C) Heatmap depicting gene expression patterns across conditions, with genes such as STSP_68000 and STSP_67970 clustered based on their temperature responsiveness. Red indicates high expression, while blue represents low expression.

Gene expression analysis revealed upregulation of STSP_03080 (*DGAT*), a key gene in triacylglycerol biosynthesis, suggesting the potential accumulation of storage lipids at 45°C. This mechanism could serve as an energy reserve to help the organism withstand thermal stress. Furthermore, STSP_61390 (*ilvE*), a gene involved in branched-chain amino acid metabolism, was also upregulated, indicating an increased need for amino acid precursors. This could be essential for maintaining protein stability and function under heat stress. Similar temperature-induced gene expression changes have been reported in other bacterial species. For example, in Escherichia coli, heat shock proteins are regulated by RNA thermometers, which are RNA sequences in the 5'-UTR of

genes. These thermometers act as thermosensors that control gene expression at the post-transcriptional level in response to temperature fluctuations[57]. Overall, the results underscore the adaptive responses of *S. jeddahensis* to high temperatures, involving modifications in metabolic pathways and the synthesis of compounds critical for stress tolerance and cellular integrity.

In addition to *acpP*, several other genes were found to be responsive to temperature changes. Among the genes that were upregulated, STSP_68010 (*fabF*), which encodes 3-Ketoacyl-ACP Synthase II, STSP_67970 (*fabD*), a transcriptional activator of the fatty acid biosynthesis operon, STSP_74190, encoding 1-Acylglycerol-3-Phosphate Acyltransferase (*AGPAT*), and STSP_03080, encoding Diacylglycerol Acyltransferase (*DGAT*) were identified. DGAT is a CoA-dependent acyltransferase enzyme essential for the synthesis of triacylglycerols (TAGs) in bacteria. Interestingly, *DGAT* shows dual functionality, acting both as an acyl-CoA:fatty alcohol acyltransferase (wax ester synthase, WS) and a diacylglycerol acyltransferase (*DGAT*). This dual activity allows DGAT to utilize a wide array of acyl-CoA substrates to synthesize either TAGs or wax esters (WEs) [58,59]. In contrast, some genes, such as STSP_12530, were downregulated in response to temperature fluctuations. The STSP_12530 gene encodes β-Glucosidase, an enzyme crucial for bacterial metabolism, particularly in the breakdown of complex carbohydrates. β-Glucosidase hydrolyzes β-glycosidic bonds in compounds like cellobiose, a degradation product of cellulose, as well as other oligosaccharides, converting them into glucose [60,61].

548 Lipid biosynthesis in bacteria is intricately connected to key metabolic
549 intermediates such as pyruvate, acetyl-CoA, and glycerol-3-phosphate. Pyruvate,
550 the end product of glycolysis, plays a pivotal role in carbon flux regulation within
551 central metabolism. It can serve as a precursor for sugar phosphate synthesis
552 through gluconeogenesis or be utilized to replenish intermediates in the
553 tricarboxylic acid (TCA) cycle via anaplerotic reactions, thereby supporting
554 anabolic processes. Together, these findings underscore the metabolic
555 adaptability of bacteria, enabling them to optimize lipid production under diverse
556 environmental conditions.
557 This research indicates that *S. jeddahensis* has potential for biodiesel production
558 due to its ability to accumulate significant amounts of lipids, especially when
559 cultured with medium-chain fatty acids under optimal temperature conditions.
560

561 ## III.4. CONCLUSION

562 This study demonstrates that *Streptomyces jeddahensis* is a promising
563 microorganism for lipid production, especially when cultured with medium-chain
564 fatty acids under optimized conditions. Sodium octanoate was identified as the
565 most effective substrate for lipid accumulation, with 37°C being the optimal
566 temperature for growth and biosynthesis. Although higher temperatures led to
567 reduced biomass, lipid production remained substantial due to stress-induced
568 metabolic adaptations. The upregulation of key lipid biosynthesis genes, including
569 STSP_03080 (*DGAT*) and STSP_67970 (*fabD*), highlights the bacterium's

potential for industrial biofuel applications. These results position *S. jeddahensis* as a strong candidate for renewable energy production, with further potential for optimization through genetic engineering and process development to enhance scalability. Future research should focus on evaluating alternative, cost-effective carbon sources, such as waste oils, molasses, and agricultural residues, to assess their impact on both biomass growth and lipid accumulation. Additionally, exploring mixed-carbon media could offer a more sustainable pathway for large-scale lipid production, providing opportunities for further optimization and industrial scalability

CHAPTER III

Development of *Streptomyces jeddahensis* as a Novel Host for Polyhydroxyalkanoate Production Using Sodium Octanoate Medium

III.1. Introduction

Polyhydroxyalkanoates (PHAs) represent a promising group of biodegradable polymers that could serve as an eco-friendly alternative to traditional plastics, offering a potential solution to the pressing issue of plastic pollution. These polymers are synthesized by a variety of microorganisms as a means of storing carbon and energy within their cells, particularly when nutrients are scarce but carbon source are plentiful. Moreover, many microorganisms produce PHAs under stress conditions, using them as a strategy for conserving carbon and energy[62,63]. A well-known medium-chain-length (mcl)-PHA is composed of various hydroxyalkanoate monomers and is recognized for its softness and elasticity. In contrast to short-chain-length (scl)-PHAs, which are typically brittle and stiff, mcl-PHAs such as P(HHx-co-3HO) demonstrate lower crystallinity, a reduced glass transition temperature, decreased tensile strength, and a higher elongation-to-break ratio. These properties make P(3HHx-co-3HO) highly suitable for a range of applications, including osteosynthesis materials, surgical sutures, stents, tissue engineering scaffolds, and drug delivery systems[64,65]. In the case of gram-negative bacteria like *Pseudomonas oleovorans* (*P. oleovorans*) selecting the appropriate carbon source is crucial. The production of P(3HHx-co-3HO) by *P. oleovorans* is achieved when the organism is cultivated

614 with sodium octanoate as the carbon source[66]. Choosing the appropriate carbon
615 source is crucial in the production of polyhydroxyalkanoates (PHAs). Typically,
616 PHAs are produced on a large scale by gram-negative bacteria. However, gram-
617 positive bacteria are preferred as hosts for PHA production in medical
618 applications because they lack the outer membrane lipopolysaccharide (LPS),
619 which is known to provoke strong immunogenic reactions[67]. *Streptomyces* species,
620 which are gram-positive bacteria, are renowned for their ability to produce a wide
621 [68]range of primary and secondary metabolites. Additionally, they are known to
622 accumulate polyhydroxyalkanoate (PHAs)[13,16]. This bacterial group has potential
623 as a source producing polyhydroxyalkanoates (PHA) with advantageous
624 properties. Through genetic engineering, *Streptomyces coelicolor* A3 has been
625 identified as a promising candidate for development into a novel PHA-producing
626 organism[13].

627 In the biosynthesis of polyhydroxyalkanoates (PHAs), PhaC enzymes are
628 essential, as they catalyze the conversion of β-hydroxyalkanoyl-CoA monomers
629 into poly-β-hydroxyalkanoate chains[68]. The classification of bacterial PHA
630 synthases depends on the carbon chain length of the substrates they process.
631 Specifically, the first two classes of phaC primarily utilize monomers containing
632 three to five carbons, whereas subunits within Class III enzymes show a preference
633 for monomers with five carbon atoms[69]. Recently, a distinct phaC enzyme from
634 the Pseudomonas genus has been identified, which can polymerize monomers
635 with four or five carbons[70]. Notable examples of these monomers include 3-

hydroxybutyrate (3HB) and 3-hydroxyvalerate (3HV), often derived from the breakdown of fatty acids via β -oxidation[71]. Oleaginous actinomycetes, known for their capability to utilize fatty acids as feedstocks, may serve as hosts for PHA synthesis. These actinomycetes exhibit a balanced metabolic state, alternating between synthesizing fatty acids from carbon sources and degrading them from triacylglyceride lipid reserves[72].

This study highlights *Streptomyces jeddahensis* as a promising new host for polyhydroxyalkanoate (PHA) production due to its exceptional lipid accumulation capacity, which can comprise up to 64% of its dry cell weight- a characteristic rarely found in other actinobacteria. Additionally, *S. jeddahensis* exhibits thermotolerance, thriving at temperature exceeding 50°C. This trait offers potential advantages for industrial applications, as it may improve process stability and lower the risk of contamination[12,24,50]. To leverage its natural lipid synthesis ability, this study integrates a PHA biosynthesis gene cluster (*phbA*, *phbB*, *phaC1*, *phaG*, and *phaC2*) into the *S. jeddahensis* genome, aiming to enable efficient PHA synthesis. By utilizing sodium octanoate as the primary carbon source, the research promotes diverse monomer incorporation, enabling the production of complex copolymers with promising industrial and medical applications. While the introduction of PHA biosynthesis genes facilitates polymer production, lipid accumulation remains a significant bottleneck. Lipid biosynthesis, particularly the formation of triacylglycerol (TAG), diverts metabolic resources away from PHA synthesis. Diacylglycerol O-acyltransferase

(*DGAT*) is a critical enzyme in the TAG biosynthesis pathway, catalyzing the final step of TAG formation. Therefore, disrupting the DGAT pathway offers a promising strategy to reduce lipid accumulation and increase carbon flux toward PHA biosynthesis. In this study, the CRISPR-Cpf1 system was employed to knock out the DGAT-encoding gene in this strain. The FnCpf1 system, a highly efficient and precise tool for genome editing, was selected due to its non-toxic nature in actinobacteria, a bacterial phylum with high GC content[73]. Unlike SpCas9, which relies on NGG PAM sequences, FnCpf1 utilizes TTTN PAM sequences and demonstrates the capability to create targeted double-stranded breaks, resulting in effective gene disruption. The overarching goal of this research is to investigate the dual impact of introducing PHA biosynthesis genes and disrupting lipid biosynthesis pathways on the production of PHAs in Streptomyces. By leveraging a combination of metabolic engineering and advanced genome editing techniques, this study aims to establish a robust microbial platform for efficient PHA production. The findings of this research are expected to contribute to the development of cost-effective and sustainable bioplastic production processes, addressing the growing demand for environmentally friendly materials and reducing reliance on fossil-based plastics.

III.2. Materials and Methods

III.2.1 Medium, bacterial strains and maintenance

All reagents were purchased from Sigma-Aldrich and Nacalai Tesque, Inc. (Kyoto, Japan). The oleaginous microorganism used in the experiments was *Streptomyces jeddahensis* DSM 101878 sourced from the Leibniz Institute DSMZ-German Collection of Microorganisms and Cell Cultures. To maintain and culture the *Streptomyces* strain used Tryptic Soy Broth (TSB) medium containing: 17 g/L peptone from casein, 3 g/L peptone from soymeal, 2.5 g/L D(+)-glucose, 5 g/L NaCl, 2.5 g/L K_2HPO_4 (20 gr/L agar). To produce polyhydroxyalkanoate (PHA), modified TSB medium (TSB0.5 medium) containing: 8.5 g/L Peptone from casein, 1.5 g/L peptone from soymeal, 1.25 g/L D(+)-glucose, 2.5 g/L NaCl, 1.75 g/L K_2HPO_4, supplemented with sodium octanoate 2.5 g/L, and Medium Salts Medium (MSM) containing: 0.25 g/L urea, 0.16 g/L yeast extract, 0.02 g/L $CaCl_2$, 1.52 g/L KH_2PO_4, 0.52 g/L $MgSO_4.7H_2O$, 4 g/L Na_2HPO_4 supplemented with sodium octanoate at 2.5 g/L, were used.

III.2.2 Plasmid construction

III.2.2.1 Plasmid 3TYM-ABCGC for polymer production

Table 3.1 details the plasmid utilized throughout this study, while Table 4.2 summarizes the primers employed. Polymerase chain reactions (PCR) were conducted using the KOD One PCR Master Mix (Toyobo Co. Ltd., Osaka, Japan), according to the manufacturer's protocols. The following three-step procedure was employed to construct the plasmid expression vector 3TYM-ABCGC, as described in Figure 3.1 Firstly, Firstly, 3TYM-ermE was constructed as follows:

initially, the ermE promoter gene fragment was amplified by polymerase chain reaction (PCR) using 22AANWMF-bglII-sjphaCGC-pMA as a template, and primer pairs IB and HW. The resulting PCR product was cloned into HindIII site of plasmid pTYM3a using In-Fusion HD Cloning Kit (TakaraBio Inc., Shiga, Japan). Secondly, 3TYM-ermEAB was constructed as follows: genes *phbA* and *phbB* were amplified by direct PCR from *Cupriavidus necator* DSM428 using the primer pairs I.C and I.D. This PCR product was then inserted into XbaI site of the previously constructed 3TYM-ermEp, utilizing the In-Fusion HD Cloning Kit (TakaraBio Inc.).

Table 3.1 Strains and plasmids used in this study.

Type	Strain	Description	Source
E. coli	Nova Blue	For routine plasmid maintenance (*endA1 hsdR17* (r_{K12}^{-} m_{K12}^{+}) *supE44 thi-1 recA1 gyrA96 relA1 lac* F′[*proA*$^{+}$*B*$^{+}$ *lacI*^{q}*ZΔM15*::Tn*10*] (Tet^{R}))	Novagen
	HST04	For cloning ((F^{-}, *ara*, Δ(*lacproAB*) [Φ80d*lacZ*ΔM15], *rpsL*(*str*), *thi*, Δ(*mrr-hsdRMS-mcrBC*), Δ*mcrA*, *dam*, *dcm*))	Takara
	JM109/pUB 307	For conjugation plasmid into *Streptomyces* (*endA1 recA1 gyrA96 thi-1 hsdR17* (r_{K}^{-}, m_{K}^{+}) *relA1 supE44* Δ(*lac-proAB*) / F' [*traD36 proA*$^{+}$*B*$^{+}$ *lacI*^{q} *lacZ*ΔM15])	Takara

Cupriavidus necator	DSM428	Wild type strain, source for *phaC*, *phbA*, *phbB* genes	Leibniz Institute DSMZ
Streptomyces jeddahensis	DSM 101878	Wild type strain	Leibniz Institute DSMZ
Plasmids	22AANWMF-bglII-sjphaCGC-pMA	- Sources for *Pseudomonas putida phaC1*, *phaG*, *phaC2*, *phaD* genes, codon optimized for *S. jeddahensis* - Source for ermE promoter (optimized for gene expression in *Streptomyces* species)	This study
	pTYM3a	Cloning vector, Apr^r	This study
	pTYCGCD	pTYM3a derivative ermE promoter, phaC1-phaG-phaC2-phaD gen	This study
	3TYM-ermE	pTYM3a derivative, ermE promoter	This study
	3TYM-ermEAB	3TYM-ermE derivative, phbA and phbB from *Cupriavidus necator* DSM428	This study
	3TYM-ABCGC	3TYM-ermEAB derivative, phaC1-phaG-phaC1	This study
	pJYS3_ΔcrtYf	$pBL1^{ts}$ $oriV_{C.\ glutamicum}$ Kn^r pSC101 $oriV_{E.\ coli}$ PlacM-FnCpf1, Pj23119-crRNA targeting *crtYf*, 1-kb upstream and downstream homologous arms flanking 705-bp deletion fragment inside *crtYf*	[73] (Addgene: 85542)
	pJY-cpf1_Δ*DGAT*	Derived from pJYS3_ΔcrtYf; 1.6-kb upstream and downstream homologous region flanking 1.3-kb deletion from *DGAT*	

711 Thirdly, 3TYM-ABCGC was finally constructed as follows: the genes *phaC1-*
712 *phaG-phaC2* were amplified by PCR using the same template as in the first step,
713 22AANWMF-bglII-sjphaCGC-pMA, with the primer pairs IE and IF. The
714 amplified fragment was introduced into EcoRI site of 3TYM-ermEAB, completing
715 the construction of the plasmid 3TYM-ABCGC, by using the In-Fusion HD
716 Cloning Kit (TakaraBio Inc.). These three steps facilitated the successful
717 assembly of the plasmid 3TYM-ABCGC, incorporating multiple gene sequences
718 under the control of the term promoter for enhanced expression of *phbA*, *phbB*,
719 *phaC1*, *phaG* and *phaC2*, important gene sets for PHA production.

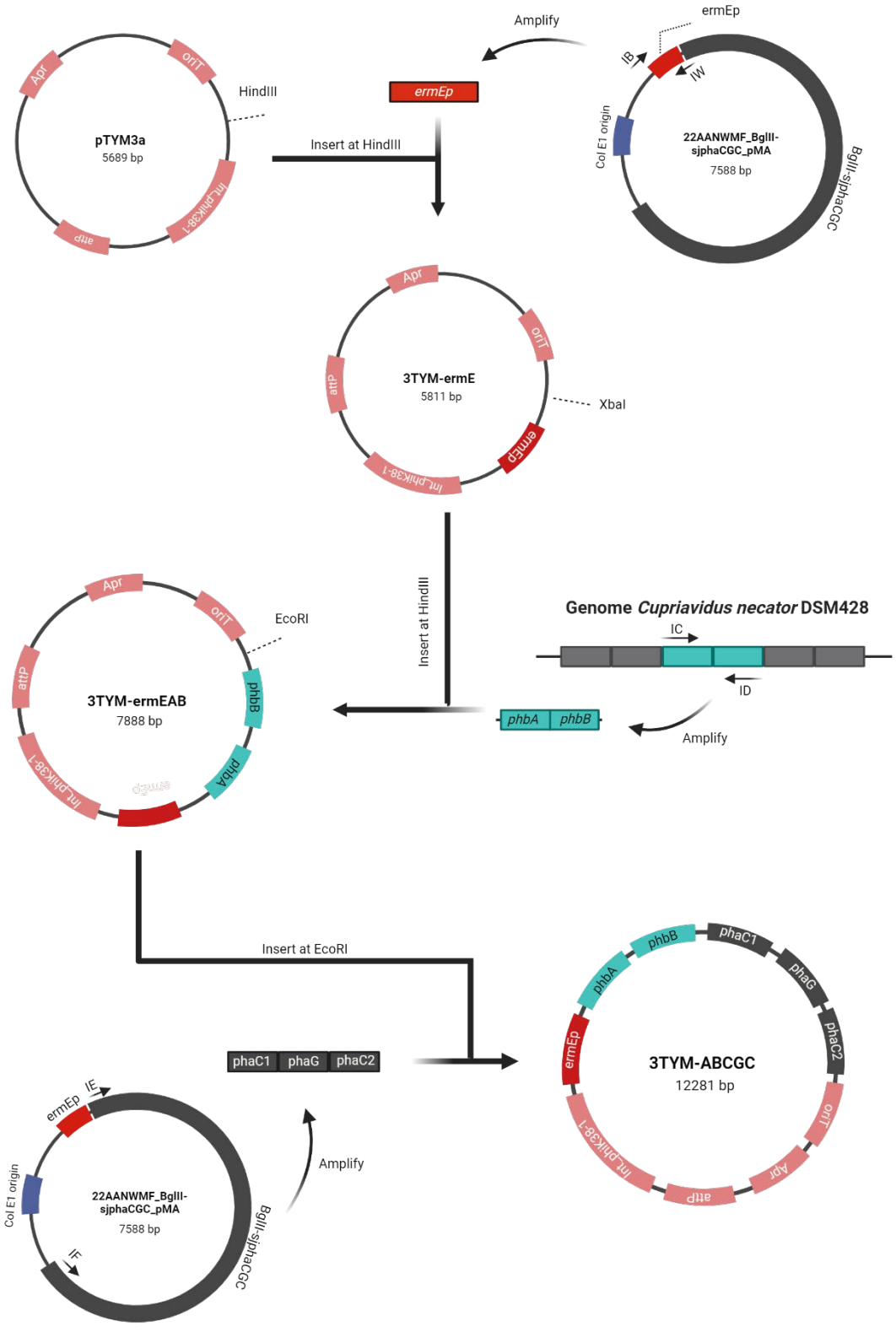

720

721 **Figure 3.1** The Illustration of the construction and restriction maps for plasmids 3TYM-ermE,
722 3TYM-ermEAB, and 3TYM-ABCGC.

723

III.2.2.2 Plasmid pJY-cpf1_Δ*DGAT* for knock out DGAT

To construct the pJY-cpf1_Δ*DGAT* plasmid, we modified the homologous arms of pJYS3_Δ*crtYf* as described in Figure 3.2. The pJYS3_Δ*crtYf* plasmid was linearized using PCR with primers I.N and I.O, resulting in the pJYS3 fragment without the *crtYf* homologous arms. Using *S. jeddahensis* genomic DNA as a template, we amplified a 1.6 kb upstream homologous arm (left arm) with primers I.P and I.Q. The PCR product was gel-extracted and used as a template to generate an overlap upstream part (left arm) with primers I.R and I.S. Similarly, a 1.3 kb downstream homologous arm (right arm) was amplified from *S. jeddahensis* genomic DNA using primers I.T and I.U. This PCR product was also gel-extracted and used as a template to create an overlap downstream part (right arm) with primers I.V and I.W. The two homologous arm fragments and the linearized pJYS3 fragment were then assembled using the In-Fusion HD Cloning Kit (TakaraBio Inc.).

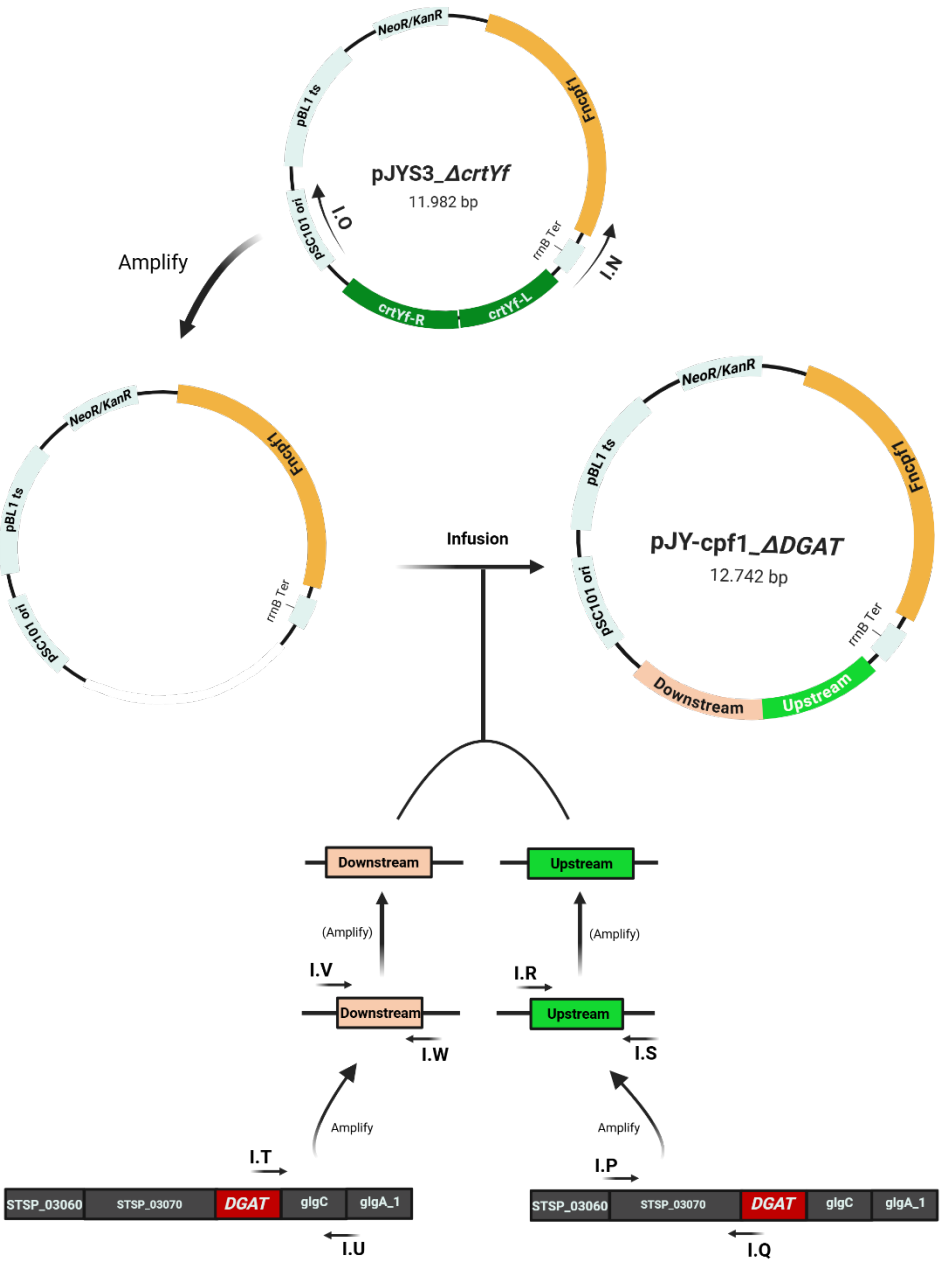

738

739 **Figure 3.2** The Illustration of the construction maps for plasmids pJY-cpf1_*ΔDGAT*.

740

741 ### III.2.3 PHA production

742 The accumulation of PHA within *S. jeddahensis* cells was assessed using

743 a modified protocol based on Sass P *et al*[33]. The experiments were conducted in

744 300-mL Erlenmeyer flasks, starting with the inoculation of approximately 1 cm^2

of *S. jeddahensis* colonies into 30 mL of Tryptic Soy Broth (TSB) liquid medium to prepare a pre-seed culture. This initial culture was incubated at 30°C with agitation at 160 rpm for 30 hours. To establish the seed culture, 5 mL of the pre-seed culture was then transferred to 50 mL of TSB medium and incubated under identical conditions for 18 hours. After incubation, cells were harvested by centrifugation, rinsed, and transferred into fermention media: 60 mL of TSB0.5 and MSM medium supplemented with 2.5 g/L sodium octanoate with OD; 1. These fermentation conditions were maintained on an orbital shaker set at 160 rpm for 144 H, with the medium refreshed every 18 hours. Sodium octanoate was used to promote PHA accumulation within the cells. Following the fermentation phase, cells were harvested by centrifugation at 10,000 x g for 5 minutes at 4°C, washed three times with sterile water, and frozen at -30°C overnight. The cells were then freeze-dried under vacuum conditions for 48 h.

III.2.4 Cell dry weight measurement

Aliquots of 1 mL of culture were taken every 24 hours, followed by centrifugation at 5,000 x g for 5 minutes. The resulting cell pellets were washed once with sterile water and then reweighed. The cell pellets were subsequently subjected to vacuum freeze-drying for 48 hours, after which the dry weight of the lyophilized cells was measured.

III.2.5 Nile red staining

For the visualization of intracellular polymers within the cell, Nile Red (Sigma-Aldrich, Tokyo, Japan; Catalog No. 7385-67-3, $C_{20}H_{18}N_2O_2$) was employed as a staining agent. The staining protocol was adapted from Spiekermann *et al*.[74]. A stock solution of Nile Red was prepared at a concentration of 0.25 mg/mL in ethanol. To stain the cells, an aliquot of approximately 100 µL of cell culture was centrifuged at 13,000 rpm for 30 seconds, and the supernatant was discarded. The cell pellets were then washed once with 100 µL of phosphate-buffered saline (PBS) at pH 7 and resuspended in 40 µL of the same buffer. To this suspension, 10 µL of Nile Red staining solution (10 µg/mL) was added and thoroughly mixed. A 10 µL sample of the stained cell suspension was subsequently placed on a microscope slide for immediate observation using a Keyence BZ-X810 fluorescence microscope.

III.2.6 Polymers determination

To analyze the monomer composition of polymers within bacterial cells, 30 mg of lyophilized bacterial cells were combined with 1.5 mL of chloroform and 1.5 mL of a methanolysis solution (comprising 85% methanol and 15% sulfuric acid by volume). The mixture was heated to 100 ° C for 2 hours and 20 minutes on a heating block, with gentle vortexing every 20 minutes. After cooling on ice for 15 minutes, 1 mL of Milli-Q water was added, and the mixture was vortexed for 1 minute before being left to rest overnight. The lower phase was carefully transferred to another tube and mixed with an equal volume of caprylate methyl

788 ester (CME) solution, serving as an internal standard, in a GC vial for subsequent
789 analysis.

790 The pretreated sample was analyzed using a Shimadzu GC-2014 gas
791 chromatograph fitted with a DB-5 capillary column, with detection carried out
792 using a flame ionization detector (FID). The gas chromatography conditions were
793 as follows: an initial temperature of 70°C for 2 minutes, ramping up to 280°C at
794 10°C/min, and held for 7 minutes. To confirm the PHA content and composition,
795 the samples were further analyzed using a Shimadzu GCMS-QP2020 NX. This
796 analysis utilized an HP-5MS UI column (30 m × 0.25 mm × 0.25 μm, Agilent
797 Co., Palo Alto, CA). The GC conditions were set with an initial temperature of
798 40 ° C held for 5 minutes, followed by a ramp at 20 ° C/min to 300 ° C, then a
799 further ramp at 10 ° C/min to 310 ° C, held for 5 minutes. The MS conditions
800 were set with an ion source temperature of 230 ° C and an interface temperature
801 of 250 ° C, with a full scan mass range of m/z 10-600.

802

803 III.2.7 Residual octanoate measurement

804 The sodium octanoate consumption was analyzed using a gas
805 chromatograph-mass spectrometer (GCMS-QP2020 NX, Shimadzu, Kyoto,
806 Japan). Separation was achieved with a DB-23 capillary column (60 m x 0.25 mm
807 x 0.15 μm, Agilent Technologies). The temperature program for chromatographic
808 analysis started at 50°C, held for 2 minutes, followed by a rapid increase of 25°C
809 per minute up to 175°C, and a subsequent slower ramp of 4°C per minute up to

230°C. Methyl esters were prepared from octanoate by derivatization using the fatty acid methylation kit (Nacalai Tesque, Inc.) in a transmethylation protocol. Specifically, 200 µL of supernatant from the culture medium was mixed with 125 µL each of Reagent A and Reagent B, followed by a 60-minute incubation at 37° C to facilitate methylation of any glycerides and sterol esters. Then, 125 µL of Reagent C was added to promote methylation of octanoate, with a further incubation for 20 minutes at 37°C. Post-methylation, the reaction mixture was treated with 250 µL of the kit's extraction solvent, centrifuged at 14,000 rpm for 1 minute, and the supernatant was transferred into a new microcentrifuge tube with 500 µL of Milli-Q (MQ) water. A second centrifugation was conducted to clarify the solution. For GC-MS analysis, 45 µL of this supernatant was combined with 5 µL of an internal standard solution (prepared by diluting 10 µL of methyl benzoate in 990 µL of chloroform) in a glass vial.

III.2.8 Residual glucose measurement

The glucose concentration in the samples was determined using the Glucose CII-Test Wako kit (FUJIFILM Wako, Osaka, Japan). To establish a standard curve, glucose solutions were prepared with concentrations of 0, 0.05, 0.1, 0.2, 0.4, 0.6, 0.8, and 1 g/L. For the assay, 190 µL of the Glucose CII-Test buffer solution was added to each well of a 96-well microplate, followed by the addition of 10 µL of each sample to the designated wells. The plate was then incubated at room temperature for four minutes to allow the reaction to occur. Absorbance was measured at 450 nm using a microplate reader, and the glucose

concentration in each sample was calculated by referencing the standard curve established from the known glucose concentrations.

Table 3.2 Primers were used for 3TYM-ABCGC plasmid construction in this study.

Primer	Sequence (5' → 3')
3pTYM3aABCGC-ermE.F (I.B)	GGTACCCGGGGATCCTCTAGAGTCGACCTGCAGGCATGCAGGTACCCGCTGGATCCTACCAACCGGCAC
HindIII pTYM3a to ermE.R (HW)	TTTTCCCAGTCACGACGTTGTAAAACGACGGCCAGTGCCACACGCGGTCGATCTTGACGGCTGGC
3pTYM3aABCGC-AB.F (I.C)	GGTAGGATCCAGCGGGTACCTGCATGCCTGCAGGTCGACTCGCTTGCATGAGTGCCGGCGTGCG
3pTYM3aABCGC-AB.R (I.D)	GACCATGATTACGAATTCGAGCTCGGTACCCGGGGATCCTTCAGCCCATATGCAGGCCGCCGT
3pTYM3aABCGC-CGC.F (I.E)	TAACAATTTCACACAGGAAACAGCTATGACCATGATTACGTCAGCGCGTGAGGACGTAGGTCCCCGGC
3pTYM3aABCGC-CGC.R (I.F)	GCCTGCATATGGGCTGAAGGATCCCCGGGTACCGAGCTCGGTTTAGAGCGCATTTTCTAAATTCAGAGCAACGGAGGTACGGTCATGTCG
pJYS3_open.F (I.N)	GGCCCGGTGAACAGTTGTTCTACTTTTGTTTGTTAGTCTTGATGCT
pJYS3_open.R (I.O)	CTAGATTGACAGCTAGCTCAGTCCTAGGTATAATGGATCCGA
Left arm_Δ*DGAT*.F (I.P)	CGGGCGCGTAGTCCTTCAGGAAGACGCC
Left arm_Δ*DGAT*.R (I.Q)	CTGGCGGAGCTGGCCGGGC
Over pJYS3_Left-right.F (I.R)	GGATCCATTATACCTAGGACTGAGCTAGCTGTCAATCTAGCGGGCGCGTAGTCCTTCAGGAAGACGC

Over Left.R (I.S)	CCGTGCTGTTCAAGTTCCACCTGGCGGAGCTGGCCGGGC
Right arm_KO DGAT.F (I.T)	GTGGAACTTGAACAGCACGGCGAAGGACGTGC
Right arm_KO DGAT.R (I.U)	GACAAGGTCTTCGCCTCGATGGGCAACTACATCTTCACC
Over Right.F (I.V)	AGCCCGGCCAGCTCCGCCAGGTGGAACTTGAACAGCACGGCGAAGGACGTGC
Over pJYS3_Left-right.R (I.W)	AAGACTAACAAACAAAAGTAGAACAACTGTTCACCGGGCCGACAAGGTCTTCGCCTCGATGGGCAACTACATCTTCACCAC

III.3. RESULTS AND DISCUSSION

III.3.1 Expression of phbA, phbB, phaC1, phaG and phaC2 in strain *S. jeddahensis*

In this research, the metabolic pathway of *S. jeddahensis*, originally incapable of synthesizing polyhydroxyalkanoates (PHAs), was genetically modified to enable PHA production. This was achieved by integrating five heterologous genes encoding key enzymes for PHA synthesis. The introduced enzymes were β-ketothiolase (*phbA*) and acetoacetyl-CoA reductase (*phbB*) from *Cupriavidus necator*, along with two PHA synthases (*phaC1* and *phaC2*), and acyl-ACP-CoA transacylase (*phaG*) from *Pseudomonas putida*. The PHB biosynthetic operon from *C. necator* was utilized due to its proven effectiveness in facilitating PHB synthesis from short-chain-length substrates (C3 to C5), predominantly using 3HB as a monomer. Additionally, the class II PHA synthase

849 from *P. putida* (*phaC1*) was selected for its extensive substrate range, allowing the
850 polymerization of medium-chain-length substrates (C6 to C12)[75,76]. The enzyme
851 phaC2 from *Pseudomonas putida* was chosen due to its broad substrate specificity,
852 allowing it to integrate both short-chain-length (scl) and medium-chain-length
853 (mcl) monomers into polyhydroxyalkanoates (PHAs)[77]. To enable PHA
854 production in *S. jeddahensis*, the genes *phbA*, *phbB*, *phaC1*, *phaG*, and *phaC2*
855 (collectively referred to as the ABCGC cassette) were successfully integrated into
856 the organism's genome. Notably, the enzyme encoded by *phaG* plays a pivotal role
857 by bridging the pathway between fatty acid biosynthesis and PHA synthesis[78]. The
858 ABCGC gene expression cassette (illustrated in Figure 4.1) was introduced into
859 the genome of *S. jeddahensis* through conjugation using a commonly used
860 integrase system, as reported in[79]. The successful transformants, referred to as
861 SJ-D2 strains, underwent evolution to produce and store PHA. The ability of
862 *Streptomyces* species to produce polyhydroxyalkanoates (PHA) has been reported
863 in several studies[13,80,81]. Among these, *S. jeddahensis* emerges as a particularly
864 promising candidate due to its oleaginous properties, which allow it to accumulate
865 lipids constituting up to 64% of its dry cell weight[12]. This lipid accumulation
866 capability is an uncommon trait among actinobacteria, distinguishing *S.*
867 *jeddahensis* as an excellent candidate for efficient PHA production. The
868 oleaginous nature of *S. jeddahensis* is especially advantageous for PHA
869 biosynthesis, as oleaginous strain exhibit carbon flux through acetyl-CoA, a pivotal
870 precursor for PHA synthesis. Acetyl-CoA, produced via fatty acid β-oxidation,

871 serves as a key substrate for the generation of PHAs[82,83]. Furthermore, the
872 metabolic pathways responsible for lipid accumulation, as illustrated in Figure 4.2,
873 can be repurposed to optimize the production of PHA precursors. This metabolic
874 engineering approach ensures an abundant supply of fatty acid intermediates,
875 facilitating the synthesis of medium-chain-length (mcl) PHA monomers.

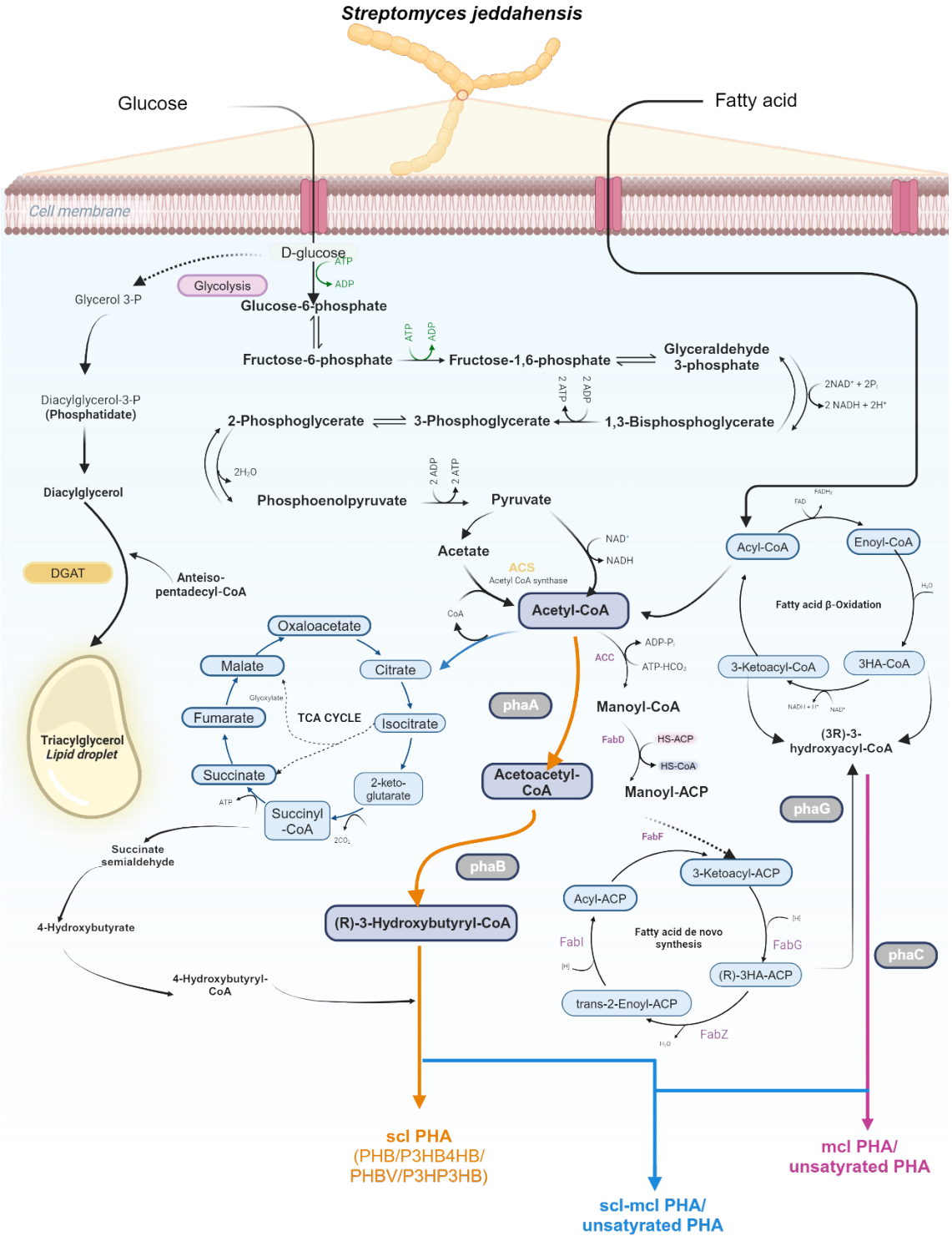

Figure 3.3 Rewiring metabolic pathway for enabling polyhydroxyalkanoate (PHA) production in *S. jeddahensis*.

III.3.2 Repeated fermentations of *S. jeddahensis* wild-type and SJ-D2 engineered strains using sodium octanoate medium for PHA production

The ability of *S. jeddahensis* SJ-D2 to accumulate medium-chain-length polyhydroxyalkanoates (mcl-PHAs) was successfully demonstrated by cultivating the strain in a medium containing sodium octanoate. This carbon source, utilized due to the expression of the *phaC1-phaG-phaC2* gene system from *P. putida* in the SJ-D2 strain, provided 3HO-CoA as a precursor for mcl-PHA synthesis. Sodium octanoate's role in supporting PHA biosynthesis was further highlighted by the incorporation of 3HO as a key building block in the polymer structure. The wild-type strain of *S. jeddahensis* was used as strain for comparison.

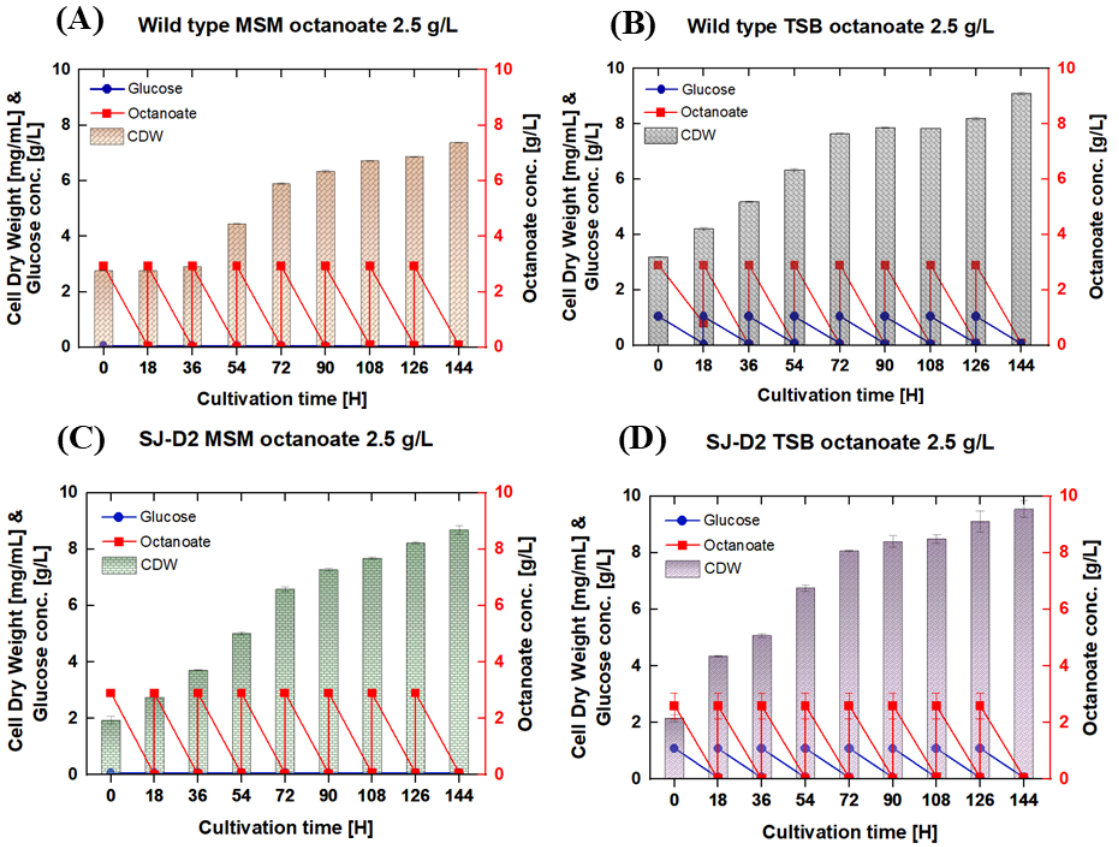

Figure 3.4 Fermentations of *S. jeddahensis* wild-type and SJ-D2 engineered strains. The strain was cultivated for 144 h by repeated batch fermentation, with triplicate samples taken. Cell Dry Weight (CDW) was measured from 1 mL samples, and standard deviations were reported. The conditions for each culture are as follows: (A) *S. jeddahensis* wild-type grown in MSM medium with 2.5 g/L sodium octanoate; (B) *S. jeddahensis* wild-type grown in TSB medium with 1 g/L glucose and 2.5 g/L sodium octanoate; (C) *S. jeddahensis* SJ-D2 strain grown in MSM medium with 2.5 g/L sodium octanoate; (D) *S. jeddahensis* SJ-D2 strain grown in TSB medium with 1 g/L glucose and 2.5 g/L sodium octanoate.

As depicted in Figure 3.3, a repeated-batch fermentation strategy was implemented to enhance productivity, where the culture broth was replaced every 18 hours and sodium octanoate was maintained at 2.5 g/L as the sole carbon source. These findings align with previous research[84], emphasizing the importance of carbon source selection on PHA yield and composition. The growth profiles of

both the wild-type and SJ-D2 strains were assessed in two different media, MSM and TSB0.5, each supplemented with 2.5 g/L sodium octanoate. In MSM, the wild-type strain achieved a dry cell weight (DCW) of 7.38 g/L, while the SJ-D2 strain reached a higher DCW of 8.7 g/L, suggesting that approximately 0.7 g/L of biomass was attributable to intracellular PHA accumulation, as confirmed by Nile red staining (Figure 3.4A, Table 3.3).

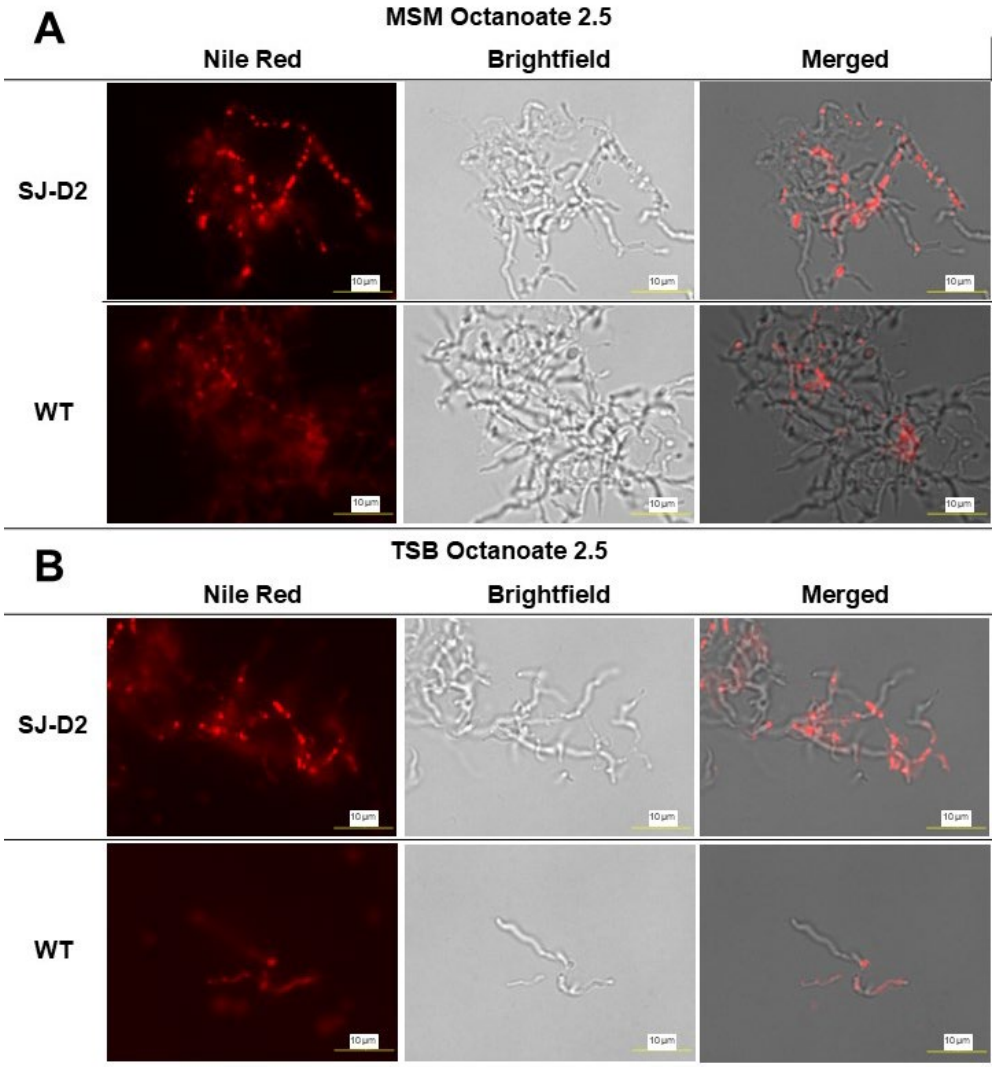

Figure 3.5 Observation of PHA accumulation in *S. jeddahensis* SJ-D2 strain. Wild-type strain was used as a background. The panel displays images of both strains as observed through Nile Red staining, phase-contrast microscopy (Brightfield), and merged (bars, 10μm). (A) strains culture into medium MSM containing 2.5 g/L sodium octanoate. (B) strains culture into medium TSB0.5 containing 1 g/L glucose and 2.5 g/L sodium octanoate.

This demonstrates the efficacy of sodium octanoate in promoting PHA biosynthesis. In TSB0.5 medium, which incorporated both sodium octanoate and glucose, both strains achieved even higher cell densities compared to MSM, with DCWs of 9.09 g/L and 9.55 g/L for the wild-type and SJ-D2 strains, respectively

(Figure 4.4B, Table 4.3). This outcome highlights the synergistic effect of glucose in supporting enhanced cell growth and PHA production, corroborating findings from earlier studies on co-substrate feeding strategies[66,85].

Table 3.3 Production of P(3HB-*co*-3HHx-*co*-3HO) in *S. jeddahensis* wild type and SJ-D2 strains[a].

Strain	Medium	CDW[b] (g/L)	%PHA	Composition by GC (% w/w)[c]		
				3HB Monomer	3HHx Monomer	3HO Monomer
Wild type	TSB0.5 Oct	8.7	n.d.	n.d.	n.d.	n.d.
	MSM Oct	7.6	n.d.	n.d.	n.d.	n.d.
SJ-D2	TSB0.5 Oct	9.3	1.7	n.d.	11.3	88.7
	MSM Oct	8.9	13.1	2.8	16	81.2

[a]Averages and standard deviations are the results of three independent replicates.
[b]CDW, cell dry weight.
[c]3HB, 3-hydroxybutyrate; 3HHx, 3-hydroxyhexanoate; 3HO, 3-hydroxyoctanoate.
n.d., not detected.

Repeated-batch fermentation effectively extended the growth phase of *S. jeddahensis*, resulting in increased cell density and mcl-PHA accumulation, with an optimal sodium octanoate concentration of 2.5 g/L. Notably, concentrations above 4 g/L exhibited inhibitory effects (data not shown), consistent with reports in other microbial systems where high substrate concentrations lead to toxicity and reduced productivity[86].

III.3.3 Influence of Media Composition and Genetic Engineering on PHA Accumulation and Composition in *S. jeddahensis*

The engineered SJ-D2 strain demonstrated consistently higher cell density compared to the wild-type strain, particularly when cultured in MSM medium. This observation suggests that SJ-D2 possesses an enhanced capability to metabolize sodium octanoate, supporting both cell growth and mcl-PHA synthesis. This improved performance may be attributed to modifications in metabolic pathways or an increased efficiency in carbon source uptake, which aligns with findings from other studies on engineered bacterial strains optimized for PHA production[76]. The inclusion of glucose in the TSB0.5 medium significantly enhanced cell densities in both strains when compared to the MSM medium. This observation suggests that glucose functions as an auxiliary carbon source, promoting more robust cell proliferation and elevated PHA production. These findings align with the concept that utilizing multiple carbon sources can improve metabolic adaptability and optimize overall yields in microbial fermentation systems[87].

The integration of *phaC1*, *phaG*, and *phaC2* genes from *Pseudomonas putida* into the genome of *S. jeddahensis* was conducted to evaluate the potential for medium-chain-length polyhydroxyalkanoate (mcl-PHA) biosynthesis using octanoate as a precursor. This aligns with prior findings that octanoate is an effective substrate for promoting PHA synthesis. Earlier studies demonstrated that various *Pseudomonas* strains grown in media containing octanoate or 1-

octanoate are capable of producing diverse mcl-PHAs, reinforcing the viability of octanoate as a key carbon source for biopolymer production[88]. Including a copolymer of 3-hydroxyhexanoate and 3-hydroxyoctanoate [P(3HHx-*co*-3HO)]. The GC-MS analysis presented in Figure 3.5 highlights the detailed composition of PHAs synthesized under different experimental conditions. Notably, the SJ-D2 strain cultured in MSM demonstrated both an increased overall PHA yield and a broader diversity in monomer composition. This is reflected in the chromatograms, which reveal a specific distribution of monomers consisting of 2.8% 3HB, 16% 3HHx, and 81.2% 3HO, consistent with the findings reported by Braunegg *et al*[89].

The broader monomer composition observed in MSM highlights the metabolic adaptations that occur in carbon-limited environments, where sodium octanoate is utilized as the primary carbon source. Notably, the detection of 3HB, which is absent in TSB0.5, suggests that the nutrient-restricted conditions in MSM activate alternative metabolic pathways, thereby enhancing the diversity of monomers in the synthesized PHA. Conversely, the metabolic activity of the SJ-D2 strain in TSB0.5 demonstrates a dependency on glucose availability, reflected in the simpler polymer composition comprising 11.3% 3HHx and 88.7% 3HO. This indicates that under these nutrient-rich conditions, the strain prioritizes growth over PHA production, resulting in a polymer with reduced monomer diversity. The comparative findings between MSM and TSB0.5, as illustrated in Figures 3.4 and 3.5, support the hypothesis that nutrient-limited environments

such as MSM favor both PHA accumulation and greater monomer diversity. This underscores the role of environmental conditions in shaping the metabolic and biosynthetic priorities of the strain. The findings show that the nutrient-rich TSB medium, when supplemented with glucose, significantly boosts cell growth, highlighting glucose as a vital nutrient and key contributor to cell proliferation[90].

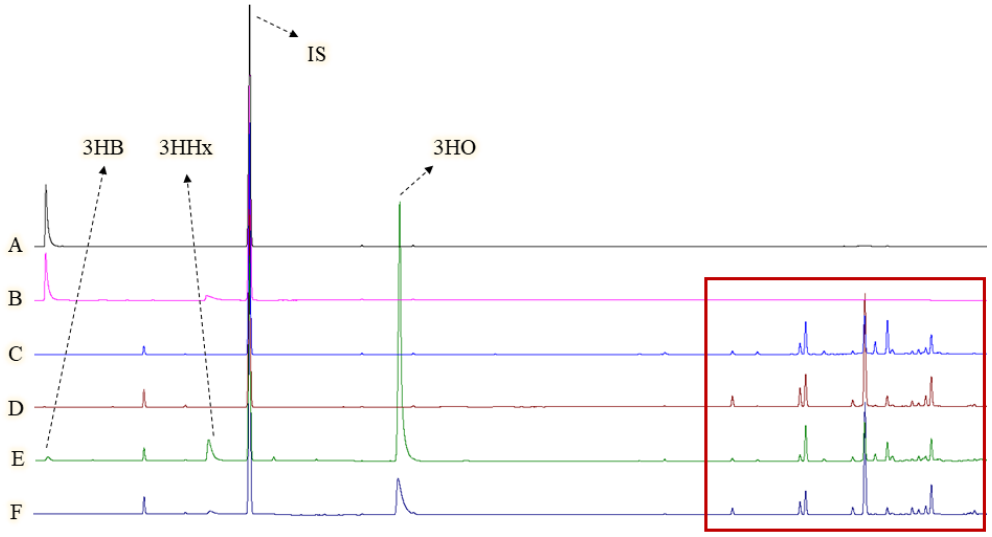

Figure 3.6 Gas chromatography analysis detects P (3HB-co-3HHx-co-3HO), indicating successful PHA production by the engineered strain (SJ-D2). (A) Standard P(3HB). (B) Standard P(3HB-co-3HV-co-3HHx). (C) *S. jeddahensis* wild-type strain cultured in MSM medium containing 2.5 g/L sodium octanoate. (D) *S. jeddahensis* wild-type strain cultured in TSB0.5 medium containing 1 g/L glucose and 2.5 g/L sodium octanoate. (E) *S. jeddahensis* SJ-D2 strain cultured in MSM medium containing 2.5 g/L sodium octanoate. (F) *S. jeddahensis* SJ-D2 strain cultured in TSB0.5 medium containing 1 g/L glucose and 2.5 g/L sodium octanoate. IS indicates the internal standard peak.

III.3.4 knock out DGAT gene to decrease lipid production through CRISPR- Cpf1 system.

To mitigate lipid accumulation and redirect metabolic flux toward polymer production. We use commercial plasmid pJYS3_ΔcrtYf to construct pJY-

cpf1_ΔDGAT, CRISPR-Cpf1 system was used to knockout the DGAT gene. This gene encodes diacylglycerol acyltransferase, a key enzyme catalyzing the final step in triacylglycerol (TAG) biosynthesis. The targeted knockout was validated through PCR analysis (Figure 3.7), which showed the absence of the DGAT gene band, confirming successful genome editing. o ensure the knockout is thoroughly confirmed, multiple rounds of verification were conducted. In the first round, colonies 16, 17, and 20 were identified as having a successful knockout of the DGAT gene (Figure 3.7B), as evidenced by the absence of PCR bands. Each of these colonies was then cultured and spread onto TSB agar media for further analysis. In the second round of PCR confirmation, colonies were randomly selected from the cultured plates. Colony 20.1 yielded a positive result (Figure 3.7C). This colony was subsequently re-cultured and spread onto TSB agar media for a third round of confirmation. Randomly selected colonies from this culture were subjected to PCR, with the results again confirming a positive knockout (Figure 3.7D). These results affirm the successful knockout of the DGAT gene in colony 20.1, which will undergo further analysis to validate the findings and assess its functional implications. We successfully knocked out the DGAT gene in strain SJ-D2, resulting in the creation of strain SJ-D2$_{cpDg}$. This result demonstrates the precision and efficiency of the CRISPR-Cpf1 system for genetic modifications in Streptomyces.

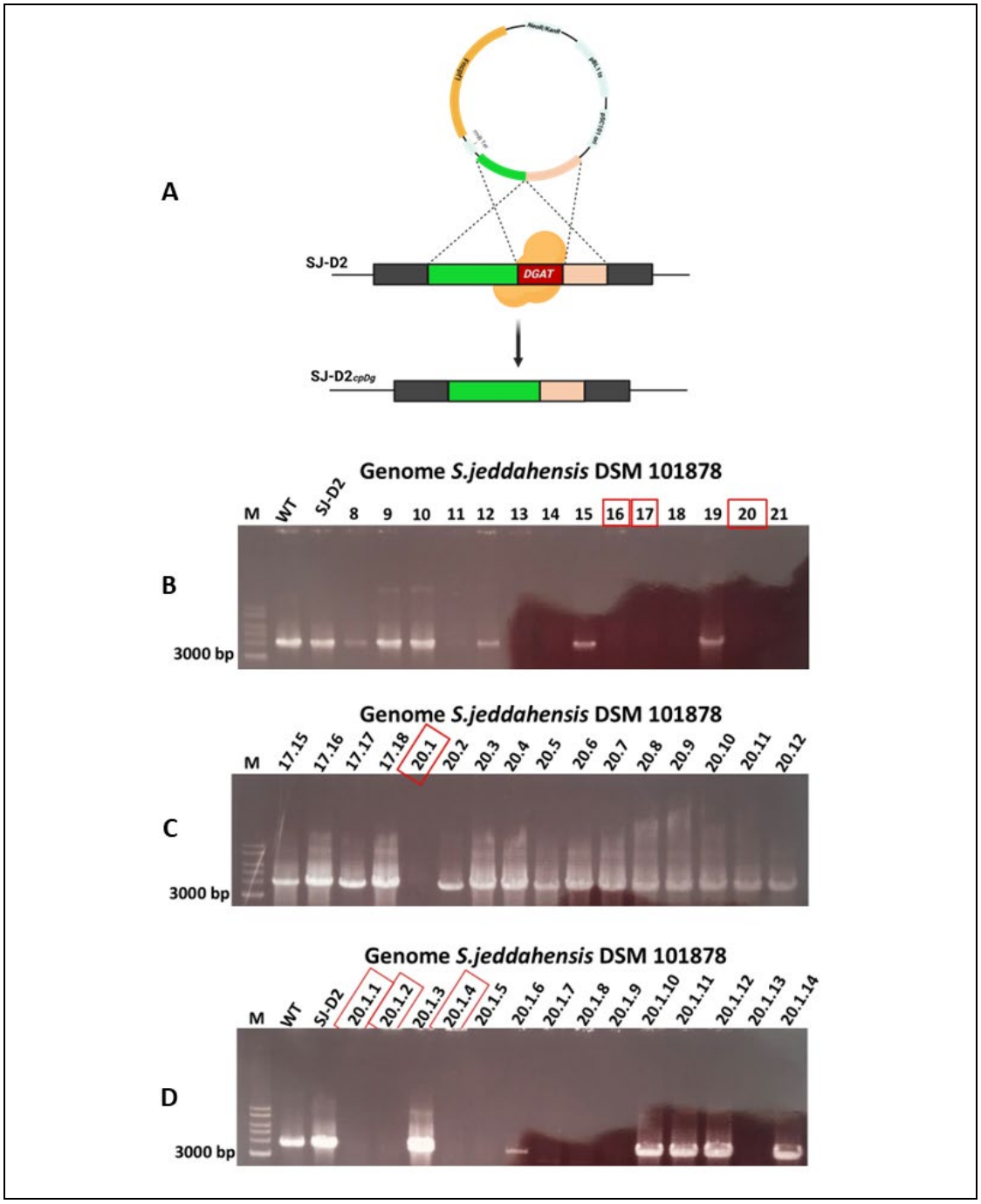

Figure 3.7 Impact of Different Repair Templates on CRISPR-Cpf1 Editing Efficiency in SJ-D2 (*S. jeddahensis ABCGC*). (A) Schematic representation of CRISPR-Cpf1-mediated repair of identical double-strand breaks (DSBs) using the pJY-cpf1_ΔDGAT plasmid. (B) PCR validation of gene deletion across various repair templates, utilizing I.U/I.P primers located outside the homologous arms. Amplified fragments are 3782 bp for the SJ-D2 strain, with no band detected in the SJ-$D2_{cpD}$g strain, representing the first PCR step. (C) Second round of PCR. (D) Third round of PCR.

The knockout of DGAT is expected to reduce TAG synthesis, thereby decreasing intracellular lipid accumulation. This metabolic intervention could potentially shift the carbon flux from lipid storage pathways to the biosynthesis of PHAs. Such a redirection is hypothesized to enhance polymer yield by increasing the availability of precursors and reducing competition between the pathways. For our current research, we have only completed the stage of successfully knocking out the SJ-D2 strain and producing the SJ-D2$_{cpDg}$ mutant, further analysis is required to determine its impact on polymer production and lipid content. The effectiveness of this genetic modification can be evaluated by comparing the polymer yield and lipid accumulation of the knockout strain with those of the wild-type strain. Analytical techniques such as gas chromatography-mass spectrometry (GC-MS), nuclear magnetic resonance (NMR) spectroscopy, and Fourier-transform infrared (FTIR) spectroscopy will be employed to quantify and characterize the produced polymers. Lipid content will be analyzed using Nile Red staining, thin-layer chromatography (TLC), or gravimetric lipid extraction methods.

III.4. CONCLUSION

The engineered *S. jeddahensis* SJ-D2 strain represents a significant advancement in the production of P(3HB-co-3HHx-co-3HO) through its enhanced *phaC1* synthase and integration of dual synthetic pathways. By combining scl- and mcl-monomer synthesis mediated by key enzymes such as

phaC1, *phaG*, and *phaC2*, this strain enables the efficient production of tailored PHA polymers. The successful integration of polymer biosynthesis genes and the efficient knockout of the DGAT gene using CRISPR-Cpf1 producing the SJ-D2$_{cpDg}$ mutant, this highlight the potential of genetic engineering to enhance biopolymer production in oleaginous Streptomyces. The use of sodium octanoate as a precursor further emphasizes the practicality of this approach for sustainable polymer production. Future studies will focus on quantifying polymer yield, assessing lipid reduction, and optimizing the strain for industrial applications. These efforts will contribute to the development of cost-effective and eco-friendly biopolymers, addressing the growing need for sustainable alternatives to conventional plastics.

CHAPTER IV

Utilizing a Target AID system for editing *Streptomyces* genome

IV.1. Introduction

The *Streptomyces* genus, a group of bacteria renowned for their extraordinary ability to generate a wide variety of bioactive substances, plays a crucial role in biotechnology and pharmaceuticals. These substances display numerous biological activities, such as antifungal, antimicrobial, antibiofilm, antitumor, anticancer, insecticidal and anthelmintic effects. Additionally, they serve as sources for enzymes with industrial applications[91–101]. One of the main challenges is fully utilizing these compounds is that many are not adequative expressed under typical laboratory conditions in their natural *Streptomyces* hosts. This limitations has driven researchers to explore genetic engineering approaches to activate biosynthetic gene clusters and enhance the production of these valuable compounds[102].

In recent years, the CRISPR-Cas system, inspired by the adaptive immune response of *Streptococcus pyogenes*, has become a groundbreaking tool in genome editing. At its core is the Cas9 protein, an RNA-guided endonuclease known for its accuracy in creating double-strand breaks in DNA. This feature is crucial for making genomic changes, including insertions, deletions, or substitutions, which can be accomplished via processes such as nonhomologous end joining or homologous recombination[103,104]. The adoption of the CRISPR-

Cas9 system in *Streptomyces* research marks a major advancement, as it enables precise genome editing in these bacteria, allowing researchers to activate biosynthetic pathways that were previously inactive[105,106]. This approach boosts the generation of established bioactive compounds and opens avenues for uncovering new compounds with promising therapeutic applications.

CRISPR-Cas9 is a powerful gene-editing tool, yet its effectiveness varies depending on the host cell. In many actinomycetes, elevated Cas9 expression can led to notable toxicity and an increase in off-target effects. The linier chromosomes of these organisms are especially unstable, making them vulnerable to extensive chromosomal deletions and rearrangements. This instability, often triggered by DNA double-strand breaks (DSBs), is a common complication in gene editing technique that rely on DSBs, such as CRISPR-Cas9[107–110]. In most bacteria, chromosomal breaks caused by nucleases often lead to cell death due to the absence of the nonhomologous end-joining (NHEJ) repair pathways. However, *Streptomyces* and other actinomycetes rely mainly on the homologous recombination (HR) pathway to repair DNA double-strand breaks. Unlike many eukaryotes, which utilize the NHEJ pathway, actinomycetes have evolved to prioritize the accuracy of HR repair, likely due to its evolutionary advantages. The frequent lack of key NHEJ proteins, such as KU and ligase D, suggest that NHEJ is generally absent in these organisms. This characteristic has facilitated precise genetic manipulations in research, allowing for controlled DNA integrations through HR and reducing the variability seen random insertions[111,112]. This

limitation can be addressed by altering a catalytically inactive Cas9 (dCas9), achieved through mutations in the HNH and RuvC domains (D10A and H840A). Although this modified system lacks endonuclease activity, it can still bind effectively to target DNA by forming a complex with sgRNA.

Recent advances in gene editing have enabled the precise alteration of individual nucleotide in DNA without requiring DNA cleavage[113,114]. This innovative approach utilizes a modified vector that fuses the deaminase enzyme PmCDA1 with dCas9 and includes the uracil DNA glycosylase inhibitor (UGI). Additionally, *E. coli*, this method leverages a degradation tag (LVA) to improve efficiency, offering new possibilities for gene regulation and visualization of specific genomic sites[115].

We introduce a method for inducing mutation in *Streptomyces* that does not require double-strand breaks (DSBs). By selectively converting cytidine (C) to thymine (T), this technique enables the generation of stop codons in target sequences. This study investigates the key characteristics of the CRISPR target-AID system and its potential for use in *Streptomyces* species, emphasizing the extensive range of applications this adaption could facilitate. Selecting an expression host with well-defined genetic properties and high flexibility is vital to achieving the desired outcomes. For this purpose, *S. coelicolor* was used to express gene clusters from actinomycetes. This system incorporates components like dCas9, PmCDA and a combined UGI structure, effectively enabling single-nucleotide edits by converting cytosine to thymine within the actinorhodin

biosynthetic genes of *S. coelicolor*, which serve as model targets. Additionally, we carried out an off-target analysis on *S. coelicolor* open reading frames (ORFs) involved in the essential pathway for actinorhodin biosynthesis.

IV.2. Materials and Methods

IV.2.1 Strains, plasmids, culture conditions, reagents, and enzymes

The bacterial strain used in this research is listed in Table 4.1. *Streptomyces coelicolor* NBRC 15146 were obtained from Biological Resource Center (NITE National Biological Resource Centre, Tokyo, Japan, https://www.nite.go.jp/en/) was utilized and maintained on ISP2 medium, which consists of Yeast extract 4 gr/L, Malts extract 10 gr/L, Dextrose 4 gr/L, Agar 20 gr/L. For conjugation experiments, strains were cultivated in ISP4 medium, composed of Soluble starch 10 gr/L, $MgSO_4 \cdot 7H_2O$, 1 gr/L NaCl, $(NH_4)2SO_4$ 2 gr/L, $CaCO_3$ 2 gr/L) supplemented with 1 mL trace salts solution ($FeSO_4 \cdot 7H_2O$ 0.1 gr/100 mL, $MnCl_2 \cdot 4H_2O$ 0.1 gr/100 mL, $ZnSO_4 \cdot 7H_2O$ 0.1 gr/100 mL). For overlaying, a medium composed of Nutrient Broth 8 gr/L, Soft agar 5 gr/L, nalidixic acid 1 μg/mL, apramycin 50 μg/mL, aztreonam 50 μg/mL). Recombinant *S. coelicolor* strains were transferred onto selective ISP2 medium, supplemented with apramycin (10 μg/mL), to ensure the selection of transformants. *Escherichia coli* (*e.coli*) JM109 (Takara Bio, Shiga, Japan) and *E. coli* HST04 (Takara Bio) were employed as hosts for plasmid transformation and conjugation, respectively. These strains were cultured in Luria-Bertani (LB)

medium at 37° C. For solid LB medium, agar was added at a concentration of 20 g/L. Antibiotics including apramycin (50 μg/mL), kanamycin (20 μg/mL), ampicillin (50 μg/mL), and tetracycline (5 μg/mL) were incorporated into the media as appropriate. All restriction enzymes used in this study were purchased from New England Biolabs Inc. (Germany), and In-Fusion HD for cloning fragment DNA was purchased from TaKaRa-Bio. The PCR technique was employed to verify the target sequence of *S. coelicolor* by amplifying nucleic acids using the high-precision polymerase KOD FX (Toyobo, Osaka, Japan).

Table 4.1. Strain and plasmids used in this study.

Strain & plasmid	Description
e.coli HST04	F^-, *ara*, Δ(*lacproAB*) [Φ80d*lacZ*ΔM15], *rpsL*(*str*), *thi*, Δ(*mrr-hsdRMS-mcrBC*), Δ*mcrA*, *dam*, *dcm*
e.coli JM109	*recA1, endA1, gyrA96, thi-1, hsdR17* ($rk^- mk^+$), *e14*$^-$ (*mcrA*$^-$), *supE44, relA1*, Δ *(lac-proAB)/F' [traD36, proAB*$^+$*,* $lacI^q$*, lacZΔM15*]
pGM1190	OriT, thiostrepton-induced gene, Apr^r, Tip A
pMA-RQ_UGI_dCasPmCDA1	Codon-optimized dCas9, PmCDA1 gene
17ACQ2GP_ermEp-gRNA_pMA-RQ	*ermE*-target and gRNA
pUB307	PΔTnA^c, IncP α replicon Km^r TC^r
pGM1190-dCas-linker-PmCDA1-UGI-AAV	OriT, thiostrepton-induced gene, Apr^r, Tip A and dCasPmCDA1 sequence
pGM1190-dCas-linker-PmCDA1-UGI-AAV-target 8	OriT, thiostrepton-induced gene, Aprr, Tip A and dCasPmCDA1-target 8 sequence

pGM1190-dCas-linker-PmCDA1-UGI-AAV- target 9	OriT, thiostrepton-induced gene, Aprr, Tip A and dCasPmCDA1-target 9 sequence
pGM1190-dCas-linker-PmCDA1-UGI-AAV-target10	OriT, thiostrepton-induced gene, Apr^r, Tip A and dCasPmCDA1-target 10 sequence
pGM1190-dCas-linker-PmCDA1-UGI-AAV-target11	OriT, thiostrepton-induced gene, Apr^r, Tip A and dCasPmCDA1-target 11 sequence
pGM1190-dCas-linker-PmCDA1-UGI-AAV-target12	OriT, thiostrepton-induced gene, Apr^r, Tip A and dCasPmCDA1-target 12 sequence
pGM1190-dCas-linker-PmCDA1-UGI-AAV- target 13	OriT, thiostrepton-induced gene, Aprr, Tip A and dCasPmCDA1-target 13 sequence
pGM1190-dCas-linker-PmCDA1-UGI-AAV-target14	OriT, thiostrepton-induced gene, Apr^r, Tip A and dCasPmCDA1-target 14 sequence
pGM1190-dCas-linker-PmCDA1-UGI-AAV-target 15	OriT, thiostrepton-induced gene, Aprr, Tip A and dCasPmCDA1-target 15 sequence
pGM1190-dCas-linker-PmCDA1-UGI-AAV-target16	OriT, thiostrepton-induced gene, Apr^r, Tip A and dCasPmCDA1-target 16 sequence
pGM1190-dCas-linker-PmCDA1-UGI-AAV-target17	OriT, thiostrepton-induced gene, Apr^r, Tip A and dCasPmCDA1-target 17 sequence
pGM1190-dCas-linker-PmCDA1-UGI-AAV-target18	OriT, thiostrepton-induced gene, Aprr, Tip A and dCasPmCDA1-target 18 sequence
pGM1190-dCas-linker-PmCDA1-UGI-AAV-target19	OriT, thiostrepton-induced gene, Aprr, Tip A and dCasPmCDA1-target 19 sequence
pGM1190-dCas-linker-PmCDA1-UGI-AAV-target20	OriT, thiostrepton-induced gene, Aprr, Tip A and dCasPmCDA1-target 20 sequence

IV.2.2 Plasmid constructions

All plasmids used in this research are listed in Table 4.1. The workflow for constructing these vectors is described in Figure 4.9. Two different plasmids, pMA-RQ_UGI_dCasPmCDA1 was used as a source of dCas9 and PmCDA1, and

17ACQ2GP_ermEp-gRNA_pMA-RQ was used as sources of ermE and gRNA sequences, for generating ermE-target- gRNA construction.

The primary temperature-sensitive pGM1190-dCas-PmCDA1-UGI plasmid was constructed from vector pGM1190 by inserting the genes for dCas9, PmCDa1, UGI, and protein degradation tag. Figure 4.1 illustrates the detailed sequence positioning of CasPmCDA-UGI along with the degradation tag.

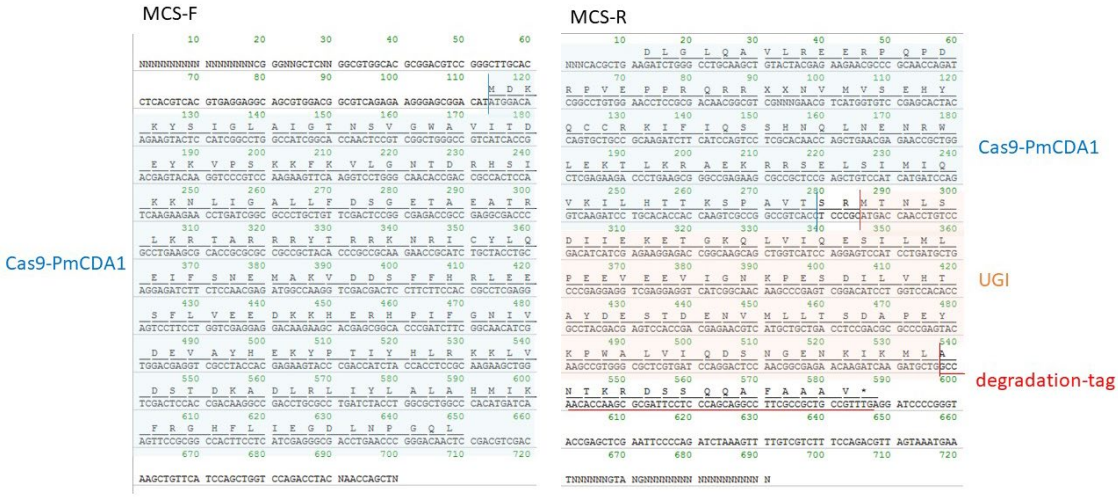

Figure 4.1 Sequence position of CasPmCDA-UGI and degradation tag

This plasmid was constructed by cutting pMA-RQ_UGI_dCasPmCDA1 (Geneart ThermoFisher) with EcoRI/BamHI and NdeI enzymes, next cloned the genes into EcoRI/BamHI and NdeI sites by ligation after verified through the gel electroporation (Figure 4.2- 4.4). To construct a completed vector, pGM1190-dCasPmCDA1-target was made as follows. Firstly, by using PCR with KOD-FX (Toyobo), the generated ermE-target, 17ACQ2GP_ermEp-gRNA_pMA-RQ as a template, using forward primer (pGM1190-SnaBI-cassette-F2)

ATGATTACGAATTGTACGTACGCGGTCGATCTTGACGGCTG and reverse primer depending on the target gene to be constructed, ermE-20 nt target will be formed, besides that forming gRNA was also using 17ACQ2GP_ermEp-gRNA_pMA-RQ as the template, forward primer (KnK9) GTTTTAGAGCTAGAAATAGCAAAG, reverse primer (pGM1190-SnaBI-cassette_R3) GTAGCTGACGCCTACGTAAAAAAAAGCACCGACTCGGTG CCACTTTTTCAAG. All primers used in listed in Table 4.2.

Table 4.2 Primers used in this study.

Primers	Sequence nucleotide	Comments
pGM1190-SnaBI-cassette-F2	ATGATTACGAATTGTACGTA-CGCGGTCGATCTTGACGGCT G	for construct ermE-target and compile with gRNA scafold (forward)
Target8 R8-SCO5085.actII-orf4.R (Code:BS)	GCTATTTCTAGCTCTAAAA-CCGGCGCGCCTGCCCATCTG--CCGCTGGATCCTACCAACCG	for construct ermE-target 8 (reverse)
Target9 R9-SCO5085.actII-orf4.R (Code:BT)	GCTATTTCTAGCTCTAAAA-CTATCGACGCGAATTGGCGG C--CCGCTGGATCCTACCAACCG	for construct ermE-target 9 (reverse)
Target10 R10-SCO5079.actVA-orf4.R (Code:BT)	GCTATTTCTAGCTCTAAAA--CGGCCGCGGAGCCGCCTTGC T-CCGCTGGATCCTACCAACCG	for construct ermE-target 10 (reverse)

Target11 R11-SCO5079.actVA-orf4.R （Code:BT）	GCTATTTCTAGCTCTAAAA-CGTGTCATCGGCGTTTGGATG-- CCGCTGGATCCTACCAACCG	for construct ermE-target 11 (reverse)
Target12 R12-SCO5079.actVA4.R (Code:BW)	GCTATTTCTAGCTCTAAAA--CGCCGGTGTCATCGGCGTTTG- CCGCTGGATCCTACCAACCG	for construct ermE-target 12 (reverse)
Target13 R13-SCO5079.actVA4.R (Code:BX)	GCTATTTCTAGCTCTAAAA-CAGCCGCCAGTTCACGCCCTC--CCGCTGGATCCTACCAACCG	for construct ermE-target 13 (reverse)
Target14 R14-actVAORF5SCO5080.R (Code:CF)	GCTATTTCTAGCTCTAAAA-CTCAGGGACGGCCGCTCCTGG-- CCGCTGGATCCTACCAACCG	for construct ermE-target 14 (reverse)
Target15 R15-actIIORF2(SCO5083) (Code:CG)	GCTATTTCTAGCTCTAAAA-CGCCGCGTTCGCGCCCCTGGA-- CCGCTGGATCCTACCAACCG	for construct ermE-target 15 (reverse)
Target16 R16-actIIORF2(SCO5083) (Code:CH)	GCTATTTCTAGCTCTAAAA-CCCTACGCGCGCCGTTGG CCGCTGGATCCTACCAACCG	for construct ermE-target 16 (reverse)
Target-R17 actIORF2(SCO5088) (Code:CH.1)	GCTATTTCTAGCTCTAAAA-CGGTCCGCCTTCGCGTCCTGG-- CCGCTGGATCCTACCAACCG	for construct ermE-target 17 (reverse)
Target18 R18-actIV(SCO5091) (Code:CI)	GCTATTTCTAGCTCTAAAA-CGGCCCTCACCGGGCTCTGG	for construct ermE-target 18 (reverse)

	C-- CCGCTGGATCCTACCAACCG	
TargetR19-actVII(SCO5090_17bp) (Code:CJ)	GCTATTTCTAGCTCTAAAA-CAACGCTTCCGGATCTGGGCG-- CCGCTGGATCCTACCAACCG	for construct ermE-target 19 (reverse)
TargetR20-actIII(SCO5086_17bp) (Code:CK)	GCTATTTCTAGCTCTAAAA-CCCCGCCTTGAGGACCTGTTT-- CCGCTGGATCCTACCAACCG	for construct ermE-target 20 (reverse)
sSCO5092.F	CGACCAGGGAATGCTCCG	For Sequencing target 6 & 7
sSCO5092.R	GGTACGCCCTTCTCCTCGAC	
sSCO5085_actIIORF4.F	AAAGCAATATCGCGCACCTG	For Sequencing target 8 & 9
sSCO5085_actIIORF4.R	TATCCGCCGGAGATTCCGAT	
target10-11-12 13_F_Cekseq2	GACTCGTGACGACGACCAAC	For Sequencing target 10-11-12-13
sSCO5079_actVAORF4.R	TTCTCCATGAAGTACGACGGC	
sSCO5083_actIIORF2.F	AAATGTTCCCGCCCAAGGAG	For Sequencing target 15
sSCO5083_actII-ORF2.R	ATCATGATGCCCATGCCGAG	
sSCO5083_actII-ORF2_t16.F	TGAGTTCCGTTGAAGCCGAC	For Sequencing target 16
sSCO5083_actII-ORF2_t16.R	GAGCCCTTGCGGAATCATCA	
sSCO5088_actI-ORF2.F	AGATCGACGACTTCCACGC	

sSCO5088_actI-ORF2.R	CCCATGTCGTAGTCGGTCAG	For Sequencing target 17
sSCO5091_actIV.F	TCAACACCCACTTCCACGG	For Sequencing target 18
sSCO5091_actIV. R	TGGACCCAGCGCAGATAGTC	
sSCO5090_actIORF4.F	CTCTACGAGCTGGTCGCAC	For Sequencing target 19
sSCO5090_actIORF4.R	GTCCTCGAACGTGAAGACCA	
sSCO5086_actIII.F	TCGAGGCGATGTTGACGATT	For Sequencing target 20
sSCO5086_actIII.R	ACGAACTCTGGCTCGATGTC	

The PCR product is purified using the Fast Gen gel/PCR extraction kit (Nippon Genetics Co., Ltd., Tokyo, Japan). Secondly, the construction combining ermE promoter, target region, and gRNA amplified using overlap PCR generated the fragment ermE promoter-20 nt target-guide RNA and carries a *SnaBI* restriction site for easy cloning of new spacers. Next, the ermE promoter 20 nt target-gRNA was cloned into the basic vector between the *SnaBI* site using an Infusion HD cloning kit (Takara-Bio). The confirming the result of target infusion into plasmid is in Figure 4.5–4.7.

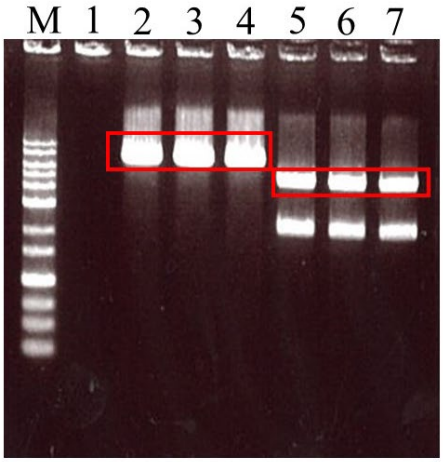

NOTE:

M : Ladder 1 kb
1 : Blank
2 : pGM1190 cutting NdeI, BamHI
3 : pGM1190 cutting NdeI, BamHI
4 : pGM1190 cutting NdeI, BamHI
5 : CasPmCDA1 cutting NdeI, BamHI
6 : CasPmCDA1 cutting NdeI, BamHI
7 : CasPmCDA1 cutting NdeI, BamHI

Figure 4.2 Utilizing *NdeI* and *BamHI* enzymes, the basic pGM1190 plasmid is electroporated (evidenced by bands 2-4). Similarly, the pMA RQ_UGI_dCasPmCDA1 is cleaved with *BamHI* and *NdeI* enzymes to isolate the CasPmCDA1 site, as indicated by bands 5-7.

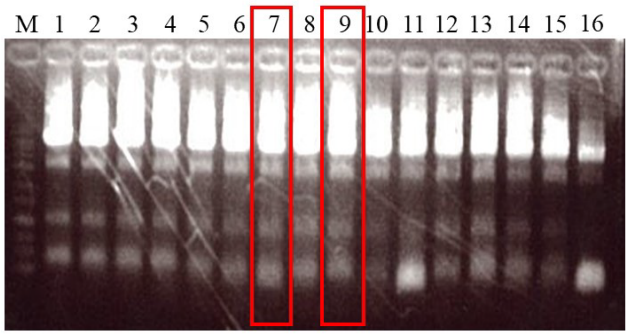

M : Ladder 1 kb
1 : pGM1190-Cas-Pm-CDAI-Knk125,126-infusion-1
2 : pGM1190-Cas-Pm-CDAI-Knk125,126-infusion-2
3 : pGM1190-Cas-Pm-CDAI-Knk125,126-infusion-3
4 : pGM1190-Cas-Pm-CDAI-Knk125,126-infusion-4
5 : pGM1190-Cas-Pm-CDAI-Knk125,126-infusion-5
6 : pGM1190-Cas-Pm-CDAI-Knk125,126-infusion-6
7 : pGM1190-Cas-Pm-CDAI-Knk125,126-infusion-7
8 : pGM1190-Cas-Pm-CDAI-Knk125,126-infusion-8
9 : pGM1190-Cas-Pm-CDAI-Knk125,126-9
10 : pGM1190-Cas-Pm-CDAI-Knk125,126-gibson-2
11 : pGM1190-Cas-Pm-CDAI-Knk125,126-gibson-3
12 : pGM1190-Cas-Pm-CDAI-Knk125,126-gibson-4
13 : pGM1190-Cas-Pm-CDAI-Knk125,126-gibson-5
14 : pGM1190-Cas-Pm-CDAI-Knk125,126-gibson-6
15 : pGM1190-Cas-Pm-CDAI-Knk125,126-gibson-7
16 : pGM1190-Cas-Pm-CDAI-Knk125,126-gibson-8

Figure 4.3 The successful integration of the casPmCDA1 into the pGM1190 plasmid was confirmed through the electroporation of PCR findings.

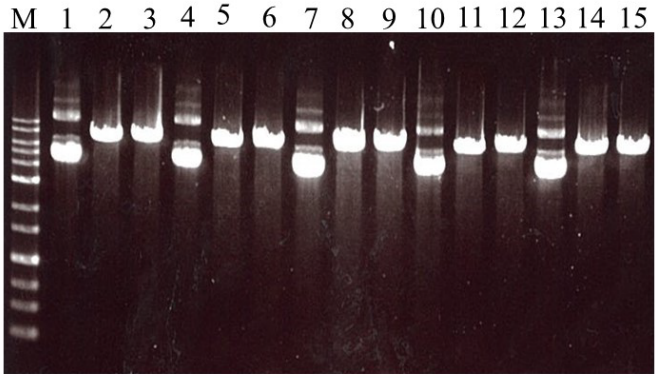

M :Ladder 1 kb
1 :lig pGM1190-CasPmCDA 1-(No cut)
2 :lig pGM1190-CasPmCDA 1-SnaBI
3 :lig pGM1190-CasPmCDA 1-NdeI, BamHI
4 :lig pGM1190-CasPmCDA 2-(No cut)
5 :lig pGM1190-CasPmCDA 2-SnaBI
6 :lig pGM1190-CasPmCDA 2-NdeI, BamHI
7 :lig pGM1190-CasPmCDA 3-(No cut)
8 :lig pGM1190-CasPmCDA 3-SnaBI
9 :lig pGM1190-CasPmCDA 3-NdeI, BamHI
10 :lig pGM1190-CasPmCDA 4-(No cut)
11 :lig pGM1190-CasPmCDA 4-SnaBI
12 :lig pGM1190-CasPmCDA 4-NdeI, BamHI
13 :lig pGM1190-CasPmCDA 5-(No cut)
14 :lig pGM1190-CasPmCDA 5-SnaBI
15 :lig pGM1190-CasPmCDA 5-NdeI, BamHI

Figure 4.4 The outcomes of the binding between pGM1190 and CasPmCDA1 plasmid were re-verified through digestion with an alternate retriction enzyme. In one instance, the plasmid was cleaved using *SnaBI*, while in another a dual enzymatic approach was employed involving *NdeI* and *BamHI*.

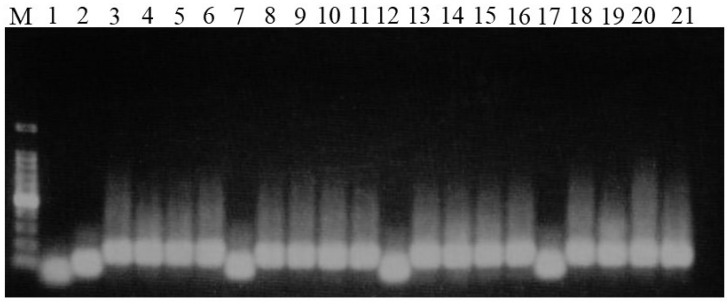

M : Ladder 100 bp
1 : gRNA
2 : ermE- target 10
3-6 : Overlap (gRNA-ermE-target 10)
7 : ermE- target 11
8-11 : Overlap (gRNA-ermE-target 11)
12 : ermE- target 12
13-16 : Overlap (gRNA-ermE-target 12)
17 : ermE- target 13
18-21 : Overlap (gRNA-ermE-target 13)

Figure 4.5. Theoutcomes of the gel electrophoreses step reveal the gRNA component, the ermE-target and combine between gRNA-ermE target by overlap PCR.

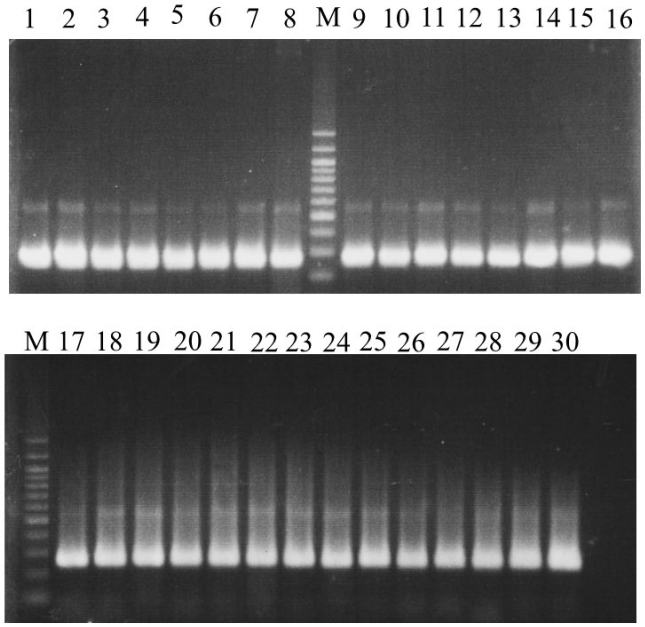

M : Ladder 100 bp
1-4 : pGM1190-dCasPmCDA-UGI-AAV target 6
5-8 : pGM1190-dCasPmCDA-UGI-AAV target 7
9-12 : pGM1190-dCasPmCDA-UGI-AAV target 8
13-15 : pGM1190-dCasPmCDA-UGI-AAV target 9
16 : pGM1190-dCasPmCDA-UGI-AAV target 13
17-18 : pGM1190-dCasPmCDA-UGI-AAV target 15
19-21 : pGM1190-dCasPmCDA-UGI-AAV target 16
22-24 : pGM1190-dCasPmCDA-UGI-AAV target 17
25-27 : pGM1190-dCasPmCDA-UGI-AAV target 18
28-30 : pGM1190-dCasPmCDA-UGI-AAV target 19

Figure 4.6 The process of confirming the results of target infusion into the pGM1190-dCasPmCDA-UGI-AAV plasmid with gRNA-ermE target.

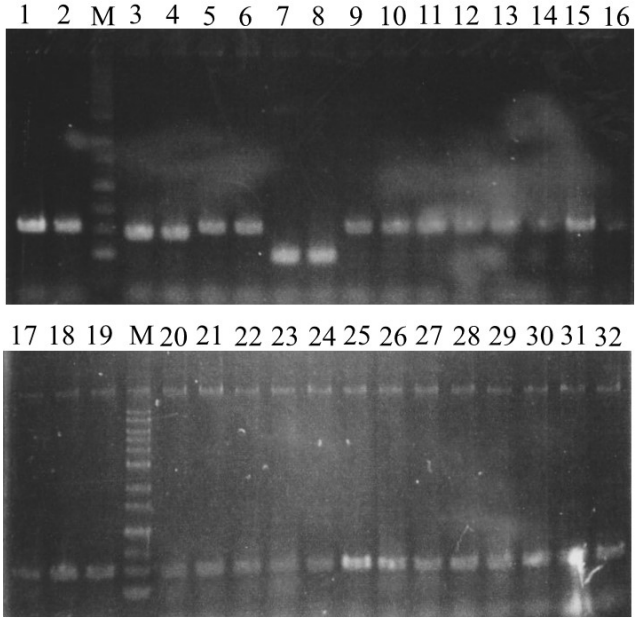

M : Ladder 1 kb
1-2 : pGM1190-dCasPmCDA-UGI-AAV target 10
3-4 : Vector AH
5-6 : Vector BH
7-8 : Empty vector
9-10 : pGM1190-dCasPmCDA-UGI-AAV target 12
11-12 : pGM1190-dCasPmCDA-UGI-LVA target 12
13-14 : pGM1190-dCasPmCDA-UGI-AAV target 13
15-16 : pGM1190-dCasPmCDA-UGI-LVA target 13
17-18 : pGM1190-dCasPmCDA-UGI-AAV target 14
19-20 : pGM1190-dCasPmCDA-UGI-LVA target 14
21-22 : pGM1190-dCasPmCDA-UGI-AAV target 17
23-24 : pGM1190-dCasPmCDA-UGI-LVA target 17
25-26 : pGM1190-dCasPmCDA-UGI-AAV target 18
27-28 : pGM1190-dCasPmCDA-UGI-LVA target 18
29-30 : pGM1190-dCasPmCDA-UGI-AAV target 20

Figure 4.7 The process of confirming the results of target infusion into the pGM1190-dCasPmCDA-UGI-AAV/LVA plasmid with gRNA-ermE target.

IV.2.3 Intrageneric conjugation

A helper plasmid PUB307 is required to assist the mobilization of pGM1190-dCasPmCDA-UGI-AAV plasmid into *Streptomyces* strains. After the PUB307 plasmid was transformed into *E. coli* JM109, it was necessarily transferred into *E. coli* HST04, which already contained pGM1190-dCasPmCDA-AAV/LVA_target, and we used the mating. The *E. coli* HST04 pGM1190-dCasPmCDAAAV/LVA_target has an apramycin resistance gene from pGM1190 plasmid and a kanamycin resistance gene from PUB307 plasmid, used as selected markers. In the end, the positive transformant was selected based on the colony formation of *E. coli* HST04 strain containing these two different plasmids, which were generated with a Kanamycin-selected helper plasmid and an Apramycin marked plasmid on the LB agar containing kanamycin and apramycin.

IV.2.4 Intergeneric conjugation for transferring plasmid from *E. coli* to *S. coelicolor*

Conjugation between *E. coli* HST04/ pGM1190-dCasPmCDA-AAV/LVA_target-PUB307 and *S. coelicolor* using a modified method[116]. Inoculation of a single colony of *E. coli* HST04 carrying pGM1190-dCasPmCDAAAV/LVA_target and PUB307 was conducted in LB medium, supplemented with 50 μg/mL apramycin and 50 μg/mL kanamycin. After incubation at 37°C for 18 h with agitation at 200 rpm, the optical density at 600 nm was measured and then adjusted to 0.5 using LB medium. The cells were harvested and washed twice with LB medium to remove antibiotics by

centrifugation at 5500 rpm for 4 min and resuspended in 1 mL LB medium. *S. coelicolor* spore suspension stored at −80°C was used as the recipient. The spores at 106 were washed using LB medium, resuspended in 200 μL 2xTY medium, and incubated at 50°C for 10 min to activate the spore germination. The *E. coli* cultured were mixed with the heat-tread spores, incubated for 1 h at 28°C, then spread in the ISP4 medium plate medium. The plate was incubated for 16–24 h at 30°C, overlaid with 3 mL soft agar containing LB medium (0.8%), 50 μg/mL nalidixic acid to eliminate *E. coli* and 50 μg/mL apramycin. The incubation process continued at 30 °C until colonies of exconjugants appeared. Each conjugant was transferred into ISP2 medium agar containing 20 μg/mL apramycine, 0.5 μg/mL thiostrepton. Generally, the experiment procedure is illustrated in Figure 4.8.

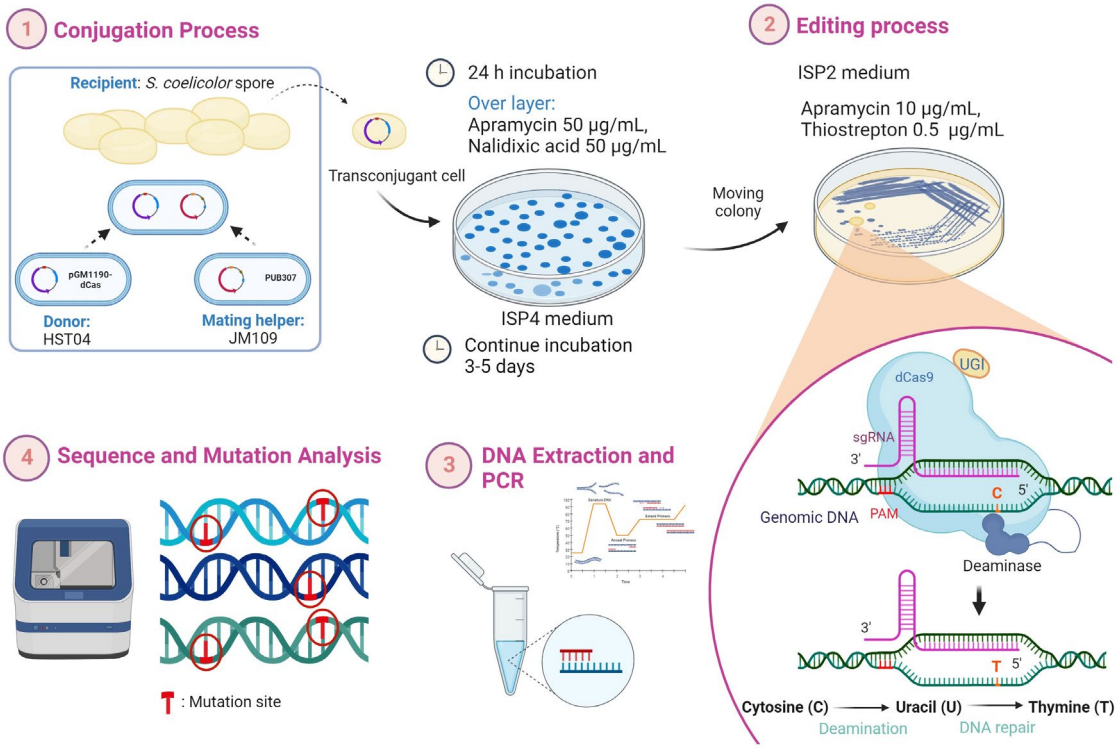

Figure 4.8 Overview of genome editing using CRISPR-dCas9-PmCDA-UGI in *S. coelicolor*.

IV.2.5 Actinorhodin detection

To investigate extracellular actinorhodin using the modified method from [116–119] *S. coelicolor* at 10^9 spores were inoculated into 15 mL of ISP2 liquid medium and grown at 30°C for 3 days with shaking, used as a seed culture. For the fermentation process, 100 mL of basal medium containing K_2SO_4 (2 g), NaCl (1 g), K_2HPO_4 (15 mmol), and NH_4Cl or NO_3K (40 mmol) prepared in 500 mL Erlenmeyer flask was inoculated with 3 mL of the seed culture. Before adjusting the pH to 7, $MgSO_4 \cdot 7H_2O$ (80 mg), $ZnSO_4 \cdot 7H_2O$ (2 mg), and 0.1 mL of trace element solution were added. The trace element solution used was composed by $CuSO_4 \cdot 5H_2O$ 0.5 g/L, $MnSO_4 \cdot H_2O$ 5 g/L, H_3BO_3 4 g/L, $CoCl_2 \cdot 6H_2O$ 0.5 g/L,

$NiCl_2 \cdot 6H_2O$ 2 g/L and $Na_2MoO_4 \cdot 2H_2O$ 3 g/L. Following autoclaving, 0.1 g/L of separately autoclaved $CaCl_2 \cdot 2H_2O$ and 5 g/L of glucose were added. The cultures were incubated at 30°C for 7 days in the dark with shaking after adding 50 mg/L of filter-sterilized yeast extract.

To extract actinorhodin, 30 mL sample was taken from each culture, centrifuged at 8000×g for 10 min at room temperature, transferred the supernatant to a 50 mL tube, adjust the pH until 2 with 1 N HCl, and added chloroform to the supernatant at a ratio of 1:4. The mixed solution was shaken vigorously and then centrifuged at 8000×g for 5 min at room temperature. The chloroform phase was collected and evaporated. After drying, 2 mL solvent (methanol: chloroform = 1:1) was added. A UV spectrophotometer was used to analyze the solutions at various absorptions.

IV.2.6 Off-target confirmation

Nonspecific mutations occurring at unintended places, known as "off-targets," are a significant problem in the CRISPR system. This study employed Next Generation Sequencing (NGS) to assess the unintended impacts following the editing process. The complete genomic sequence of *S. coelicolor* (wild type) and genetically modified strains were compared and analyzed using CRISPR tools provided by Geneious prime (Biomatters, Inc., Auckland, New Zealand). A search was conducted for the gRNA CRISPR sites within the targeted gene, as well as for

off-target binding sites within the genome of interest. This study focused only on conducting off-target evaluation specifically for the actinorhodin gene.

IV.3. RESULTS AND DISCUSSION

IV.3.1 Basic vector construction and AID system

The constructed a host-vector CRISPR complex utilizing a high copy number temperature-sensitive vector, pGM1190, which uses apramycin as a selection marker. The sgRNA expression was driven by a constitutive ermE promoter and terminated by the fd terminator, while the expression of dCas9 was regulated by the thiostrepton inducible tipA promoter. The vector was equipped with oriT, enabling its mobility. We used an enzyme-deactivated Cas9 variant (dCas9), which lacks endonuclease activity due to inactivating mutations in its RuvC and HNH catalytic domains[113,120]. For precise control over targeted modifications at the desired site, the protein was fused to transcriptional activator, repressor, and effector domains. To tightly regulate this protein's cellular level, LVA and AAV tag variants were utilized. Additionally, to enhance the base conversion process by blocking the cell's natural repair mechanisms, Uracil Glycosylase Inhibitor (UGI) was incorporated. In practice, after cytidine deaminase converts a target cytosine to uracil, UGI prevents the cell from reversing this edit, thereby making the modification permanent[121]. After transforming *E. coli* JM109, the foundational vector was successfully constructed. The ermE promoter, along with the target region and gRNA, was amplified via

PCR. In this process, the 128 bp gRNA and the 178 bp ermE promoter-target region were combined using overlap PCR, resulting in a gRNA-ermE-target cassette with a total length of 306 bp (as shown in Figure 4.9). This gRNA-ermE-target fragment was then inserted into the pre-digested basic plasmid (cut with SnaBI) through the use of an In-Fusion HD Cloning Kit.

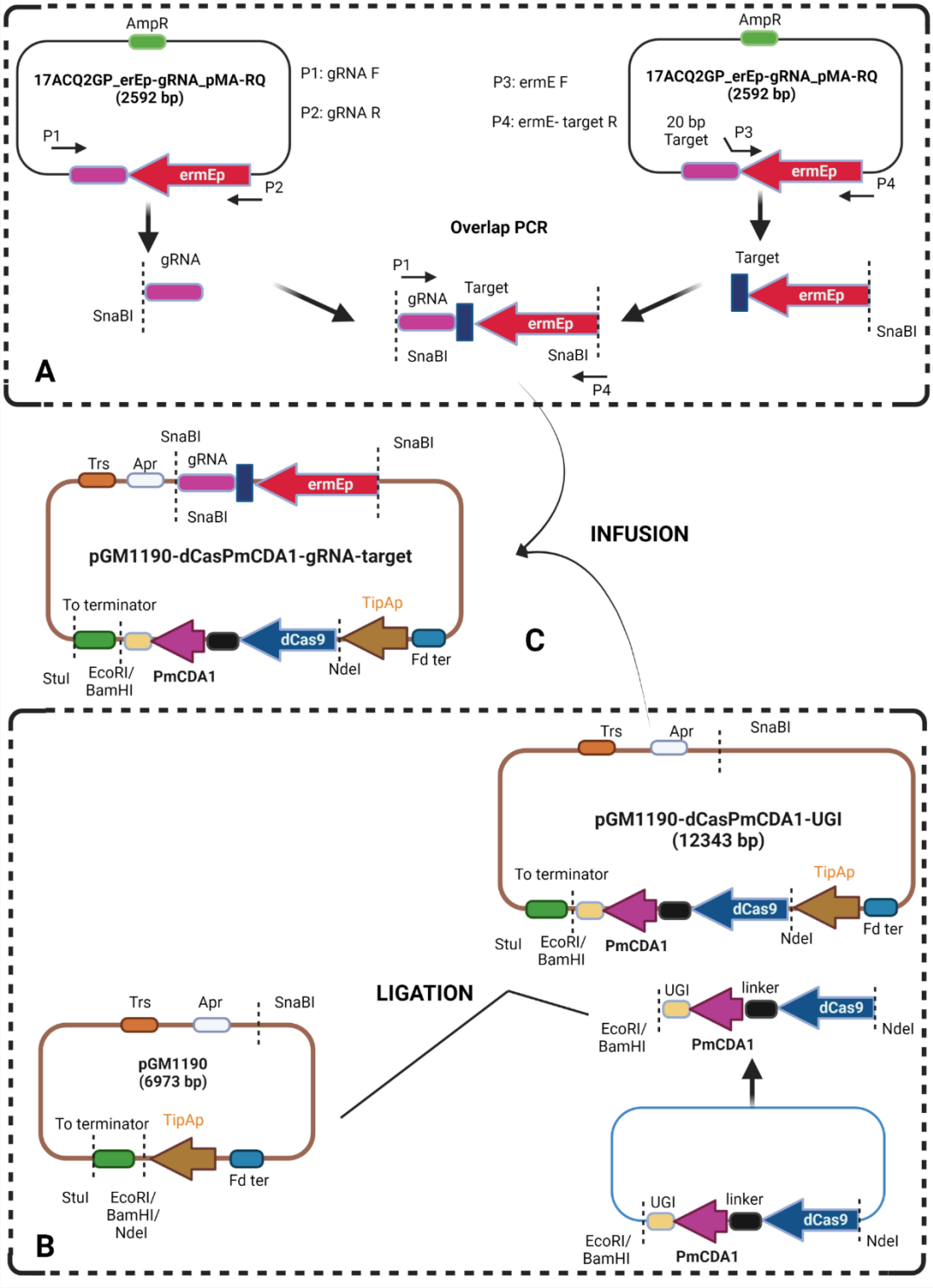

Figure 4.9 Plasmid construction. (A) Step to prepare ermE promoter and gRNA region. (B) The construction of vector backbones integrating the fused dCasPmCDA1-UGI. (C) Complete vector.

IV.3.2 Evaluation of the CRISPR-dCas9-AID-UGI-AAV/LVA fusion system in *Streptomyces*

In model strain *S. coelicolor*, the Target-AID system was assessed using a combination of dCas9 from *Streptococcus pyogenes*, activation-induce cytidine deaminase (AID), PmCDA from sea lamprey (*Petromyzon marinus*) and a uracil DNA glycosylase inhibitor (UGI). The *S. coelicolor* has the capability to produce Actinorhodin (ACT), a distinctive blue pigment[122]. Actinorhodin belongs to the class of polyketides and is synthesized through a specific polyketide synthase (PKS) pathway. This synthesis pathways comprises a sequence of enzyme-driven reactions that eventually result in Actinorhodin production. It begins with the formation of precusor molecules like acetyl-CoA and malonyl-CoA, which act as foundational units for building polyketides. Through the catalytic action of PKS, the polyketide chain elongates progressively. Subsequently, this growing chain undergoes cyclization, chemical modifications, and structural rearrangements, forming a stable aromatic system essential for Actinorhodin synthesis[122].

In this study, the application of dCas9-PmCDA-UGI_AAV based base editing proved effective in *Streptomyces*. Prior research demonstrated the success of Target-AID in *E.coli* by fusing PmCDA1 with an LVA tag and UGI. According to these studies, target-AID facilitates the conversion of cytosine (C) to thymine (T), which introduces a stop codon[115]. To evaluate the potential of deaminase-mediated targeting within *Streptomyces*, we developed e Target-AID-dCas-PmCDA system. This fusion protein was engineered to enhance mutation

efficiency by incorporating UGI (Uracil-DNA glycosylase inhibitor) and a degradation tag at the C-terminus of dCas-CDA[115]. UGI, derived from Bacillus subtilis bacteriophage, inhibits the action of uracil-DNA glycosylase (UDG), preventing DNA repair on the targeted sequence[123]. Additionally, the degradation tag, a short peptide sequence, directs the protein toward the cellular degradation machinery. Variants of these tags, such as AAV, ASV, LVA, and LAA, have been designed with differences in the final three amino acids to adjust protein stability[124]. Banno et al[115]. emphasized the LVA tag's significance for genome editing in *E. coli*, highlighting its role in enhancing editing efficiency. The LVA tag facilitates the degradation of the dCas9-CDA-UGI fusion protein, thereby reducing potential toxicity. By regulating the concentration of this fusion protein, the LVA tag improves genome editing efficiency and helps prevent off-target effects and unintentional mutations. When applied to *Streptomyces* strains, the strains continued to produce Actinorhodin. In other research, the AAV tag has been used to target specific proteins for degradation, a technique particularly advantageous for synthetic circuits that rely on a stable presence of functional proteins[125]. We continue to use the AAV degradation tag for ongoing research, as it has consistently yielded favorable results throughout the studies.

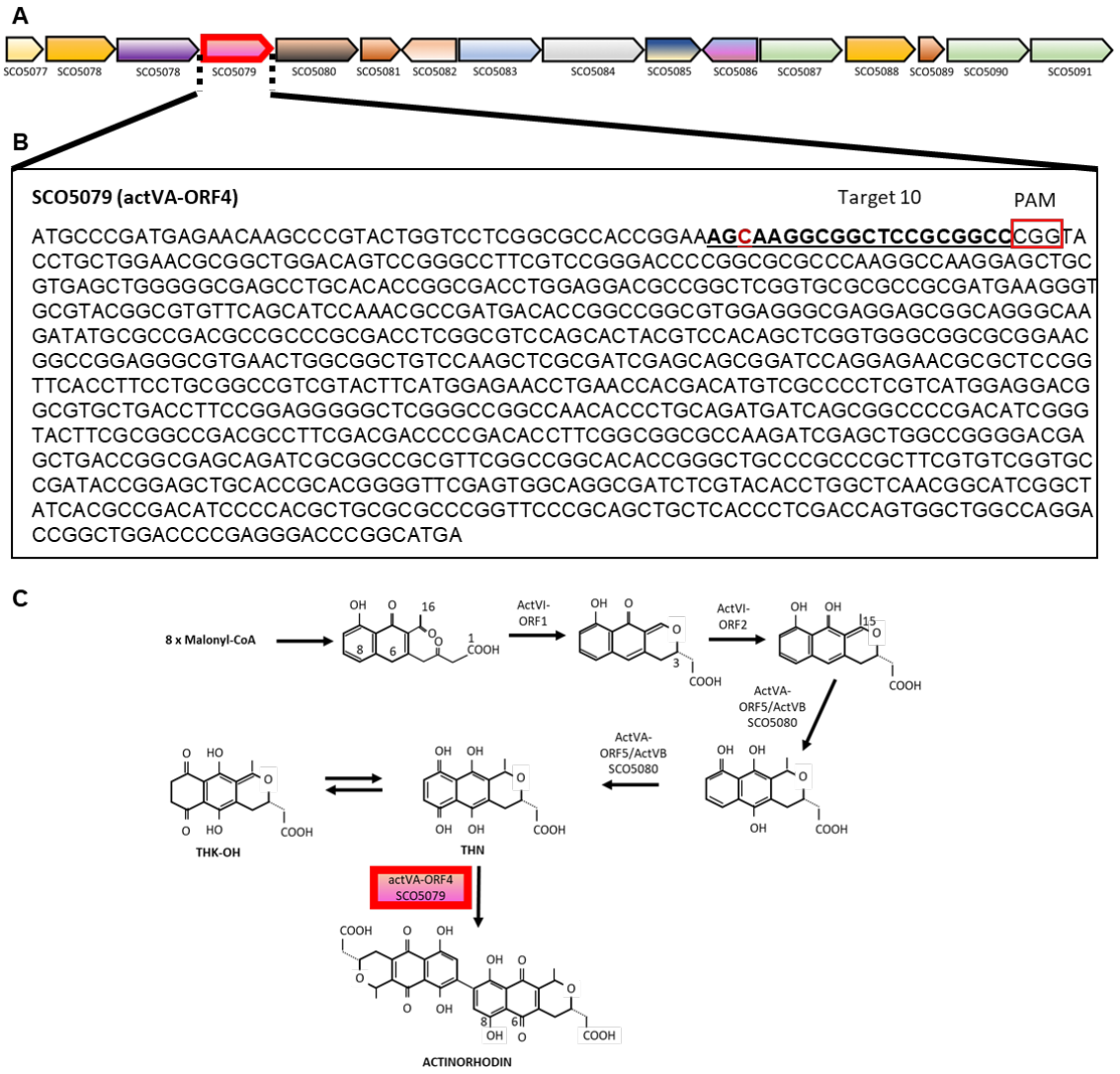

Figure 4.10 Essential genes for actinorhodin production. (A) Actinorhodin gene cluster. (B) Mutated target gene actVA-ORF4. The positions of PAM sequence (GGC) and target 10 are given. (C) The position of SCO5079 protein (actVA-ORF4) in actinorhodin biosynthesis.

In this study, *Streptomyces coelicolor* was utilized to investigate key genes involved in the biosynthesis pathway of actinorhodin, focusing specifically on several genes related to this process (as shown in Figure 4.10). The targeted genes included *actVA-ORF4* (SCO5079), *actVA-ORF5* (SCO5080), *actII-ORF2* (SCO5083), *actI-ORF2* (SCO5088), *actIV* (SCO5091), *actI-ORF4* (SCO5090),

and *actIII* (SCO5086). Additionally, *actII-ORF4* (SCO5085), which has a length of 768 nucleotides, was examined for two specific target regions: target 8 at nucleotide positions 628–646 and target 9 at positions 510–529. Similarly, the *actVA-ORF4* (SCO5079) gene, which is 885 bp long, presented four targets: target 10 at positions 46–66, target 11 at 230–250, target 12 at 235–254, and target 13 at 361–380. The 1737 bp *actII-ORF2* (SCO5083) gene contained two targets, with target 15 located at positions 755–774 and target 16 at 106–123. The 1224 bp *actI-ORF2* (SCO5088) had one target (target 17) at positions 249–268, while the 894 bp *actIV* (SCO5091) included a single target, target 18, at 309–328. Finally, the 951 bp *actI-ORF4* (SCO5090) gene had one target region, target 19, spanning positions 155–174. A detailed summary of these target positions is presented in Table 4.3.

Table 4.3 Target sequence position in *S. coelicolor* NBRC15146 genome.

Name	Sequence nucleotide	Pam	Position
Target 8 (5 ’- 3’)	CAGATGGGCAGGCGC GCCG	AGG	5.528.721-5.528.739
Target 9 (5’ - 3’)	TATCGACGCGAATTG GCGGC	TGG	5.528.603-5.528.622
Target 10 (5’ - 3’)	AGCAAGGCGGCTCCG CGGCC	CGG	5.520.903-5.520.922

Target 11 (5’ - 3’)	GCATCCAAACGCCGA TGACAC	CGG	5.521.086-5.521.106
Target 12 (5’ - 3’)	CAAACGCCGATGACA CCGGC	CGG	5.521.091-5.521.110
Target 13 (3’ - 5’)	CTCCCGCACTTGACC GCCGA	CGG	5.521.217-5.521.236
Target 14 (5’ - 3’)	CCAGGAGCGGCCGTC CCTGA	CGG	5.521.758-5.521.777
Target 15 (5’ - 3’)	TCCAGGGGCGCGAAC GCGGC	TGG	5.524.827-5.524.846
Target 16 (3’ - 5’)	GGGATGCGCGCGGC AACC	CGG	5.524.178-5.524.195
Target 17 (5’ - 3’)	CCAGGACGCGAAGGC GGACC	CGG	5.531.449-5.531.468
Target 18 (3’ - 5’)	CCGGGAGTGGCCCGA GACCG	AGG	5.533.961-5.533.980
Target 19 (3’ - 5’)	TTGCGAAGGCCTAGA CCCGC	CGG	5.532.860-5.532.879
Target 20 (3’ - 5’)	GGGCGGAACTCCTGG ACAAA	CGG	5.529.335-5.529.354

In our study, we designed 13 sgRNAs targeting specific genes, positioning each approximately 17-20 nucleotides upstream of the PAM sequence. These sgRNAs were introduced into *Streptomyces coelicolor* via the pGM1190 vector, which carries the CRISPR editing system. For controls, we used the empty vector, pGM1190-dCas9-PmCDAUGI-AAV/LVA, without any inserted target, following an identical approach. The editing mechanism was under strict regulation by the tipA promoter, with thiostrepton as an inducer to initiate the system. After conjugation on ISP4 medium, we transferred the exconjugants to ISP2 medium containing thistrepton to induce editing.

We assessed editing efficiency by performing PCR and DNA sequencing on the target regions from colonies that did not produce the characteristic blue pigment. Among all targets, only one achieved a successful mutation, introducing a stop codon and thereby creating a knockout effect (Figure 4.11B, C). This mutant strain CrA10, harbored the pGM1190-dCas9-PmCDAUGI-AAV vector targeting *actVA-ORF4* (SCO5079) and demonstrated a lack of actinorhodin production. In contrast, the strains corresponding to the other 12 sgRNA exhibited single-nucleotide mutations that did not result in stop codons capable of disrupting gene expression. Consequently, these mutants retained the ability to produce ACT, as confirmed by the data (data not shown).

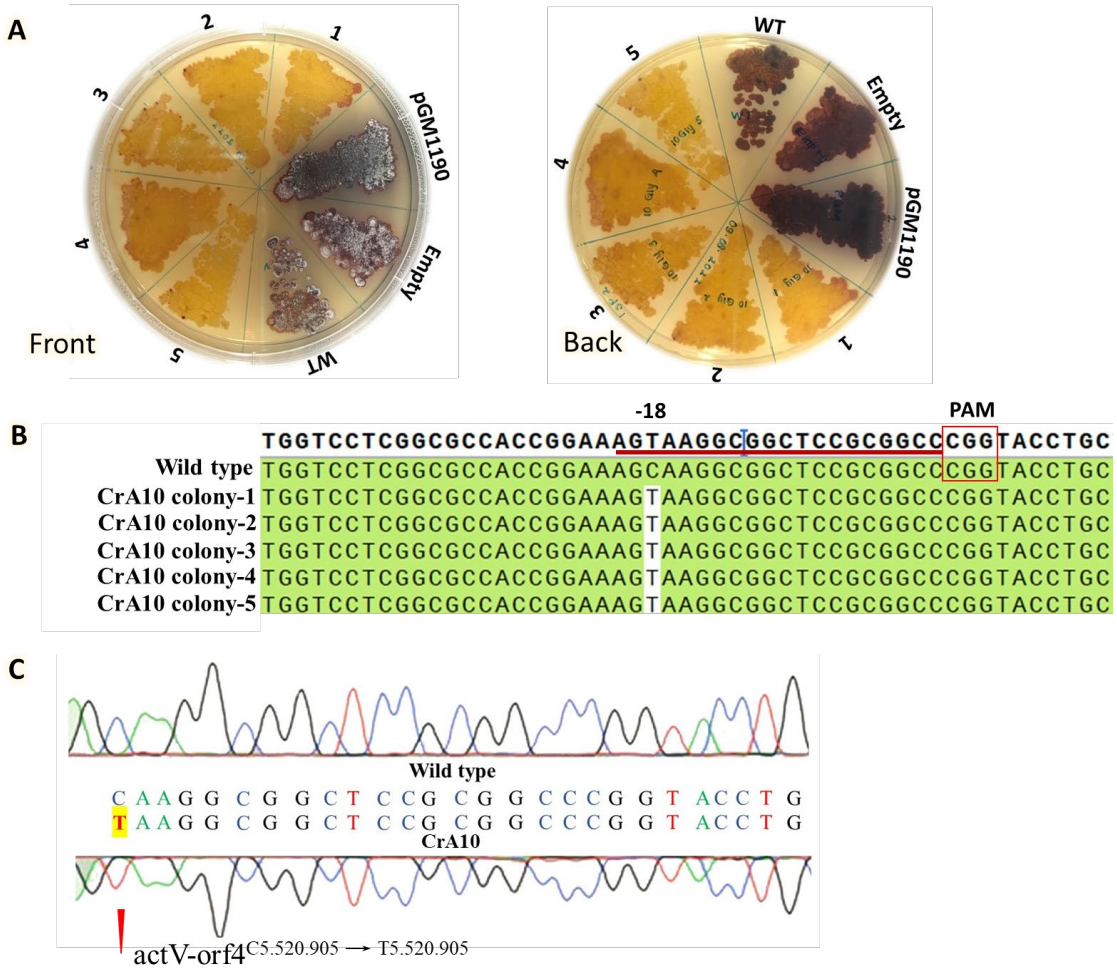

Figure 4.11 Genome editing using dCas9-PmCDA-UGI-AAV system. (A) Phenotypical analysis of five mutants selected and grew on ISP2 medium agar, the mutant with targeted actVA-ORF4. Wild-type *S. coelicolor*, pGM1190, and Empty vector (dcas9-PmCDA-UGI-AAV without target) were used as control experiments. (B) Sequence alignment between Wild type and target 10 (*actVA-ORF4*) edited by dCas9-PmCDA-UGI-AAV. The PAM sequence is shown in the red box, and the site targeted by sgRNA is indicated by a brown underline. Uncolored bases are seen in single mutation results. (C) A typical sequencing chromatogram showing the mutation from C to T in the target location. *S. coelicolor* wild-type strain was used as a control.

The *actVA-ORF4* gene, part of the *actVA-actVB* system in *Streptomyces coelicolor*, is essential to the flavin-dependent monooxygenase system that facilitates actinorhodin (ACT) biosynthesis. Specifically, it enables the

dimerization of a benzoisochromanequinone (BIQ) intermediate during ACT production. Disruption or deletion of the actVA-ORF4 gene halts ACT synthesis, highlighting its critical role in ACT biosynthesis and its potential involvement in cellular energy management. In the absence of actVA-ORF4, a genetic variant produces 8-hydroxy-DHK, a modified form of hydrokalafungin that resembles the single unit of ACT. This finding suggests that actVA-ORF4 is key in catalyzing the C-C bond formation for BIQ dimerization in ACT synthesis[126,127].

The streaking result on ISP2 medium confirmed that the engineered system effectively inhibited actinorhodin production in the CrA10 mutant, as evidenced by the observed phenotype. In contrast, strains containing control vectors (pGM1190-dCas-PmCDA-UGI-AAV/LVA without the specific target sequence) continued to produce actinorhodin, as shows in Figure 4.11 A.

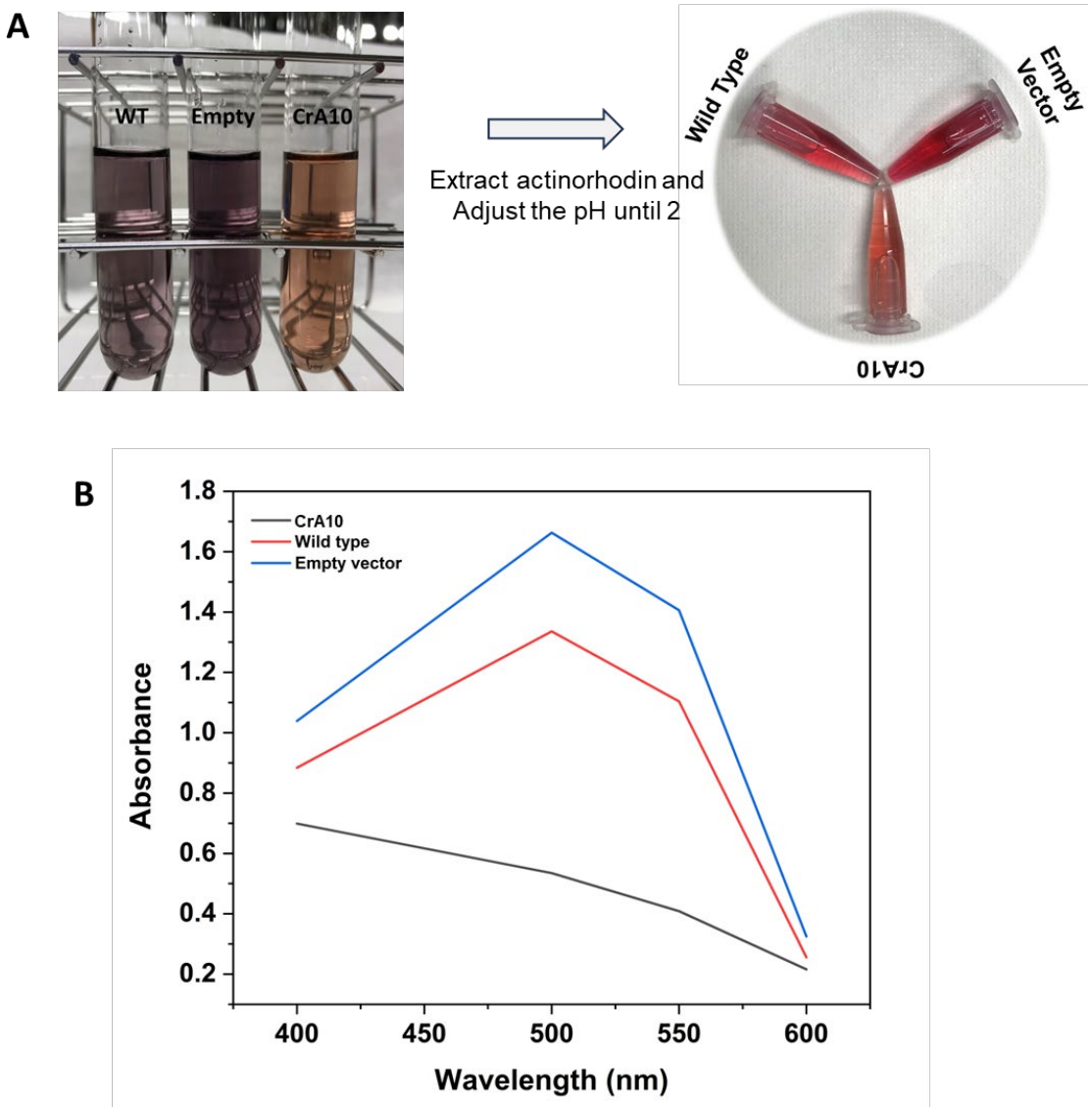

Figure 4.12 The actinorhodin color differences from the cultures of WT (Wild type), Empty (plasmid CRISPR system with no expected target), Target 10 (plasmid CRISPR system with 20 nucleotides from gen actVA-ORF4 as targets) At a pH of 2, actinorhodin undergoes a color change, shifting from its initial blue to a distinct red are depicted in the photograph (A) and observed at various absorbances (B).

To further validate these results from the agar plate experiments, we cultured the clones in a liquid basal medium and quantified actinorhodin levels using UV-visible spectroscopy. Notably, actinorhodin undergoes a color shift from blue to red under acidic condition (pH 2), as illustrated in Figure 4.12 A. Absorbance

measurements were taken across multiple wavelengths, with results presented in Figure 4.12B. These data revealed that absorbance peaks at 500 nm were prominent in both the wild-type and control vector sample, while CrA10 mutant (target 10) exhibited significantly lower absorbance values compared to wild-type. This reduction in absorbance suggests that the system successfully targeted the *actVA-ORF4* (SCO5079) gene, effectively inhibiting their expression and leading to a suppression of actinorhodin biosynthesis.

IV.3.3 Characterization of mutation and off-targets

To facilitate conjugation from E. coli to *Streptomyces*, the plasmid pUB307 is required. During the mating process, the AID-system vector contained within pGM1190 is mobilized into E. coli strain HST04. Here, pUB307 enables the transfer of the AID-system vector into *Streptomyces* spore. To initiate germination, *S. coelicolor* spore were incubate at 50°C for 15 minute, then mixed with *E. coli* HST04/pUB307 and pGM1190, and subsequently plated on ISP4 agar. After 18 hours, 3 mL of an upper layer NB medium (containing 0.8% NB and 0.5% soft agar with Aztreonam at 50 μg/mL, Nalidixic acid at 5 μg/mL, and Apramycin at 50 μg/mL) was overlaid on each plate.

For genome editing, we developed a CRISPR system that combines the dead cas9 protein (dCas9), cytidine deaminase (PmCDA1) derived from *Petromyzon marinus*, a uracil glycosylation inhibitor (UGI), and a degradation tag (AAV). The codon-optimized dCas9 gene is controlled by a promoter from the *tipA* gene,

which is activated by thiostrepton induction[128,129]. The ermE promoter drives gRNA expression[119,130]. Additionally, the Activation-induced Cytidine Deaminase (AID), part of the apolipoprotein B mRNA-editing catalytic family, acts as an RNA editor capable of converting C to U in DNA and RNA, leading to mutations. While increasing UGI copy number at the C terminus does not further enhance editing efficiency, adding a single UGI copy at the C terminus boosts editing levels three- to tenfold, even in cases without UGI[131].

Understanding and minimizing off-target effects in genome editing is critical, as these unintended modifications can have long-term impacts on the viability and functionality of edited cells. This highlights the importance of reliable methods for off-target detection[132]. Previously, the T7 endonuclease assay was commonly employed for this purpose; however, its sensitivity is limited, particularly in detecting mutations occurring at frequencies below 1%[133,134]. To address these limitations, numerous computational tools have been developed to predict and identify CRISPR off-target sites. Advanced techniques such as Digenome-seq[135], CIRCLE-seq[136], and GUIDE-seq[137] have emerged, enhancing detection capabilities. Early algorithms for off-target prediction primarily relied on analyzing potential off-target regions based on the sgRNA sequence.

We conducted a thorough examination of the complete genome sequence of CrA10 laboratory strains, comparing it with the reference genome to investigate potential off-target effects induced by the Target-AID system. Our focus was on key genes involved in actinorhodin synthesis. Our detailed analysis of single

nucleotide variants (SNVs) revealed multiple mutations: two in *actVA-OFR4* (SCO5079), 24 in *actVA5* (SCO5080), 83 in actII-ORF2 (SCO5083), three in *actII-ORF4* (SCO5088), and 26 in *actIII* (SCO5086). Notably, no mutations were detected in *actI-ORF2* (SCO5088), *actI-ORF4* (SCO5090), and *actIV* (SCO5091).

We also identified deletions and insertions in various other genes, as illustrated in Figure 4.13B. A significant observation was the frequent substitution of cytosine (C) with thymine (T), highlighted in Figure 4.13A. This substitution pattern strongly suggests that the Target-AID system was responsible for these SNVs. Interestingly, the Geneious program failed to predict the unintended mutations and did not correlate with any of the spacers we utilized. To validate our findings, we re-examined the mutation sites relative to the PAM sequence. However, this validation showed a limited number of changes, none of which resulted in the insertion of stop codons, as depicted in Figure 4.13C.

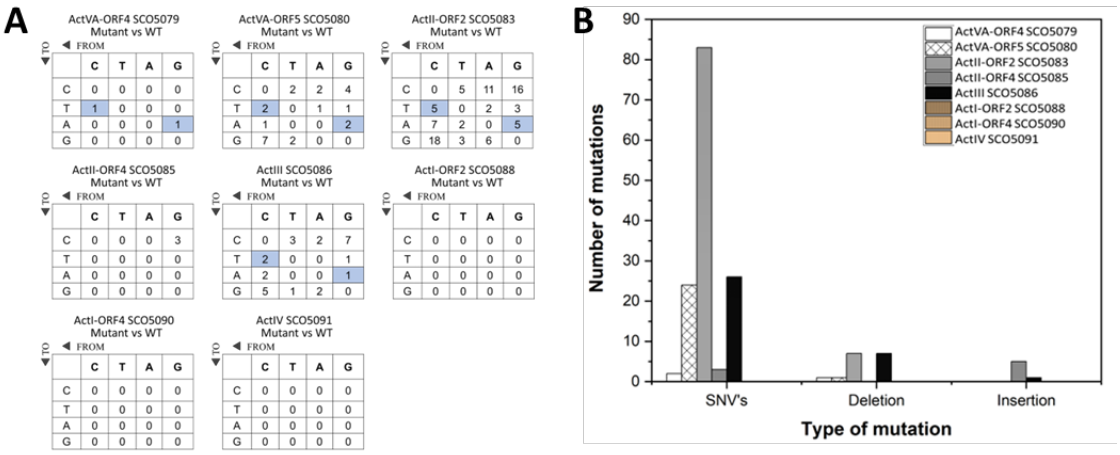

C

Gene	Mutation			PAM	Position
	from	to			
ActVA-ORF4 SCO5079	C	T	18 bp	CGG	5573921
	G	A	18 bp	GGG	5573952
ActII-ORF2 SCO5083	A	C	22 bp	CGG	5577904
	C	G	20 bp	AGG	5578657
	C	G	18 bp	GGG	5578749
ActIII SCO5086	G	C	19 bp	CGG	5582313
	C	G	20 bp	CGG	5582377

Figure 4.13 The outcome of assessing mutations in the open reading frame (ORF) genome plays a crucial role in producing actinorhodin. (A) The mutated gene critical for actinorhodin production was analyzed and compared to the reference sequence from the *S. coelicolor* wild type. The study recorded the total count of single nucleotide variants (SNVs) in this analysis. (B) The number of mutations based on the mutation types, including SNVs, deletions, and insertions, were observed in the critical genes. (C) The single nucleotide variations (SNPs) are observed in multiple ORFs, these mutations do not result in the creation of a stop codon.

IV.4. CONCLUSION

This study explored the application of a CRISPR-dCas9-AID-UGI-AAV/LVA fusion system in *Streptomyces* strains, utilizing a high copy number vector, pGM1190, with distinct genetic control elements. The method effectively targeted specific genes in *S. coelicolor*, leading to the suppression of actinorhodin synthesis. Through precise genome editing and subsequent analysis to assess off-target effects, the study revealed unexpected genetic changes. These results demonstrate the system's capability in gene disruption while highlighting the critical need for thorough evaluation of unintended genetic modifications. This underscores both the potential and challenges of advanced genome editing technologies in bacterial research.

CHAPTER V

General Conclusions and Future Research

This dissertation comprehensively explores the biotechnological potential of the *Streptomyces* genus, emphasizing its role in producing secondary metabolites, lipids, and biopolymers. By integrating advances in genetic engineering and metabolic insights, the research contribute significantly to biotechnology, particularly in addressing global challenges in medicine, industry, and environmental sustainability. Below the conclusions are synthesized in the context of each preceding chapter to maintain coherence, followed by future research dirrections.

highlighting its pivotal role in secondary metabolite production, lipid biosynthesis, biopolymer synthesis, and advancements in genetic engineering. The study begins by establishing the significance of *Streptomyces* in biotechnology and microbiology, particularly its capacity to produce antibiotics and other bioactive compounds. This ability is underpinned by the genus's remarkable genomic plasticity and ecological adaptability, enabling it to thrive in diverse and extreme environments. Additionally, *Streptomyces* exhibits key enzymatic activities, such as cellulase and chitinase production, which contribute to nutrient cycling and ecosystem dynamics. Its high-GC-content linear chromosomes provide a genetic foundation for the synthesis of a vast array of bioactive molecules, solidifying its position as a cornerstone of pharmaceutical, agricultural, and industrial innovation, as outlined in Chapter I.

Building on this foundation, in **Chapter II** the dissertation delves into lipid biosynthesis, particularly within *Streptomyces jeddahensis*, revealing the genus's potential to produce triacylglycerols (TAGs) and other lipids that serve as renewable alternatives to fossil fuels. Metabolic engineering approaches, including the optimization of fatty acid synthase (FAS) and acyltransferase activity, were shown to enhance lipid accumulation. This study also highlighted *Streptomyces*' capacity for biopolymer production, focusing on polyhydroxyalkanoates (PHAs), which present sustainable solutions to plastic pollution. By integrating genetic and metabolic tools, the research offers a pathway to advance biopolymer synthesis technologies, aligning with global efforts to reduce environmental impacts.

The genetic engineering capabilities of *Streptomyces* were further explored using a CRISPR-Cas9-based system. In **Chapter III**, this novel adaptation of the CRISPR-dCas9 system enabled precise single-nucleotide edits without inducing double-strand breaks, thereby minimizing off-target effects. By targeting genes involved in actinorhodin biosynthesis in *Streptomyces coelicolor*, the research demonstrated the system's effectiveness in suppressing actinorhodin production while highlighting the potential of CRISPR technologies to activate cryptic biosynthetic gene clusters. However, challenges such as single nucleotide variants (SNVs), deletions, and insertions were identified, emphasizing the need for more refined predictive tools to further enhance the precision and applicability of these technologies.

Finally, the **Chapter IV** investigated the development of *Streptomyces jeddahensis* as a host for polyhydroxyalkanoate production. The genus's ability to metabolize specific carbon sources, such as sodium octanoate, to produce medium-chain-length PHAs with favorable properties for biomedical and industrial applications was demonstrated. This finding reinforces *Streptomyces*' potential as a sustainable biotechnological platform to address critical challenges, including the need for biodegradable materials and alternatives to conventional plastics.

In summary, this dissertation positions *Streptomyces* as a versatile and invaluable genus for tackling pressing global challenges in medicine, agriculture, and environmental sustainability. By combining metabolic engineering, cutting-edge genetic tools, and applied biotechnological methods, this research provides a robust framework for future exploration and practical application of this remarkable microorganism.

LIST OF PUBLICATIONS

Chapter II

P.Apriliana, P. Kahar, N. Rachmadona, W. K. Restu, A. Kondo, C. Ogino. Lipid Production in *Streptomyces jeddahensis* Driven by Glucose and Fatty Acid Derivatives. (Draft to be submitted).

Chapter III

P. Apriliana, P. Kahar, N. Kashiwagi, A. Kondo, C. Ogino, Editing *Streptomyces* genome using target AID system fused with UGI-degradation tag. Eng Life Sci. 2024; 24:e2400005. https://doi.org/10.1002/elsc.202400005

Chapter IV

P. Apriliana, P. Kahar, M. Yara, N. Afiqah, A. Kondo, C. Ogino, Polyhydroxyalkanoate production by oleaginous *Streptomyces jeddahensis* from sodium octanoate. (Draft to be submitted)

Co-authored Publications

S. Ratnakomala, P. Kahar, N. Kashiwagi, J. Lee, M. Kudou, H. Matsumoto, **P. Apriliana,** Y. Yopi, B.Prasetya, C.Ogino, A. Kondo. Manno-Oligosaccharide Production from Biomass Hydrolysis by Using Endo-1,4-β-Mannanase (ManNj6-379) from *Nonomuraea jabiensis* ID06-379. Processes 2022. https://doi.org/10.3390/pr10020269

REFERENCE

1. Schrempf, H. Streptomycetaceae: Life Style, Genome, Metabolism and Habitats. in *Encyclopedia of Life Sciences* (Wiley, 2008). doi:10.1002/9780470015902.a0020393.
2. Nodwell, J. R. Microbe Profile: Streptomyces coelicolor: a burlesque of pigments and phenotypes. *Microbiology (N Y)* **165**, 953–955 (2019).
3. Salwan, R. & Sharma, V. Bioactive compounds of Streptomyces: Biosynthesis to applications. in 467–491 (2020). doi:10.1016/B978-0-12-817903-1.00015-2.
4. Zhou, Z., Gu, J., Li, Y.-Q. & Wang, Y. Genome plasticity and systems evolution in Streptomyces. *BMC Bioinformatics* **13**, S8 (2012).
5. Zhao, F. *et al.* Biogeography and Adaptive evolution of Streptomyces Strains from saline environments. *Sci Rep* **6**, 32718 (2016).
6. Zhou, L. *et al.* Diversity Analysis and Biocontrol Potential of Cultivatable Terrestrial Bacterial Streptomyces in Southern China. *Agronomy* **13**, 2500 (2023).
7. Quezada, M. *et al.* Diverse Cone-Snail Species Harbor Closely Related Streptomyces Species with Conserved Chemical and Genetic Profiles, Including Polycyclic Tetramic Acid Macrolactams. *Front Microbiol* **8**, (2017).
8. Lucas, X. *et al.* StreptomeDB: a resource for natural compounds isolated from Streptomyces species. *Nucleic Acids Res* **41**, D1130–D1136 (2013).
9. Glaeser, S. P. & Kämpfer, P. Streptomycetaceae: Phylogeny, Ecology and Pathogenicity. in *Encyclopedia of Life Sciences* 1–12 (Wiley, 2016). doi:10.1002/9780470015902.a0020392.pub2.
10. Arabolaza, A., Rodriguez, E., Altabe, S., Alvarez, H. & Gramajo, H. Multiple Pathways for Triacylglycerol Biosynthesis in *Streptomyces coelicolor*. *Appl Environ Microbiol* **74**, 2573–2582 (2008).
11. Chen, Y., Metz, J., Miller-Xavier, R. K. & Wang, G. Unlocking a new target for streptomycetes strain improvement. *Synth Syst Biotechnol* **5**, 33–34 (2020).

12. Röttig, A. *et al.* Streptomyces jeddahensis sp. nov., an oleaginous bacterium isolated from desert soil. *Int J Syst Evol Microbiol* **67**, 1676–1682 (2017).

13. Krishnan, S., Chinnadurai, G. S. & Perumal, P. Polyhydroxybutyrate by Streptomyces sp.: Production and characterization. *Int J Biol Macromol* **104**, 1165–1171 (2017).

14. Narayanan, M. *et al.* A Novel Insight Into the Fabrication of Polyhydroxyalkanoates from Actinobacteria Streptomyces toxytricini D2: Screening, Optimization, and Biopolymer Characterization. *J Polym Environ* **30**, 2128–2141 (2022).

15. Ramachander, T. V. N. & Rawal, S. K. PHB synthase from Streptomyces aureofaciens NRRL 2209. *FEMS Microbiol Lett* **242**, 13–18 (2005).

16. Verma, S., Bhatia, Y., Valappil, S. P. & Roy, I. A possible role of poly-3-hydroxybuiyric acid in antibiotic production inStreptomyces. *Arch Microbiol* **179**, 66–69 (2002).

17. Dávila Costa, J. S., Leichert, L., Alvarez, H. M. & Herrero, O. M. Label-free and redox proteomic analyses of the triacylglycerol-accumulating Rhodococcus jostii RHA1. *Microbiology (N Y)* **161**, 593–610 (2015).

18. Wältermann, M., Luftmann, H., Baumeister, D., Kalscheuer, R. & Steinbüchel, A. Rhodococcus opacus strain PD630 as a new source of high-value single-cell oil? Isolation and characterization of triacylglycerols and other storage lipids. *Microbiology (N Y)* **146**, 1143–1149 (2000).

19. Amara, S. *et al.* Characterization of key triacylglycerol biosynthesis processes in rhodococci. *Sci Rep* **6**, 24985 (2016).

20. Zhang, J. *et al.* Microbial lipid production by the oleaginous yeast Cryptococcus curvatus O3 grown in fed-batch culture. *Biomass Bioenergy* **35**, 1906–1911 (2011).

21. Kim, H. M., Chae, T. U., Choi, S. Y., Kim, W. J. & Lee, S. Y. Engineering of an oleaginous bacterium for the production of fatty acids and fuels. *Nat Chem Biol* **15**, 721–729 (2019).

22. Hernández, M. A. *et al.* Central Metabolism of Species of the Genus Rhodococcus. in 61–85 (Springer, Cham, 2019). doi:10.1007/978-3-030-11461-9_3.

23. Yang, X., Jin, G., Wang, Y., Shen, H. & Zhao, Z. K. Lipid production on free fatty acids by oleaginous yeasts under non-growth conditions. *Bioresour Technol* **193**, 557–562 (2015).

24. Röttig, A. *et al.* Analysis and optimization of triacylglycerol synthesis in novel oleaginous Rhodococcus and Streptomyces strains isolated from desert soil. *J Biotechnol* **225**, 48–56 (2016).

25. Heath, R. J., Jackowski, S. & Rock, C. O. Chapter 3 Fatty acid and phospholipid metabolism in prokaryotes. in 55–92 (2002). doi:10.1016/S0167-7306(02)36005-8.

26. Gago, G., Arabolaza, A., Diacovich, L. & Gramajo, H. Components and Key Regulatory Steps of Lipid Biosynthesis in Actinomycetes. in *Biogenesis of Fatty Acids, Lipids and*

Membranes 1–25 (Springer International Publishing, Cham, 2018). doi:10.1007/978-3-319-43676-0_65-1.

27. Kim, G. J., Lee, I. Y., Yoon, S. C., Shin, Y. C. & Park, Y. H. Enhanced yield and a high production of medium-chain-length poly(3-hydroxyalkanoates) in a two-step fed-batch cultivation of Pseudomonas putida by combined use of glucose and octanoate. *Enzyme Microb Technol* **20**, 500–505 (1997).

28. Lin, J. *et al.* Lipid production by Lipomyces starkeyi cells in glucose solution without auxiliary nutrients. *J Biotechnol* **152**, 184–188 (2011).

29. Fei, Q., Wewetzer, S. J., Kurosawa, K., Rha, C. & Sinskey, A. J. High-cell-density cultivation of an engineered Rhodococcus opacus strain for lipid production via co-fermentation of glucose and xylose. *Process Biochemistry* **50**, 500–506 (2015).

30. Hu, C. *et al.* Simultaneous utilization of glucose and xylose for lipid production by Trichosporon cutaneum. *Biotechnol Biofuels* **4**, 25 (2011).

31. Cabecas Segura, P. *et al.* Study of the Production of Poly(Hydroxybutyrate- *co* -Hydroxyhexanoate) and Poly(Hydroxybutyrate- *co* -Hydroxyvalerate- *co*-Hydroxyhexanoate) in Rhodospirillum rubrum. *Appl Environ Microbiol* **88**, (2022).

32. Fontaine, P., Mosrati, R. & Corroler, D. Medium chain length polyhydroxyalkanoates biosynthesis in Pseudomonas putida mt-2 is enhanced by co-metabolism of glycerol/octanoate or fatty acids mixtures. *Int J Biol Macromol* **98**, 430–435 (2017).

33. Sass, P. (ed.). *Antibiotics: Methods and Protocols, Methods in Molecular Biology 2nd Edition*. http://www.springer.com/series/7651 (2022) doi:https://doi.org/10.1007/978-1-0716-2855-3.

34. Livak, K. J. & Schmittgen, T. D. Analysis of Relative Gene Expression Data Using Real-Time Quantitative PCR and the 2−ΔΔCT Method. *Methods* **25**, 402–408 (2001).

35. Bosdriesz, E. *et al.* Low affinity uniporter carrier proteins can increase net substrate uptake rate by reducing efflux. *Sci Rep* **8**, 5576 (2018).

36. Shukla, V. & Phulara, S. C. Impact of Culture Condition Modulation on the High-Yield, High-Specificity, and Cost-Effective Production of Terpenoids from Microbial Sources: a Review. *Appl Environ Microbiol* **87**, (2021).

37. Wang, Z. *et al.* Isolation and thermo-acclimation of thermophilic bacteria in hyperthermophilic fermentation system. *Bioprocess Biosyst Eng* **45**, 75–85 (2022).

38. Demirjian, D. C., Morís-Varas, F. & Cassidy, C. S. Enzymes from extremophiles. *Curr Opin Chem Biol* **5**, 144–151 (2001).

39. Schilling, O. A protein-dependent riboswitch controlling ptsGHI operon expression in Bacillus subtilis: RNA structure rather than sequence provides interaction specificity. *Nucleic Acids Res* **32**, 2853–2864 (2004).

40. Trakunjae, C. *et al.* Statistical optimization of P(3HB-co-3HHx) copolymers production by Cupriavidus necator PHB−4/pBBR_CnPro-phaCRp and its properties characterization. *Sci Rep* **13**, 9005 (2023).

41. Lindenkamp, N., Volodina, E. & Steinbüchel, A. Genetically Modified Strains of Ralstonia eutropha H16 with β-Ketothiolase Gene Deletions for Production of Copolyesters with Defined 3-Hydroxyvaleric Acid Contents. *Appl Environ Microbiol* **78**, 5375–5383 (2012).

42. Iram, S. H. & Cronan, J. E. The β-Oxidation Systems of *Escherichia coli* and *Salmonella enterica* Are Not Functionally Equivalent. *J Bacteriol* **188**, 599–608 (2006).

43. Schroda, M. & deVitry, C. Molecular chaperones, proteases, and unfolded protein responses. in *The Chlamydomonas Sourcebook* 647–689 (Elsevier, 2023). doi:10.1016/B978-0-12-821430-5.00023-7.

44. Russell, A. D. Lethal Effects of Heat on Bacterial Physiology and Structure. *Sci Prog* **86**, 115–137 (2003).

45. Alvarez, H. M. & Steinbüchel, A. Physiology, Biochemistry, and Molecular Biology of Triacylglycerol Accumulation by Rhodococcus. in 263–290 (2010). doi:10.1007/978-3-642-12937-7_10.

46. Yang, Y. *et al.* Potential of oleaginous microbes for lipid accumulation and renewable energy generation. *World J Microbiol Biotechnol* **40**, 337 (2024).

47. Koreti, D., Kosre, A., Jadhav, S. K. & Chandrawanshi, N. K. A comprehensive review on oleaginous bacteria: an alternative source for biodiesel production. *Bioresour Bioprocess* **9**, 47 (2022).

48. Patel, A. *et al.* Lipids detection and quantification in oleaginous microorganisms: an overview of the current state of the art. *BMC Chemical Engineering* **1**, 13 (2019).

49. Gorte, O., Kugel, M. & Ochsenreither, K. Optimization of carbon source efficiency for lipid production with the oleaginous yeast Saitozyma podzolica DSM 27192 applying automated continuous feeding. *Biotechnol Biofuels* **13**, 181 (2020).

50. Röttig, A. *et al.* Role of wax ester synthase/acyl coenzyme A: Diacylglycerol acyltransferase in oleaginous Streptomyces sp. strain G25. *Appl Environ Microbiol* **82**, 5969–5981 (2016).

51. Moon, S. *et al.* Temperature Matters: Bacterial Response to Temperature Change. *Journal of Microbiology* **61**, 343–357 (2023).

52. Zhu, L. *et al.* Functions of the Clostridium acetobutylicium FabF and FabZ proteins in unsaturated fatty acid biosynthesis. *BMC Microbiol* **9**, 119 (2009).

53. Ogawa, T., Tanaka, A., Kawamoto, J. & Kurihara, T. Purification and characterization of 1-acyl-sn-glycerol-3-phosphate acyltransferase with a substrate preference for polyunsaturated fatty acyl donors from the eicosapentaenoic acid-producing bacterium Shewanella livingstonensis Ac10. *The Journal of Biochemistry* **164**, 33–39 (2018).

54. Shi, K. *et al.* Reactive Oxygen Species-Mediated Cellular Stress Response and Lipid Accumulation in Oleaginous Microorganisms: The State of the Art and Future Perspectives. *Front Microbiol* **8**, (2017).

55. Paulsen, I. T. Carbon metabolism and its regulation in Streptomyces and other high GC Gram-positive bacteria. *Res Microbiol* **147**, 535–541 (1996).

56. Bucca, G. *et al.* Translational control plays an important role in the adaptive heat-shock response of Streptomyces coelicolor. *Nucleic Acids Res* **46**, 5692–5703 (2018).

57. Narberhaus, F., Waldminghaus, T. & Chowdhury, S. RNA thermometers. *FEMS Microbiol Rev* **30**, 3–16 (2006).

58. Kalscheuer, R. & Steinbüchel, A. A Novel Bifunctional Wax Ester Synthase/Acyl-CoA:Diacylglycerol Acyltransferase Mediates Wax Ester and Triacylglycerol Biosynthesis inAcinetobacter calcoaceticus ADP1. *Journal of Biological Chemistry* **278**, 8075–8082 (2003).

59. Wältermann, M., Stöveken, T. & Steinbüchel, A. Key enzymes for biosynthesis of neutral lipid storage compounds in prokaryotes: Properties, function and occurrence of wax ester synthases/acyl-CoA:diacylglycerol acyltransferases. *Biochimie* **89**, 230–242 (2007).

60. Santos, C. A. *et al.* An engineered GH1 β-glucosidase displays enhanced glucose tolerance and increased sugar release from lignocellulosic materials. *Sci Rep* **9**, 4903 (2019).

61. Zhang, X. *et al.* Mechanism of differential expression of β-glucosidase genes in functional microbial communities in response to carbon catabolite repression. *Biotechnology for Biofuels and Bioproducts* **15**, 3 (2022).

62. Obruča, S. *et al.* Polyhydroxyalkanoates synthesis by halophiles and thermophiles: towards sustainable production of microbial bioplastics. *Biotechnology Advances* vol. 58 Preprint at https://doi.org/10.1016/j.biotechadv.2022.107906 (2022).

63. Müller-Santos, M. *et al.* The protective role of PHB and its degradation products against stress situations in bacteria. *FEMS Microbiology Reviews* vol. 45 Preprint at https://doi.org/10.1093/femsre/fuaa058 (2021).

64. Rai, R., Keshavarz, T., Roether, J. A., Boccaccini, A. R. & Roy, I. Medium chain length polyhydroxyalkanoates, promising new biomedical materials for the future. *Materials Science and Engineering: R: Reports* **72**, 29–47 (2011).

65. Muhr, A. *et al.* Biodegradable latexes from animal-derived waste: Biosynthesis and characterization of mcl-PHA accumulated by Ps. citronellolis. *React Funct Polym* **73**, 1391–1398 (2013).

66. Davis, R. *et al.* High cell density cultivation of *Pseudomonas putida* KT2440 using glucose without the need for oxygen enriched air supply. *Biotechnol Bioeng* **112**, 725–733 (2015).

67. Lee, S. Y. Bacterial polyhydroxyalkanoates. *Biotechnol Bioeng* **49**, 1–14 (1996).

68. Chek, M. F. *et al.* Structure of polyhydroxyalkanoate (PHA) synthase PhaC from Chromobacterium sp. USM2, producing biodegradable plastics. *Sci Rep* **7**, 5312 (2017).

69. Mozejko-Ciesielska, J., Szacherska, K. & Marciniak, P. Pseudomonas Species as Producers of Eco-friendly Polyhydroxyalkanoates. *J Polym Environ* **27**, 1151–1166 (2019).

70. Vicente, D., Proença, D. N. & Morais, P. V. The Role of Bacterial Polyhydroalkanoate (PHA) in a Sustainable Future: A Review on the Biological Diversity. *Int J Environ Res Public Health* **20**, 2959 (2023).

71. Rigouin, C. *et al.* Production and characterization of two medium-chain-length polydroxyalkanoates by engineered strains of Yarrowia lipolytica. *Microb Cell Fact* **18**, 99 (2019).

72. Lamers, D. *et al.* Selection of oleaginous yeasts for fatty acid production. *BMC Biotechnol* **16**, 45 (2016).

73. Jiang, Y. *et al.* CRISPR-Cpf1 assisted genome editing of Corynebacterium glutamicum. *Nat Commun* **8**, 15179 (2017).

74. Spiekermann, P., Rehm, B. H. A., Kalscheuer, R., Baumeister, D. & Steinbüchel, A. A sensitive, viable-colony staining method using Nile red for direct screening of bacteria that accumulate polyhydroxyalkanoicacids and other lipid storage compounds. *Arch Microbiol* **171**, 73–80 (1999).

75. Matsusaki, H., Abe, H., Taguchi, K., Fukui, T. & Doi, Y. Biosynthesis of poly(3-hydroxybutyrate- co -3-hydroxyalkanoates) by recombinant bacteria expressing the PHA synthase gene phaC1 from Pseudomonas sp. 61-3. *Appl Microbiol Biotechnol* **53**, 401–409 (2000).

76. Taguchi, S. *et al.* A microbial factory for lactate-based polyesters using a lactate-polymerizing enzyme. *Proceedings of the National Academy of Sciences* **105**, 17323–17327 (2008).

77. Chen, J.-Y., Song, G. & Chen, G.-Q. A lower specificity PhaC2 synthase from Pseudomonas stutzeri catalyses the production of copolyesters consisting of short-chain-length and medium-chain-length 3-hydroxyalkanoates. *Antonie Van Leeuwenhoek* **89**, 157–167 (2006).

78. Fiedler, S., Steinbüchel, A. & Rehm, B. H. A. PhaG-Mediated Synthesis of Poly(3-Hydroxyalkanoates) Consisting of Medium-Chain-Length Constituents from Nonrelated Carbon Sources in Recombinant *Pseudomonas fragi*. *Appl Environ Microbiol* **66**, 2117–2124 (2000).

79. Apriliana, P., Kahar, P., Kashiwagi, N., Kondo, A. & Ogino, C. Editing *Streptomyces* genome using target AID system fused with UGI-degradation tag. *Eng Life Sci* **24**, (2024).

80. Trakunjae, C. *et al.* Enhanced polyhydroxybutyrate (PHB) production by newly isolated rare actinomycetes Rhodococcus sp. strain BSRT1-1 using response surface methodology. *Sci Rep* **11**, 1896 (2021).

81. Demir Öksüz, Z., Doruk, T., Yağci, N. & Tunca Gedik, S. Polyhydroxyalkanoate accumulation in streptomyces coelicolor affected by sco761gene region. *Turkish Journal of Biology* **45**, 275–286 (2021).

82. Tourang, M., Xiong, X., Sarkhosh, S. & Chen, S. Polyhydroxybutyrate (PHB) Biosynthesis by an Engineered Yarrowia lipolytica Strain Using Co-Substrate Strategy. *Fermentation* **9**, 1003 (2023).

83. Magdouli, S., Brar, S. K., Blais, J. F. & Tyagi, R. D. How to direct the fatty acid biosynthesis towards polyhydroxyalkanoates production? *Biomass Bioenergy* **74**, 268–279 (2015).

84. Kim, T. K., Jung, Y. M., Minh, T. V., Shioya, S. & Lee, Y. H. Metabolic engineering and characterization of phaC1 mid phaC2 genes from Pseudomonas putida KCTC1639 for overproduction of medium-chain-length polyhydroxyalkanoate. *Biotechnol Prog* **22**, 1541–1546 (2006).

85. Ansari, N. F., Annuar, M. S. M. & Murphy, B. P. A porous medium-chain-length poly(3-hydroxyalkanoates)/hydroxyapatite composite as scaffold for bone tissue engineering. *Eng Life Sci* **17**, 420–429 (2017).

86. Steinbüchel, A. & Lütke-Eversloh, T. Metabolic engineering and pathway construction for biotechnological production of relevant polyhydroxyalkanoates in microorganisms. *Biochemical Engineering Journal* vol. 16 81–96 Preprint at https://doi.org/10.1016/S1369-703X(03)00036-6 (2003).

87. Madkour Mohamed H, Heinrich Daniel, Alghamdi, M. A., Shabbaj, I. I. & Steinbüchel Alexander. PHA Recovery from Biomass. *Biomacromolecules* **14**, 2963–2972 (2013).

88. De Smet, M. J., Eggink, G., Witholt, B., Kingma, J. & Wynberg, H. *Characterization of Intracellular Inclusions Formed by Pseudomonas Oleovorans During Growth on Octane*. *JOURNAL OF BACTERIOLOGY* vol. 154 (1983).

89. Braunegg, G., Sonnleitner, B. & Lafferty, R. M. A rapid gas chromatographic method for the determination of poly-β-hydroxybutyric acid in microbial biomass. *European Journal of Applied Microbiology and Biotechnology* **6**, 29–37 (1978).

90. Shao, D. *et al.* Glucose promotes cell growth by suppressing branched-chain amino acid degradation. *Nat Commun* **9**, 2935 (2018).

91. Ahsan, T., Chen, J., Zhao, X., Irfan, M. & Wu, Y. Extraction and identification of bioactive compounds (eicosane and dibutyl phthalate) produced by Streptomyces strain KX852460 for the biological control of Rhizoctonia solani AG-3 strain KX852461 to control target spot disease in tobacco leaf. *AMB Express* **7**, (2017).

92. Mangamuri, U. *et al.* Bioactive metabolites produced by Streptomyces Cheonanensis VUK-A from Coringa mangrove sediments: isolation, structure elucidation and bioactivity. *3 Biotech* **6**, 1–8 (2016).

93. Monthon Lertcanawanichakul & Kittisak Chawawisit. Bioactive Compound from Streptomyces sp. KB1 TISTR2504 as Effective Disinfectant against Microorganisms. *Journal of Pharmacy and Pharmacology* **9**, 1–7 (2021).

94. Nakashima, T. *et al. NOTE Productivity of Bioactive Compounds in Streptomyces Species Isolated from Nagasaki Marine Environments*. (2009).

95. Balasubramanian, S. *et al.* A new bioactive compound from the marine sponge-derived Streptomyces sp. SBT348 inhibits staphylococcal growth and biofilm formation. *Front Microbiol* **9**, (2018).

96. Wang, J., Nong, X. H., Amin, M. & Qi, S. H. Hygrocin C from marine-derived Streptomyces sp. SCSGAA 0027 inhibits biofilm formation in Bacillus amyloliquefaciens SCSGAB0082 isolated from South China Sea gorgonian. *Appl Microbiol Biotechnol* **102**, 1417–1427 (2018).

97. Ahmad, M. S. *et al.* Exploring the antimicrobial and antitumor potentials of Streptomyces sp. AGM12-1 isolated from Egyptian soil. *Front Microbiol* **8**, (2017).

98. Nguyen, H. T. *et al.* Streptomyces sp. VN1, a producer of diverse metabolites including non-natural furan-type anticancer compound. *Sci Rep* **10**, (2020).

99. Zhao, H. *et al.* Insecticidal Endostemonines A-J Produced by Endophytic Streptomyces from Stemona sessilifolia. *J Agric Food Chem* **68**, 1588–1595 (2020).

100. Haruo Ikeda. Genetic Analysis of Biosynthesis of Polyketide Anthelmintic Macrolide Avermectin in Streptomyces avermitilis. *Actinomycetologica* **13**, 94–112 (1999).

101. Sevillano, L., Vijgenboom, E., van Wezel, G. P., Díaz, M. & Santamaría, R. I. New approaches to achieve high level enzyme production in Streptomyces lividans. *Microb Cell Fact* **15**, (2016).

102. Rutledge, P. J. & Challis, G. L. Discovery of microbial natural products by activation of silent biosynthetic gene clusters. *Nature Reviews Microbiology* vol. 13 509–523 Preprint at https://doi.org/10.1038/nrmicro3496 (2015).

103. Xu, T., Li, Y., Van Nostrand, J. D., He, Z. & Zhou, J. Cas9-based tools for targeted genome editing and transcriptional control. *Applied and Environmental Microbiology* vol. 80 1544–1552 Preprint at https://doi.org/10.1128/AEM.03786-13 (2014).

104. Selle, K. & Barrangou, R. Harnessing CRISPR-Cas systems for bacterial genome editing. *Trends in Microbiology* vol. 23 225–232 Preprint at https://doi.org/10.1016/j.tim.2015.01.008 (2015).

105. Jia, H. *et al.* Development of a crispr/cas9-mediated gene-editing tool in streptomyces rimosus. *Microbiology (United Kingdom)* **163**, 1148–1155 (2017).

106. Zhang, M. M. *et al.* CRISPR-Cas9 strategy for activation of silent Streptomyces biosynthetic gene clusters. *Nat Chem Biol* **13**, 607–609 (2017).

107. Alberti, F. & Corre, C. Editing streptomycete genomes in the CRISPR/Cas9 age. *Nat Prod Rep* **36**, 1237–1248 (2019).

108. Tong, Y., Weber, T. & Lee, S. Y. CRISPR/Cas-based genome engineering in natural product discovery. *Natural Product Reports* vol. 36 1262–1280 Preprint at https://doi.org/10.1039/c8np00089a (2019).

109. Hoff, G., Bertrand, C., Piotrowski, E., Thibessard, A. & Leblond, P. Genome plasticity is governed by double strand break DNA repair in Streptomyces. *Sci Rep* **8**, (2018).

110. Volff, J. N. & Altenbuchner, J. Genetic instability of the streptomyces chromosome. *Molecular Microbiology* vol. 27 239–246 Preprint at https://doi.org/10.1046/j.1365-2958.1998.00652.x (1998).

111. Riha, K., Heacock, M. L. & Shippen, D. E. The role of the nonhomologous end-joining DNA double-strand break repair pathway in telomere biology. *Annual Review of Genetics* vol. 40 237–277 Preprint at https://doi.org/10.1146/annurev.genet.39.110304.095755 (2006).

112. Kieser, T., Bibb, M. J., Buttner, M. J., Chater, K. F. & Hopwood, D. A. *Practical Streptomyces Genetics*. (The John Innes Foundation, Norwich, England, 2000).

113. Qi, L. S. *et al.* Repurposing CRISPR as an RNA-guided platform for sequence-specific control of gene expression. *Cell* vol. 152 1173–1183 Preprint at https://doi.org/10.1016/j.cell.2013.02.022 (2013).

114. Jinek, M. *et al.* A Programmable Dual-RNA–Guided DNA Endonuclease in Adaptive Bacterial Immunity. *Science (1979)* **337**, 816–821 (2012).

115. Banno, S., Nishida, K., Arazoe, T., Mitsunobu, H. & Kondo, A. Deaminase-mediated multiplex genome editing in Escherichia coli. *Nat Microbiol* **3**, 423–429 (2018).

116. Blaesing, F. *et al.* Introduction of DNA into Actinomycetes by bacterial conjugation from E. coli - An evaluation of various transfer systems. *J Biotechnol* **120**, 146–161 (2005).

117. Bystrykh, L. V. *et al.* Production of actinorhodin-related 'blue pigments' by Streptomyces coelicolor A3(2). *J Bacteriol* **178**, 2238–2244 (1996).

118. Coisne, S., Béchet, M. & Blondeau, R. Actinorhodin production by *Streptomyces coelicolor* A3(2) in iron-restricted media. *Lett Appl Microbiol* **28**, 199–202 (1999).

119. Tong, Y., Charusanti, P., Zhang, L., Weber, T. & Lee, S. Y. CRISPR-Cas9 Based Engineering of Actinomycetal Genomes. *ACS Synth Biol* **4**, 1020–1029 (2015).

120. Bikard, D. *et al.* Programmable repression and activation of bacterial gene expression using an engineered CRISPR-Cas system. *Nucleic Acids Res* **41**, 7429–7437 (2013).

121. Komor, A. C., Kim, Y. B., Packer, M. S., Zuris, J. A. & Liu, D. R. Programmable editing of a target base in genomic DNA without double-stranded DNA cleavage. *Nature* **533**, 420–424 (2016).

122. Bentley, S. D. *et al.* Complete genome sequence of the model actinomycete Streptomyces coelicolor A3(2). *Nature* **417**, 141–147 (2002).

123. Mol, C. D. *et al.* Crystal structure of human uracil-DNA glycosylase in complex with a protein inhibitor: Protein mimicry of DNA. *Cell* **82**, 701–708 (1995).

124. Keiler, K. C., Waller, P. R. H. & Sauer, R. T. Role of a Peptide Tagging System in Degradation of Proteins Synthesized from Damaged Messenger RNA. *Science (1979)* **271**, 990–993 (1996).

125. Jadhav, P., Chen, Y., Butzin, N., Buceta, J. & Urchueguía, A. Bacterial degrons in synthetic circuits. *Open Biology* vol. 12 Preprint at https://doi.org/10.1098/rsob.220180 (2022).

126. Taguchi, T. *et al.* Identification of the actinorhodin monomer and its related compound from a deletion mutant of the actVA-ORF4 gene of Streptomyces coelicolor A3(2). *Bioorg Med Chem Lett* **22**, 5041–5045 (2012).

127. Valton, J., Mathevon, C., Fontecave, M., Nivière, V. & Ballou, D. P. Mechanism and regulation of the two-component FMN-dependent monooxygenase ActVA-ActVB from Streptomyces coelicolor. *Journal of Biological Chemistry* **283**, 10287–10296 (2008).

128. Murakami, T., Holt, T. G. & Thompson, C. J. Thiostrepton-induced gene expression in Streptomyces lividans. *J Bacteriol* **171**, 1459–1466 (1989).

129. Mo, J. *et al.* Efficient editing DNA regions with high sequence identity in actinomycetal genomes by a CRISPR-Cas9 system. *Synthetic and Systems Biotechnology* vol. 4 86–91 Preprint at https://doi.org/10.1016/j.synbio.2019.02.004 (2019).

130. Zeng, H. *et al.* Highly efficient editing of the actinorhodin polyketide chain length factor gene in Streptomyces coelicolor M145 using CRISPR/Cas9-CodA(sm) combined system. *Appl Microbiol Biotechnol* **99**, 10575–10585 (2015).

131. Mok, B. Y. *et al.* A bacterial cytidine deaminase toxin enables CRISPR-free mitochondrial base editing. *Nature* **583**, 631–637 (2020).

132. Atkins, A. *et al.* Off-Target Analysis in Gene Editing and Applications for Clinical Translation of CRISPR/Cas9 in HIV-1 Therapy. *Front Genome Ed* **3**, (2021).

133. Kim, H. J., Lee, H. J., Kim, H., Cho, S. W. & Kim, J.-S. Targeted genome editing in human cells with zinc finger nucleases constructed via modular assembly. *Genome Res* **19**, 1279–1288 (2009).

134. Cho, S. W., Kim, S., Kim, J. M. & Kim, J.-S. Targeted genome engineering in human cells with the Cas9 RNA-guided endonuclease. *Nat Biotechnol* **31**, 230–232 (2013).

135. Kim, D. *et al.* Digenome-seq: genome-wide profiling of CRISPR-Cas9 off-target effects in human cells. *Nat Methods* **12**, 237–243 (2015).

136. Tsai, S. Q. *et al.* CIRCLE-seq: A highly sensitive in vitro screen for genome-wide CRISPR-Cas9 nuclease off-targets. *Nat Methods* **14**, 607–614 (2017).

137. Tsai, S. Q. *et al.* GUIDE-seq enables genome-wide profiling of off-target cleavage by CRISPR-Cas nucleases. *Nat Biotechnol* **33**, 187–197 (2015).

Doctoral Dissertation, Kobe University

“Engineering *Streptomyces* Strains for Bioproduct Production through CRISPR Systems and Gene Integration”

CRISPR システムと遺伝子導入によるバイオ生産のための *Streptomyces* 菌株の遺伝子工学

（101 pages）

Submitted on February 20, 2024.

The date of publication is printed on the cover of the repository version published with the Kobe University Repository Kernel.

© Pamella apriliana

All Rights Reserved,

2025